ISBN 978-82-326-3186-5 (printed version)
ISBN 978-82-326-3187-2 (electronic version)
ISSN 1503-8181

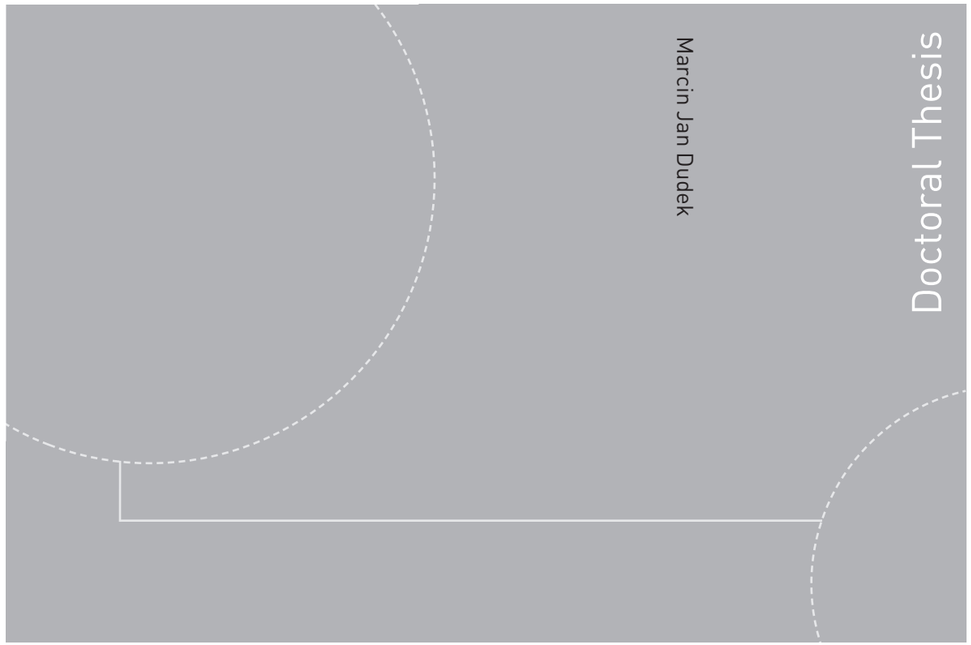

Doctoral theses at NTNU, 2018:198

Marcin Jan Dudek

Produced Water Quality and Microfluidic Methods for Studying Drop-Drop and Drop-Bubble Interactions in Produced Water

NTNU
Norwegian University of
Science and Technology
Faculty of Natural Sciences
Department of Chemical Engineering

NTNU
Norwegian University of
Science and Technology

Doctoral theses at NTNU, 2018:198

NTNU

NTNU
Norwegian University of
Science and Technology

Marcin Jan Dudek

Produced Water Quality and Microfluidic Methods for Studying Drop-Drop and Drop-Bubble Interactions in Produced Water

Thesis for the degree of Philosophiae Doctor

Trondheim, June 2018

Norwegian University of Science and Technology
Faculty of Natural Sciences
Department of Chemical Engineering

NTNU
Norwegian University of
Science and Technology

NTNU
Norwegian University of Science and Technology

Thesis for the degree of Philosophiae Doctor

Faculty of Natural Sciences
Department of Chemical Engineering

ISBN 978-82-326-3186-5 (printed version)
ISBN 978-82-326-3187-2 (electronic version)
ISSN 1503-8181

Doctoral theses at NTNU, 2018:198

Printed by Skipnes Kommunikasjon as

PREFACE

This thesis is submitted to partly fulfil the requirements for the degree of *Philosophiae Doctor* (Ph.D.) at the Norwegian University of Science and Technology (NTNU). The work presented here was carried out at the Ugelstad Laboratory in the Department of Chemical Engineering under the supervision of Professor Gisle Øye, and consists of four manuscripts.

I obtained my *Master of Science in Engineering* in Chemical and Process Engineering (specialization: Chemical Engineering) in the Faculty of Chemical Technology at Poznań University of Technology (Poland) in June 2015. I started to pursue my Ph.D. degree in August later that year. I was affiliated to the SUBPRO project, a Centre for Innovation-based Research (SFI) within subsea production and processing. This project was funded by the Research Council of Norway, NTNU and major industry partners: ABB, Aker Solutions, Aker BP, DNV GL, Neptune Energy Norge, Lundin, Shell, Statoil and VNG Norge.

ACKNOWLEDGMENTS

Throughout the project I have received a lot of support from many people, and I will not be able to fit all of you in this short paragraph. Even if you did not find yourself on that list, please know that I am grateful for your help.

First and foremost, I would like to express my sincere gratitude to Professor Gisle Øye for giving me a chance on this project and then supporting me all the way till the end. I was very lucky to have you as my supervisor. To Bartek for helping me in the beginning (and probably a little before), and making this new surrounding a little bit more familiar. I also want to thank the staff of the Ugelstad Laboratory, namely May Grete, Camilla, Sébastien, Jens and Bicheng for all their advice, both of technical and more personal nature. And of course, to all other colleagues in the Ugelstad Laboratory and the Department of Chemical Engineering, present and past, who made this a unique workplace!

To all the people from SUBPRO for the support and self-development opportunities. To Gro and Jon, the management team, PhDs, Postdocs and industrial partners. I am very glad to have been a part of this project.

To Karin Schroën and Kelly Muijlwijk from the Wageningen University for all their useful advice and patience during my research stay there.

To my family, for supporting my education and life choices. *Nie dotarłbym tutaj bez Waszego wsparcia i wiary we mnie.*

And finally, to all of you with whom I also spent time outside of the lab. To Sandra, Aleksandar, Are, Eirik and Jost, who were there from the beginning, and Marzieh and Tomas, who arrived a little bit later. Thank you for accepting me to your social circle and making my stay here not only about work.

ABSTRACT

Produced water originates from crude oil production, during which it is extracted to the surface together with hydrocarbons. It consists of various dissolved and dispersed components, such as dissolved organic and inorganic compounds, suspended solids, production chemicals, and oil dispersed in the form of droplets. The latter is typically targeted by the treatment processes before the water can be discharged to sea or re-injected to an underground formation.

Most of the produced water treatment processes are gravity-based separation. For example, gravity separators or hydrocyclones strongly rely on the rising velocity of the dispersed droplets, whereas gas flotation process aims at enhancing the density difference between the continuous and the dispersed phases through attachment of gas bubbles. This means that the fundamental phenomena occurring on a microscale, like droplet growth through coalescence or bubble-droplet interactions will play a key role during these separation processes. That is why the development of new, microfluidic research tools and their application for studying these interactions in various conditions was one of the main goals of this project.

First, the produced water quality and its connection to both crude oil and water compositions was investigated. The water was mixed with crude oil and later analysed with respect to the total oil concentration, droplet size, total organic carbon and pH change. Next, a microfluidic method was developed to study the coalescence of model oils in the presence and absence of dissolved atmospheric gases, also at elevated pressures. This was followed by a report on the application of microfluidics for probing coalescence between crude oil droplets in produced water. Various aspects, like the oil and water composition, the presence of dissolved components or pressure levels were studied. Finally, a novel methodology for investigating the removal of dispersed hydrocarbons through spreading on gas bubbles was presented. It also involved changing relevant parameters and testing their effect on the spreading process.

LIST OF PUBLICATIONS

PAPER 1

Marcin Dudek, Eugénie Kancir and Gisle Øye

Influence of the Crude Oil and Water Compositions on the Quality of Synthetic Produced Water

Energy & Fuels **2017**, *31(4)*, 3708-3716

DOI: 10.1021/acs.energyfuels.6b03297

PAPER 2

Marcin Dudek, Kelly Muijlwijk, Karin Schroën and Gisle Øye

The Effect of Dissolved Gas on Coalescence of Oil Drops Studied with Microfluidics

Journal of Colloid and Interface Science **2018**, *528*, 166-173

DOI: 10.1016/j.jcis.2018.05.083

PAPER 3

Marcin Dudek, Are Bertheussen, Thomas Dumaire and Gisle Øye

Microfluidic Tools for Studying Coalescence of Crude Oil Droplets in Produced Water

Submitted to Chemical Engineering Science; under review.

PAPER 4

Marcin Dudek and Gisle Øye

Removal of Crude Oil Droplets through Spreading on Gas Bubbles Studied with Microfluidics

Submitted to Industrial & Engineering Chemistry Research; under review.

CONFERENCES AND OTHER CONTRIBUTIONS

Poster at the 21st International Conference on Miniaturized Systems for Chemistry and Life Sciences (MicroTAS 2017)

Title: A Microfluidic Method to Study the Coalescence of Crude Oil Drops in Water – the Effect of Crude Oil and Water Composition

Authors: Marcin Dudek, Thomas Dumaire and Gisle Øye

Location and date: 22-26 October 2017; Savannah, USA.

Oral presentation at the International Workshop on Advanced Hybrid Separation Techniques in Industrial Wastewater Management

Title: Microfluidics within Produced Water Treatment

Authors: Marcin Dudek and Gisle Øye

Location and date: 8-9 December 2017; Kolkata, India.

Oral presentation at the Tekna Produced Water Management 2018 Conference

Title: Application of Microfluidics in Produced Water Research

Authors: Marcin Dudek and Gisle Øye

Location and date: 24-25 January 2018; Stavanger, Norway.

Poster at the 6th Population Balance Modelling Conference (PBM 2018)

Title: PBE Model Regression Applied to Water and Petroleum Dispersions

Authors: Sindre B. Øyen, Seok Ki Moon, Marcin Dudek, Christoph J. Backi, Gisle Øye, Sigurd Skogestad and Brian A. Grimes

Location and date: 7-9 May 2018; Ghent, Belgium.

TABLE OF CONTENTS

1. Crude oil

Crude oil is a mixture of hydrocarbons and other organic components. It can be found in underground geological formations around the world. Together with natural gas and coal, it is considered a fossil fuel and a non-renewable energy resource. Regardless of today's heated debate about the role of oil in climate change, petroleum-derived products are still an irreplaceable source of energy and precursors for a variety of manufacturing industries.

1.1. Composition

The composition of crude oil is highly dependent on the geographical location of the reservoir it is produced from. In general, it is composed of saturated, non-saturated, cyclic and aromatic hydrocarbons with the addition of certain fractions containing heteroatoms, such as nitrogen, oxygen and sulphur, and to smaller extent also metals, for instance nickel, vanadium or copper[1]. To simplify, a division of crude oil components into **s**aturates, **a**romatics, **r**esins and **a**sphaltenes (**SARA**) was introduced. It classifies different fractions of petroleum based on their polarity and solubility[2]. The least polar group, **saturates**, is mostly composed of saturated hydrocarbons with straight-, branched- or cyclic configuration. **Aromatics** have more polar nature due to one or more aromatic rings, as well as some heteroatoms in their structure. **Resins** and **asphaltenes** are usually highly aromatic and have polar moieties that can be of acidic or basic nature. They also contain a significant percentage of oxygen, nitrogen and sulphur. Asphaltenes and resins are distinguished by their solubility in light alkanes (C5-C7): resins dissolve readily in such solvents, whereas asphaltenes precipitate out. Both groups consist of amphiphilic molecules that can diffuse and adsorb on various interfaces. This may result in flow assurance issues, i.e. asphaltene aggregation, corrosion or emulsion formation. In addition, crude oils can be described by the total acid and base numbers (TAN and TBN, respectively). They indicate the acidic or basic nature of the oil. It is worth noting that the chemical composition of a crude oil largely determines its physical (density, viscosity) and interfacial (interfacial tension, viscoelastic behaviour) properties.

1.2. Recovery

After successful exploration and appraisal phases, the reservoir is ready to start producing hydrocarbons. Figure 1-1 illustrates a typical hydrocarbon formation, composed of three phases: gas, oil and water.

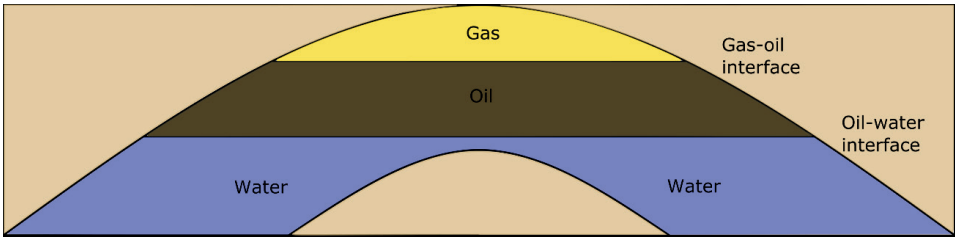

Figure 1-1 Simplified illustration of an underground hydrocarbon reservoir.

The reservoir fluids are initially under high pressure, which allows to maintain a steady flow of hydrocarbons in the beginning of the production without any additional energy. Later, this process may be supported with pumping. This stage of production is called **primary recovery** and only a small percentage of the hydrocarbons is retrieved, usually not more than 15%. After expansion of gas in the reservoir and subsequent reduction of its pressure, the formation requires an external pressure support in order to sustain production. This marks the beginning of the **secondary recovery** stage, where injection of water or gas is needed for a pressure boost in the formation, and maintaining the required flow of the produced hydrocarbons. The water injected into the reservoir can be either treated formation water or purified seawater. Approximately 50-60% of the original oil in place can be extracted from the reservoir thanks to the two combined recovery stages. Still, little less than half of the oil remains in the formation, predominantly trapped by capillary forces in small, micron-sized pores. This is when the enhanced oil recovery techniques (**tertiary recovery**) are employed. Most commonly, tertiary recovery methods can be categorized into gas (foam) injection, chemical injection or thermal displacement.

1.3. Transport and processing

Produced hydrocarbons leave the geological formation through an oil well. In an offshore facility several oil wells are usually connected to a production manifold, which collects the produced fluids. From there they are pumped topside for further processing (Figure 1-2).

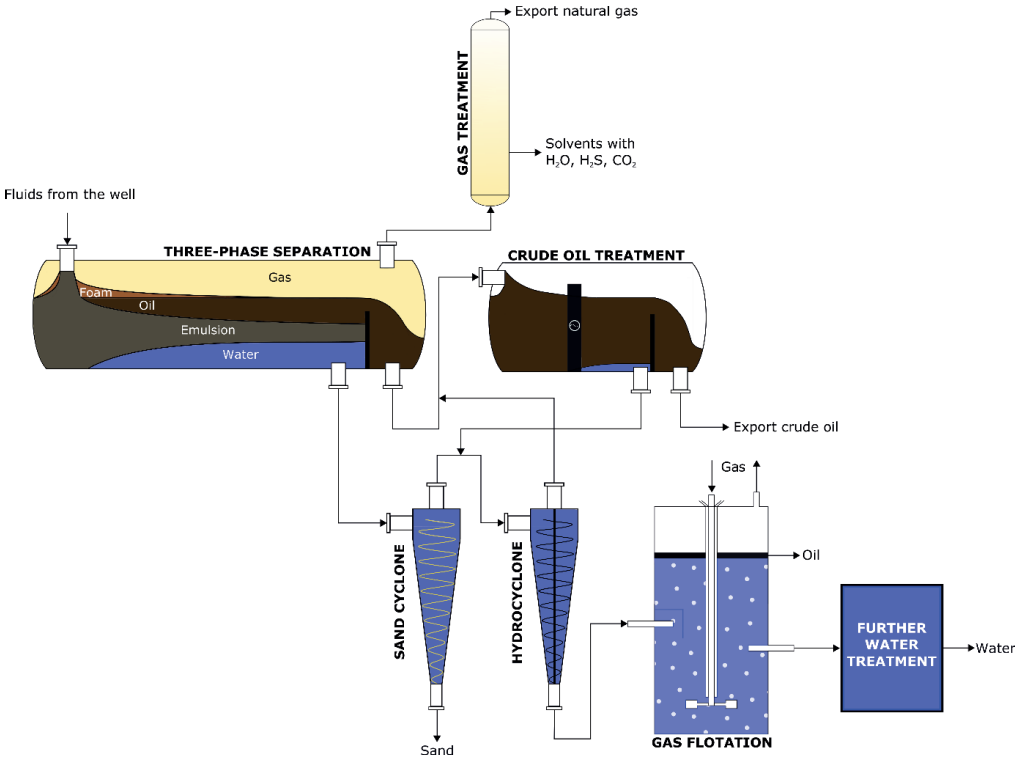

Figure 1-2 Schematic of an offshore crude oil, natural gas and water processing.

First, all fluids enter a gravity separator, where bulk three-phased separation takes place. Gas phase proceeds to natural gas treatment units, where it is dehydrated, sweetened (H_2S and CO_2 removal) and compressed. Crude oil flows to a second stage gravity separator, often equipped with an electrocoalescer. It enhances the water removal by forcing the growth of water droplets with an electric field. In order to reach the export quality, the water content in the crude oil has to be lowered to 0.5%. Frequently, oil and gas after treatment are recombined and pumped in one pipeline to shore or a floating production, storage and offloading (FPSO) unit. Lastly, produced water is treated through a series of processes. This, together with a comprehensive description of the produced water and its fate, will be described in detail in the next section.

2. Produced water

Produced water (PW) is largely composed of trapped formation water, extracted to the surface together with hydrocarbons. In the later stages of production, it can be a mix of formation and seawater. It is by far the largest by-product of petroleum production. Shortly after initializing production, relatively small volumes of water are produced. However, with the progressing age of an oilfield, water is steadily replacing hydrocarbons in the production stream. In the end, the water cut (ratio of water to total volume of produced fluids) can reach as high as 95%[3]. Typical production profile for an oilfield, located on the Norwegian Continental Shelf (NCS), is illustrated in Figure 2-1.

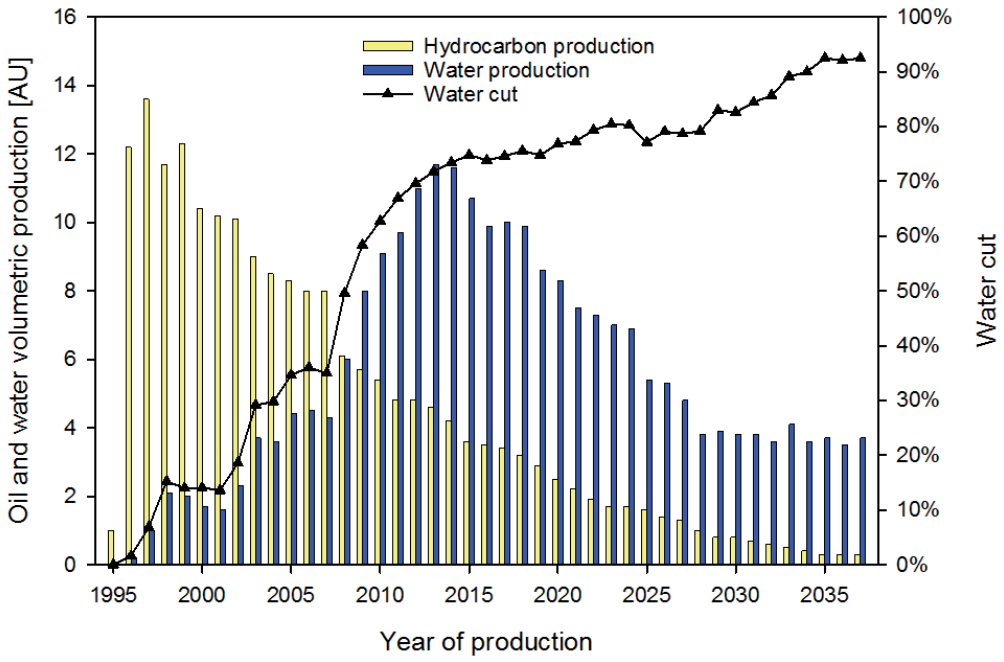

Figure 2-1 Crude oil and water production profiles in Heidrun oilfield. Based on[4].

Crude oil production, initially much higher than water production, starts to decline rapidly within 10 years or so. Inversely, volume of produced water steadily increases over the first 20 years of the field life time. It is also worth noting that even though the water production eventually starts to decrease, the water-to-oil ratio keeps growing, as indicated by the black

line in Figure 2-1. Global estimates say that for every barrel of crude oil (≈159L), three barrels of water are produced[5].

2.1. Composition

Water produced from a geological formation has been trapped there for millions of years. The composition of the produced water is further changed during various production steps. As a consequence, it is extremely complex and varies from field to field. Major constituents of the produced water are[6]: **dispersed hydrocarbons**, **dissolved inorganic** and **organic compounds**, **solid particles**, **production chemicals**, **dissolved gases** and **heavy metals**. General properties of PW are listed in Table 2-1.

Table 2-1 Basic properties of produced water and seawater. Based on[5, 7-9]

Parameter	Produced water		Seawater
	North Sea	World	
Density [kg/m^3]	1 014-1 085	1 014-1 140	1 020-1 029
Temperature [°C]	3-80	N/D	3-17
pH	6-7.7	4.3-10	7.6-8.3
Surface tension [mN/m]	N/D	43-78	72-73
Total Organic Carbon [mg/dm^3]	0-1500	100-1 000	0-1
Chloride [g/dm^3]	12.4-100	0.08-200	18.8-20.8

2.1.1. Dissolved minerals

Water trapped in a geological formation continuously dissolves the mineral material of the reservoir. The type of the formation determines the composition of the brine. Produced water contains various anions and cations, as well as heavy metals and even naturally occurring radioactive materials[5]. Table 2-2 provides an overview of different ions that are usually found in the North Sea produced water, together with a comparison to seawater.

Table 2-2 Concentrations of inorganic ions in produced water and seawater. Based on[9].

Ion	Concentration [mg/dm^3]	
	Produced water	**Seawater**
Cl^-	12 400-81 000	18 800-20 800
HCO_3^-	420-1430	134-155
SO_4^{2+}	18-1 650	2 810-2 960
Na^+	5 000-43 600	10 700-11 500
K^+	160-744	472-564
Mg^{2+}	25-791	1 180-1 322
Ca^{2+}	151-5 700	393-427
$Fe^{2+/3+}$	1-33	0-0.5
Ba^{2+}	1-218	0-0.1

These anions and cations can affect production processes in terms of scaling[10-11], separation[12-13] and environmental issues[14].

2.1.2. Solid particles

A variety of solid state materials can be present in the produced water, including formation solids, inorganic scale, wax and asphaltene precipitates, gas hydrates and dead microorganisms[5]. All of these can contribute to the stabilization of emulsions[15] or flow assurance problems[16]. The extent of precipitation can be managed with an injection of inhibitors (wax, scale, hydrates, corrosion) or adequate treatment of the injection water (bacteria, scale).

2.1.3. Dispersed oil

In the produced water crude oil is dispersed in the form of micron-sized droplets. They appear in the water phase as a result of turbulent flow and pressure drops, which can induce mixing between oil and water, and facilitate dispersion of drops. Their removal is the primary objective during most of the produced water treatment (PWT) processes. The approximate drop size and oil concentration after each water treatment stage is presented in Figure 2-2.

	Produced water from a gravity separator	After primary treatment	After secondary treatment	After tertiary treatment
Size range [µm]	>100-150	0-15	0-5	0
Dispersed oil concentration [mg/l]	500-1000	10-300	10-40	0

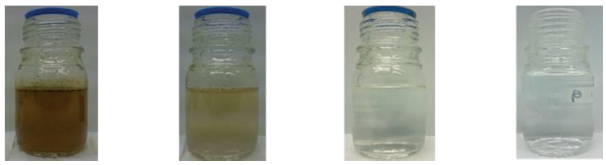

Figure 2-2 Drop size and oil concentration from different water treatment processes. (based on[17-23]). Below typical appearance of produced water with the oil-in-water concentration from appropriate concentration ranges.

Except of the last stage, all PWT processes rely, to a lesser or greater extent, on the droplet size distribution. In produced water, droplets below 100 µm are considered metastable. Their rising velocity is too low for them to separate from water during standard gravity separation. The majority of environmental regulations specifies only limitation of the dispersed (or total) oil-in-water[6]. On the Norwegian Continental Shelf this limit is set to 30 ppm[24], however an implementation of the Zero Harmful Discharge Policy by the Norwegian government is ongoing. This regulation greatly reduces the dispersed oil limit for the discharge water and additionally aims at decreasing the concentration of the dissolved organics.

2.1.4. Dissolved organics

Certain components of crude oil can be water-soluble. Formation water spends millions of years in contact with hydrocarbons, during which some partitioning from the oil to the water phase may occur. Further transfer of water-soluble crude oil components can take place during the production and processing of fluids due to changes in fluid properties and solubility conditions. Several papers reported the complexity of the dissolved organics found in the produced water[9, 25-26]. Figure 2-3 illustrates the averaged concentration of different organic species in the PW samples from the Norwegian Continental Shelf[27].

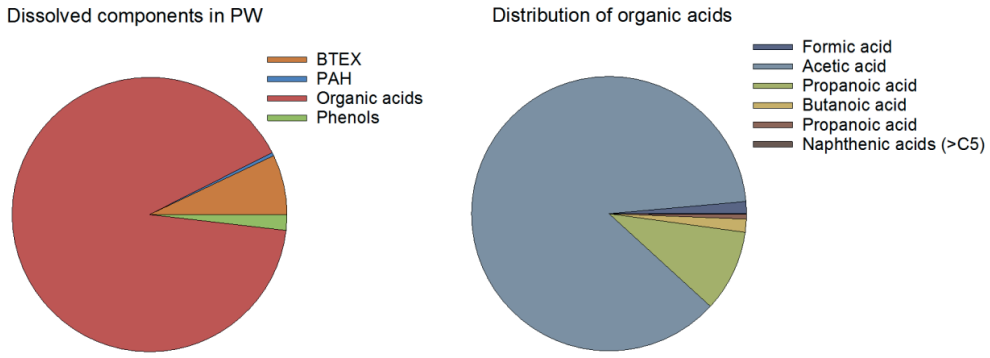

Figure 2-3 Distribution of organic species and detailed distribution of organic acids in PW samples, based on [27]. BTEX – Benzene, Toluene, Ethylbenzene, Xylene; PAH – Polycyclic aromatic hydrocarbon.

The majority of the dissolved components is of acidic nature, mostly short-chained, such as C1-C5 acids. Certain production chemicals, such as scale inhibitors or degreasers can also contribute to the presence of organic acids[9]. Nevertheless, the predominant share of the acidic species in the dissolved components in produced water was confirmed by other reports[8-9]. The acids are much more water-soluble than other non-polar species. This is further enhanced by their low pK_a and the salting-out effect, which can decrease the solubility of pure hydrocarbons, compared to the polar ones[28]. These dissolved components had already been proven to influence the air-water surfaces[29-31] and oil-water interfaces[32].

2.1.5. Production chemicals

Various chemicals are added during the production of crude oil in order to keep control over the process and mitigate issues affiliated with undesired phenomena, such as pipeline blockage or corrosion of metal surfaces. These chemicals include[8]: (1) inhibitors against bacterial growth, corrosion, foam, hydrate formation, asphaltene, scale and wax deposition; (2) de-emulsifiers or flocculants and (3) chemicals for natural dehydration. The type and concentration of the additives varies from field to field. Some of them are water-soluble and can appear in the discharged PW composition. At the Norwegian Continental Shelf, most of the production chemicals are from the “green chemicals” category. It is classified as having no or very minor effect on the natural environment[33].

2.1.6. Dissolved gases

Produced water can also contain dissolved gases, especially CO_2, O_2 and H_2S. Their presence is the effect of bacterial activity or chemical reactions in the PW[6]. The concentration of the dissolved gases is highly dependent on the process conditions (pressure, temperature) and is rather insignificant during the topside PW treatments. However, this may be different if the separation is to be performed in a subsea produced water treatment facility, where the dissolved gas can cause flow assurance problems[34].

2.2. Fate of produced water

Current trends indicate that the production of produced water will keep increasing. Oil producers are required to deal with the gigantic volume of what is now considered a production waste. Presently, the universally accepted practice is to treat PW to a specified level and discharge it to sea or dispose of it in another way, for instance through re-injection into a geological formation. However, in the past years, thanks to the advancement of separation technologies, oil companies found other, more eco-friendly ways of dealing with produced water that can turn this problematic by-product into a useful commodity.

2.2.1. Discharge

As discussed above, the most common way of managing produced water is to discharge it to sea. More than 40% of the total PW volume is disposed into the environment[6]. According to the newest data[27], approximately 75% of the produced waste water at the Norwegian Continental Shelf is dealt with in that way (Figure 2-4).

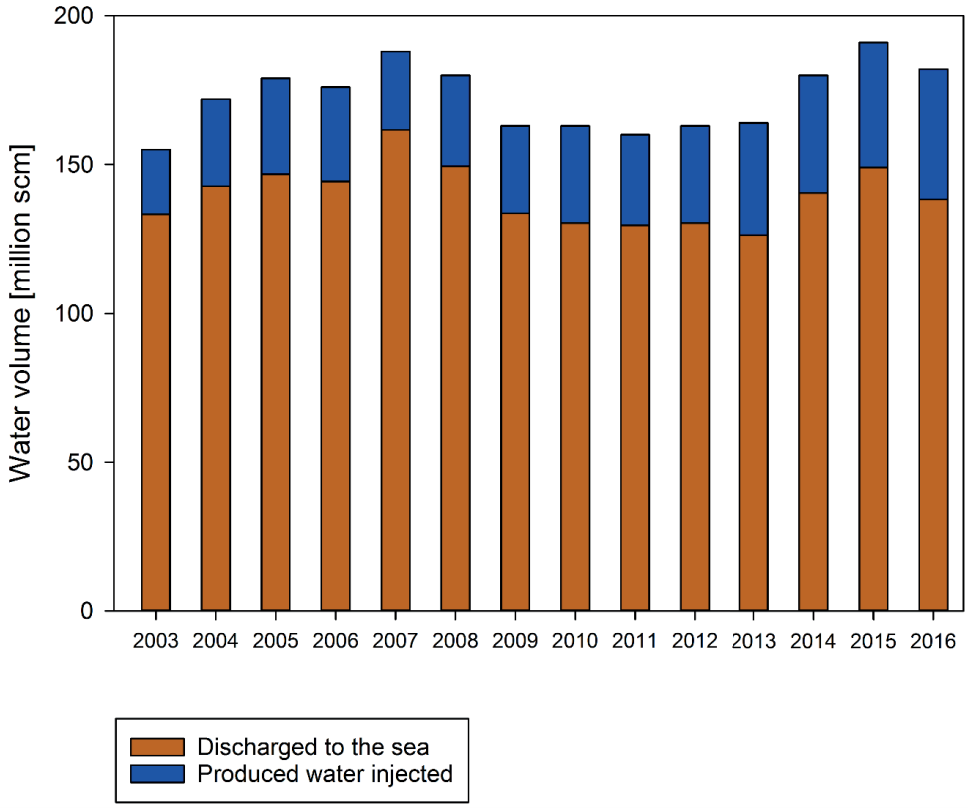

Figure 2-4 Volumes of discharged and reinjected produced water at the NCS. Data based on[27].

Local and international regulations ensure that the amount of harmful products present in the waste stream is minimal, which decreases the potential damage to the marine environment.

2.2.2. Re-injection

An increasingly more popular way of dealing with produced water is to re-inject it to an underground formation, either for disposal or production boosting[35]. In the past, only seawater was used as a pressure support during the secondary recovery stage, however more oil producers switch to re-injection of PW instead, both for environmental and economical reasons[36]. Figure 2-4 also illustrates the slow, but steady increase of the produced water re-injection (PWRI) percentage in the total volume of water produced. Re-injected PW is more compatible with formation water, compared to seawater. This means less risk of scale

formation, H_2S and bacteria growth[34]. In addition, all production chemicals, and dispersed and dissolved oil components are being trapped in the underground geological formation, instead of being discharged into the marine environment. Nevertheless, the injection of produced water has to be carefully managed to avoid production issues including injectivity decline or formation damage. Additionally, PWRI carries an increased risk of reservoir souring due to the abundant presence of carbon sources (dissolved components) and increased concentration of sulphate-reducing bacteria[37]. These microorganisms were identified as a primary source of H_2S production, and therefore are the main cause of reservoir souring.

2.2.3. Reuse

Produced water can also be reused for other purposes, such as irrigation, livestock farming or even drinking water[5, 18]. This, however, is limited to only a few examples, and occurs mostly in onshore operations in countries with water shortage.

2.3. Produced water treatment

The previous sections stressed the need for treating the produced water to certain quality in order to minimize the harm it causes to the natural environment. The processes that aid in meeting these requirements are typically divided into three categories:

- **Primary produced water treatment**, predominantly gravity-based separation, targeting the dispersed oil and suspended solids;
- **Secondary produced water treatment**, such as gas flotation or filtration, focusing on further reduction of the dispersed oil-in-water concentration;
- **Tertiary produced water treatment**, or water polishing step, targeting the smallest oil drops and dissolved components, both organic and inorganic.

The overview of each PWT step is illustrated in Figure 2-5.

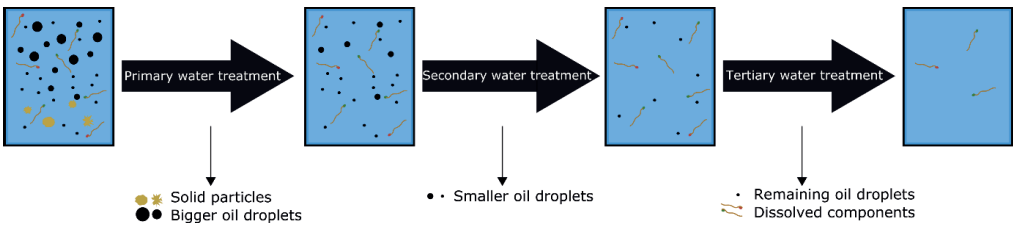

Figure 2-5 Produced water treatment steps and targeted contaminants.

2.3.1. Primary produced water treatment

After a bulk three-phase separation, produced water can contain up to 1000 ppm of oil-in-water and up to 350 ppm of suspended solid particles[38]. The majority of oil droplets are below 150 µm in size[39], while the solid particle size distribution may reach as high as millimetre size[40]. The goal of the primary water treatment process is to reduce the oil-in-water concentration well below 500 ppm and significantly decrease or completely remove solid particles in certain size ranges to avoid settling in process facilities or during re-injection to the formation[36]. Two types of separators are typically used in the primary PWT: gravity settlers and hydrocyclones.

- Gravity separator (skimmer)

Like the three-phase separator, the gravity separator for the produced water treatment utilizes the density difference between the two separated phases (Figure 2-6).

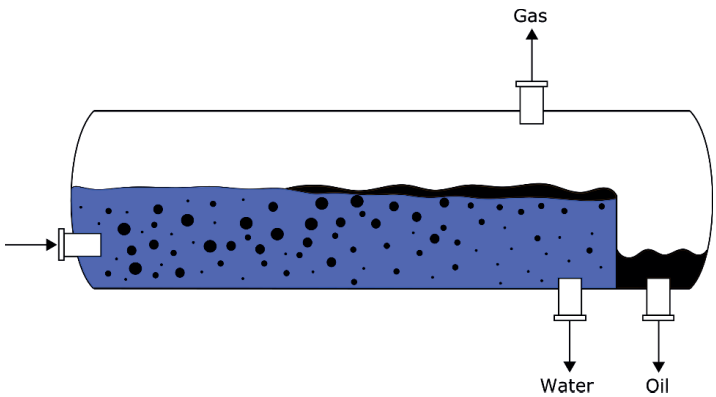

Figure 2-6 Gravity separator for primary PWT.

The contaminated produced water enters the skimmer from one side. As a consequence of the lower oil density, the dispersed droplets start to move upwards and form an oil layer on the top of the water surface. The skimmed oil is collected, typically after passing over a baffle shown in Figure 2-6. The baffle also blocks the flow of the purified water and directs it towards the water outlet. The droplet velocity can be calculated with the Stokes law (Equation 1):

$$v = \frac{\Delta\rho * g * d^2}{18 * \mu} \quad (1)$$

where $\Delta\rho$ is the density difference, g is the standard gravity, d is the droplet diameter and μ is the viscosity of the continuous phase. It can be concluded that the drop size has the biggest impact on the separation rate, as both density and the viscosity of water are affected only marginally by the process conditions (pressure, temperature). The gravity separator is relatively insensitive to the inlet oil-in-water concentration, but it requires high retention times for sufficient separation. Its footprint can be reduced with certain modifications, for instance by introducing plate coalescers that stimulate the growth of the droplet size. These internal plates improve the coalescence process by decreasing the rising distance and capturing droplets on the horizontally inclined plates. As a result, droplets can get in contact with each other and, given enough time, merge into bigger particles which rise much faster. With the addition of plate coalescers, the minimum drop size removed is reduced from approximately 150 µm for the standard gravity separators to 20-40 µm in the modified units[41].

- Hydrocyclone

Hydrocyclones, or enhanced gravity separators, utilize the centrifugal force to remove the dispersed oil droplets from water (Figure 2-7).

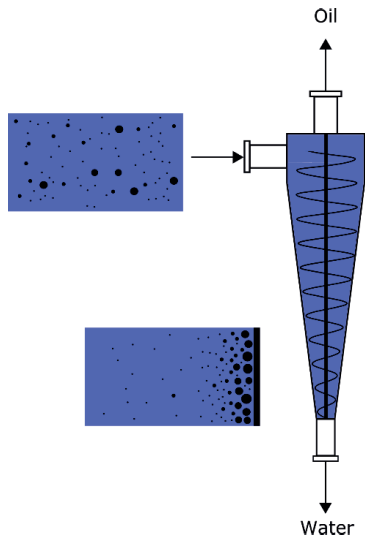

Figure 2-7 Hydrocyclonic produced water treatment.

The produced water enters the separator through a tangential inlet. It creates a vortex that swirls downwards the reducing section with an increasing velocity. The lighter phase is pushed towards the central core of the unit, where the upward reject flow removes the separated

oil. At the same time, the purified aqueous phase is pushed towards the walls of the separator and exits the hydrocyclone from the bottom. Larger droplets are removed in the upper part of the separator, whereas higher centrifugal forces and lower rising distance facilitates separation of smaller particles in the lower part. Unlike gravity separators, hydrocyclones require a minimum pressure of 7 bar in order to obtain high separation efficiencies and effectively remove droplets down to 10-20 μm in size[39]. Their compact size and robustness makes them good candidates for offshore produced water treatment. Cyclonic separation is also often utilized for sand management processes[40].

2.3.2. Secondary produced water treatment

The initial PW treatment usually reduces the oil-in-water concentration to 100-500 ppm and removes the droplets as small as 20 μm in diameter. The level of pollution in the water phase is still too high to be safely discharged and the water quality is insufficient to reach most of the re-injection specifications. The most common technique in secondary PWT is gas flotation, however recently membrane processes are also being considered as a viable option for further treatment of produced water. Both these methods can provide high separation efficiency. However, their performance decreases considerably when the initial oil-in-water concentration exceeds 500 ppm.

- Gas flotation

Gas flotation is a technique that relies on the generation and dispersion of very fine gas bubbles in water. These bubbles attach to the dispersed contaminant and, with increased size and enhanced density difference, rise to the surface, where the pollutant can be removed. Two types of flotation, distinguished by the bubble generation method, are used in the oilfield water treatment: induced and dissolved gas flotation (IGF and DGF, respectively).

In IGF, the gas bubbles are dispersed with either an eductor or by mechanical rotors. In the first type, the flow of the recycled water sucks the gas in the stream and is ejected through a nozzle, creating a jet of gas bubbles. Figure 2-8 shows the induced gas flotation with a hydraulic eductor.

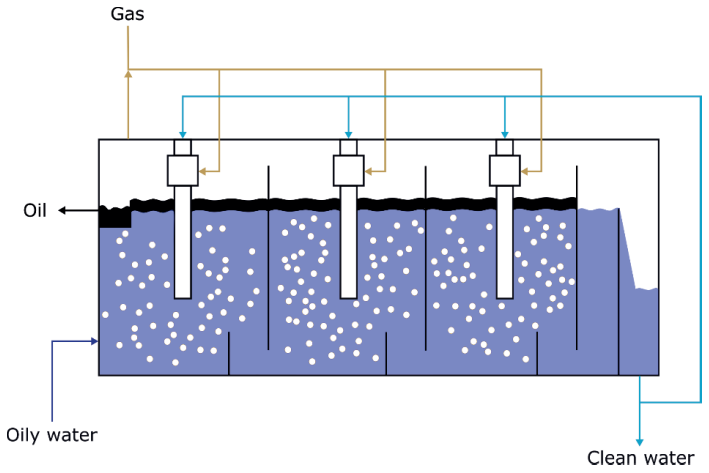

Figure 2-8 Induced gas flotation unit.

In the other type, motor-driven rotors are drawing gas from above the liquid and dispersing it into the water. The bubble size range in IGF is usually between 100 and 1000 µm[42].

The dissolved gas flotation relies on nucleation of bubbles in an oversaturated water or oil phase. For example, part of the clean water is pressurized in the presence of gas in a saturation vessel and re-introduced to the flotation unit, where the decreased pressure forces the gas to break out of the solution in the form of small bubbles (Figure 2-9).

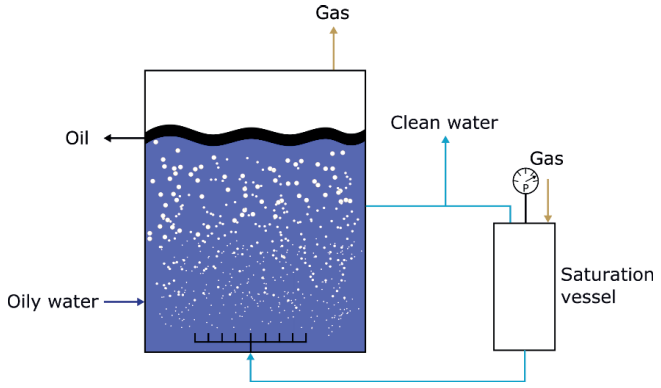

Figure 2-9 Dissolved gas flotation.

The amount of dissolved gas can be boosted by increasing the pressure in the saturation vessel to improve the separation performance. The typical size range of gas bubbles in DGF is below 100 µm[42].

IGF is more frequently used in the produced water treatment. Still, the dissolved gas flotation occurs to some extent in the degasser drums, where the remaining dissolved gas is removed from the water phase by pressure reduction. In both types of flotation, natural gas is commonly used to avoid the presence of oxygen in the process[42]. Flotation can be aided by the addition of flocculants, which increases the size of the dispersed particles and consequently improves the performance of the process. This treatment method can remove up to 95% of the dispersed oil in water and particles down to 5 µm[41]. At this point, the produced water can be discharged to the environment.

- Membrane filtration

Recently, membrane technology (micro- and ultrafiltration) is considered a promising alternative for secondary produced water treatment. This process can reduce the oil concentration in treated water below 5 mg/L and also remove droplets with few micrometres in diameter[43]. In contrast to gas flotation units, membrane treatment is reported to also lower the concentration of the dissolved components[44]. Typically, ceramic membranes are preferred over the polymer type, due to higher chemical, mechanical and thermal resistance. One of the biggest obstacles in the application of this treatment in the PWT is the fouling process. Over time, the membrane pores will clog with residual oil and particles. This will gradually decrease the permeability of the membrane and reduce its performance. Therefore, cleaning and proper maintenance are critical to ensure robustness and efficient separation.

2.3.3. Tertiary produced water treatment

Tertiary PWT, or water polishing step, usually aims at almost complete removal of the dispersed oil and considerable reduction of the dissolved organic and/or inorganic components from the water phase. Various treatments can be applied to obtain this goal[5, 8]:

- Ion exchange (replacement of metal ions);
- Adsorption on activated carbon or synthetic zeolites (removal of dissolved organics);
- Membrane filtration – nanofiltration and reverse osmosis (reduction of salinity and dissolved organics concentration);
- Gas stripping (elimination of volatile components);
- Biological treatment (removal of dissolved organics);
- Extraction with liquid condensate (elimination of dissolved organics).

3. Subsea production and processing

Oil producers are slowly running out of hydrocarbon reservoirs, which are easily accessible with relatively simple technological solutions. The remaining crude oil and gas is typically located offshore, in more remote places (>200 km from the nearest shore) and deeper waters (>2000 m). In addition, the climate conditions of those places are usually more uncertain and extreme. Examples include oil- and gas fields in the Barents Sea or deep-water oil supplies in the Gulf of Mexico and off the Brazilian coast.

Subsea technology is of growing interest in the production and processing of crude oil and gas. Subsea wells, multiphase pumps and seabed separation are currently considered as feasible options for many green and brown oilfields[45]. The application of subsea systems can extend the lifetime of existing fields and increase the overall recovery. Furthermore, partial or complete separation on the seabed can de-bottleneck processing facilities through removal of water. Subsea production also opens the possibility of gaining access to more remote hydrocarbon reservoirs in harsher environments through eliminating the need for manned production platforms. A futuristic vision of a subsea factory is depicted in Figure 3-1.

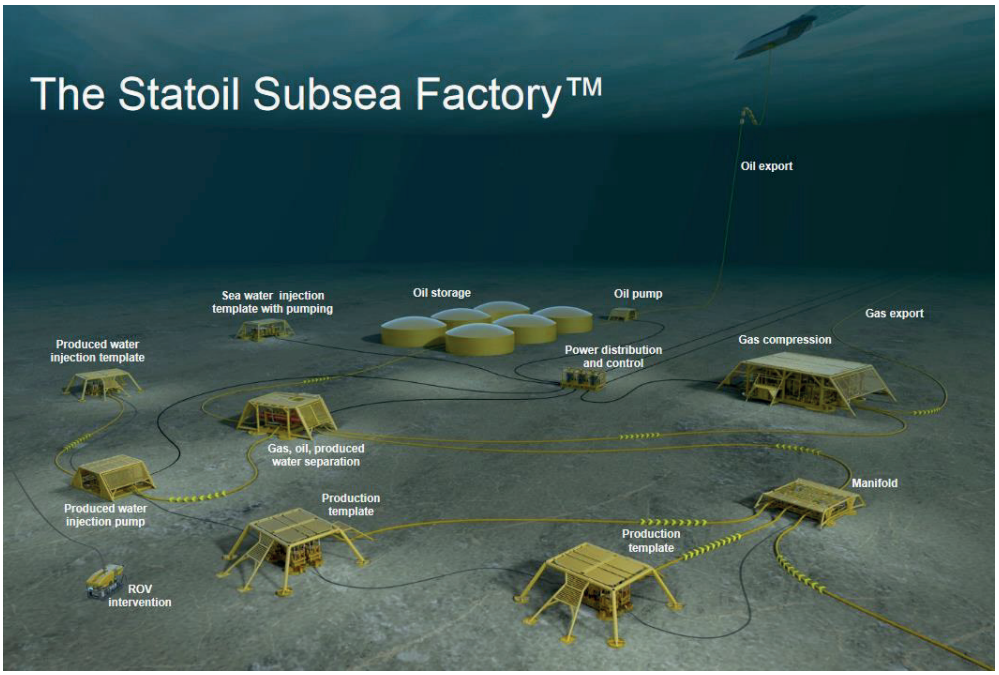

Figure 3-1 The Statoil Subsea Factory™ illustration.

In this system, produced fluids from different templates are combined in a manifold and pumped to a separation module. The gas, after reaching export quality, is compressed and exported. Dewatered crude oil can be stored in seabed tanks or pumped to an oil tanker. The separated produced water finds its way back to the reservoir for production support. The subsea technology differs from the conventional equipment as the process takes place much closer to the well, where the operating pressure and temperature are significantly higher than what is expected topside. Even the most proven solutions need to be requalified for subsea use. Figure 3-2 illustrates the status of maturity for subsea processing technologies.

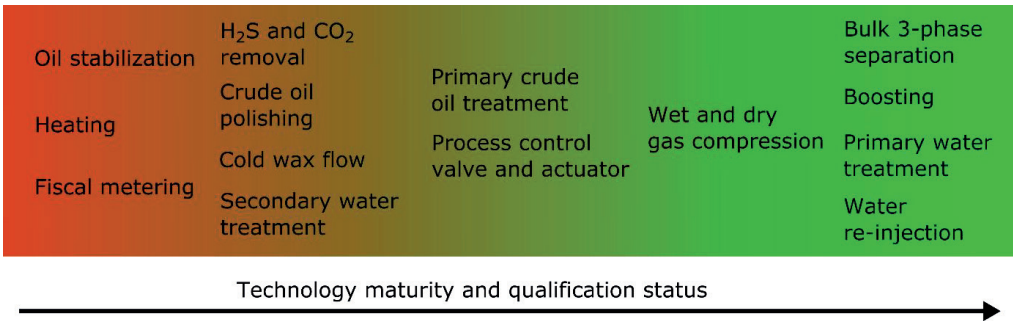

Figure 3-2 Status of maturity for the subsea production and processing technology. Based on[45].

Most of the major separation and transportation technologies are qualified for the subsea applications. Still, several processes, that are crucial during the production of hydrocarbons, require additional development. Further treatment of the produced fluids and processes related to flow assurance are among the most pressing issues to address within the subsea production and processing of petroleum products. Subsea systems are required to be mechanically and operationally robust to avoid frequent maintenance and failure. Major part of the instrumentation is divided into modules for easier installation, replacement and decommissioning. Also for this reason, the subsea processing units are usually much more compact compared to the topside facilities. They must sustain high external and internal pressure, and high temperature gradient between the produced fluids and the surrounding water. The fluid behaviour in the high pressure/temperature conditions will also be different.

Nevertheless, the advantages of subsea treatment may outweigh strict requirements for the processing units. Closer proximity to the well can reduce the wellhead pressure and help stabilize the flow of the produced fluids. In addition, higher pressure and temperature should

facilitate a more effective bulk separation process resulting from the decreased viscosities, increased density difference and avoided issues with asphaltene or wax precipitation. Regarding water treatment, partial or complete removal of water at the seabed offers more compact topside facilities, reduced use of chemicals and decreased backpressure on the reservoir[34]. Subsea-treated produced water will still be pressurized, which lowers the required pumping energy to re-inject it. All in all, the idea of a complete subsea factory, envisioned by several oil producers, should lead to reduced CAPEX, increased hydrocarbon recovery and lower environmental footprint.

4. Fundamental phenomena involved in separation processes

Like many industrial processes, the produced water treatment is quite complicated, and is influenced by various parameters. Emulsions, such as produced water, are inherently unstable and given enough time they will phase-separate. During the production process, however, the residence time of fluids in separators is limited, therefore fast and efficient separation is critical. The efficiency of separation processes can be broken down to several crucial factors. On the one hand, the design of the separator, fluid dynamics or physical properties of the phases are extremely important when considering the performance of the process. On the other hand, fundamental phenomena occurring in gravity separators, hydrocyclones and gas flotation units will also have great influence on the efficiency of the produced water treatment. While many researchers focus on the process parameters, such as liquid recycle percentage or gas-to-liquid ratio, the fundamental part of separation is often overlooked. Understanding the interactions between droplets, and droplets and bubbles in crude oil systems is usually more elusive due to the extreme complexity of the fluids involved. Nevertheless, these interactions are important and can determine the performance of the entire produced water system.

The following sections will describe mechanisms and important aspects of the **dispersion stability**, **oil droplet coalescence** and **bubble-drop interactions**. These phenomena were identified as crucial during the most common produced water treatments, like gravity or enhanced gravity separation, and gas flotation.

4.1. Dispersion stability

Dispersions consist of at least one phase dispersed in another continuous phase. Dispersions are thermodynamically unstable. Therefore, in the absence of any stabilizing mechanisms, the involved phases will separate. Basically, their stability depends on the attractive and repulsive forces, and their relative magnitude, and other important factors, including the dispersed particle size and the physicochemical properties of the phases. Especially the presence of surface-active molecules contributes to the stability of dispersions through increased repulsion between the dispersed particles[46]. The presence of ionic surfactants will give rise to electrostatic repulsions, whereas steric repulsion will often be the effect of polymers or non-ionic surfactants at the interface. These effects, together with other molecular interaction

forces, are described further in the next section. Dispersions can be destabilized through gravity forces (creaming or sedimentation), flocculation, coalescence or Ostwald ripening.

4.2. Droplet coalescence

Merging of two fluid particles, or coalescence, is one of the main mechanisms of droplet growth in dispersed systems. Together with particle break-up, it is relevant to many industrial processes involving multiphase flow. The equilibrium between the two phenomena will govern the size distribution and the stability of the dispersed phase, which in turn will determine the properties of the dispersion and can influence the characteristics of the flow.

There are several theories proposed for the coalescence process. The most popular and generally accepted is the **film drainage model**, developed by Shinnar and Church[47]. It states that the coalescence of two fluid particles is limited by the drainage of the thin film of the continuous phase, formed between the interfaces. Thus, coalescence is usually divided into three subprocesses: **collision of particles**, **drainage of the thin film** and **film rupture**[48]. These stages are depicted in Figure 4-1.

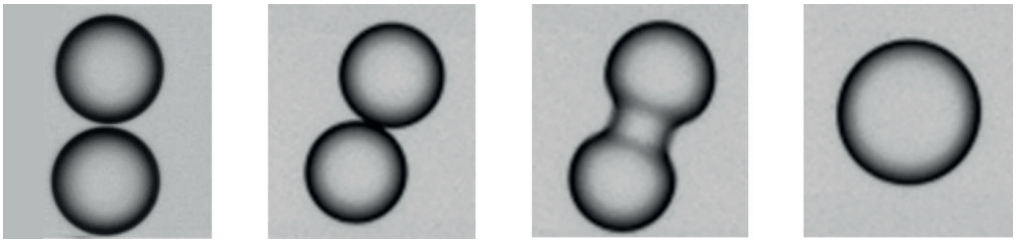

Figure 4-1 Coalescing oil droplets. From left to right: Pending collision between drops, film drainage, film rupture and newly formed drop.

The collisions between fluid particles are frequently a function of the flow, however they can occur through different mechanisms. Bubbles or droplets can collide with each other via fluctuating turbulent velocity of the continuous phase, for example induced by mixing. Another mechanism involves local velocity gradients, where the colliding fluid particles are in two different, high- and low-velocity fields. Two droplets can also encounter each other when captured by a single turbulent eddy. Lastly, fluid particles of dissimilar sizes will experience various buoyancy forces. Therefore, they will have different creaming (or sedimenting) velocities that can lead to a collision. If dispersed bubbles or droplets are small enough, their

thermal motion (Brownian motion) should also be considered as a process leading to collisions.

The force upon collision is determined by the hydrodynamic characteristics of the flow, in which the droplets are moving. If this force is too large, the droplets may simply bounce off each other. However, if the fluid particles stay in contact after the collision, a thin film of the continuous phase is formed. Due to the thickness of this film, certain molecular forces acting on it are no longer negligible and become of similar magnitude as the hydrodynamic forces. These **surface forces** are usually a combination of van der Waals forces, electrostatic repulsion, steric and hydrophobic interactions.

The van der Waals forces are averaged intermolecular dipole-dipole interactions, consisting of three major contributions: (1) Keesom force, between two permanent dipoles; (2) Debye force, between a permanent and an induced dipole; (3) London dispersion force, between two induced dipoles. These forces are in most cases attractive and relatively short-range. **Electrostatic repulsion** is effective when the electrical double layers from two surfaces start to overlap each other. It arises from the presence of negatively or positively charged ions at the vicinity of interfaces. Both air-water and oil-water interfaces typically exhibit negative charge due to preferential adsorption of hydroxyl ions[49-50]. Electrostatic repulsion can occur through the presence of ionic surfactants. The extent of the electrical double layer is reduced by the addition of an electrolyte. **Steric interactions** are typically observed in systems with non-ionic surfactants or polymers. The repulsive effect takes place through the decrease of entropy and excluded volume effect during confinement of polymeric chains. Attraction may occur when the polymers are in poor solvent or when the two opposite ends of molecules adsorb to another approaching surface. Besides, the presence of either type of surfactants may invoke additional interfacial effects. First, upon collision and onset of film drainage, the motion of the liquid disturbs the interfacial distribution of surfactants, creating a concentration gradient. As a result, molecules in the higher concentration region will transfer towards the regions of lower concentration, creating a flux in the opposite direction of the film drainage process. This so-called **Marangoni effect** can retard the film thinning rate[51]. Secondly, the interfacial concentration gradient also causes a flux of solvent into the region with high concentration through the **osmotic effect**. This is caused by the differences in the chemical potential and can occur in systems with both ionic and non-ionic surfactants. In

addition, the surface-active components can influence the rheological properties of the interface, causing further changes in the film drainage process[52]. The origin of the **hydrophobic surface forces** is still elusive. In general, the literature sources agree that they can be divided into at least two categories[51]: attraction caused by the presence of the dissolved gas, and the ordering of water molecules at the vicinity of hydrophobic surfaces. The dissolved gas molecules in the water phase will preferentially adsorb at hydrophobic surfaces, which can lead to the formation of nanobubbles[53]. Upon approach, these nanobubbles can form gaseous bridges, giving rise to an attractive force that can facilitate coalescence. The removal of the dissolved gases from the water phase was reported to significantly reduce the attraction between hydrophobic oil drops and result in the formation of very stable surfactant-free oil-in-water emulsions[54-55].

Finally, the droplets have to stay in contact sufficiently long for the film to be drained to a critical thickness and rupture. At this critical thickness, the attractive forces start to dominate and destabilize the film, causing it to break. The critical thickness depends on the fluid parameters and the drop size; nevertheless it should be in the range of tens to hundreds of ångströms[56]. The drainage time is usually orders of magnitude higher than the rupture time[57].

It has been shown that only a fraction of collisions results in merging. The remaining drops have too high approach velocity that results in bouncing-off, not sufficient energy to overcome the energy barrier or shorter contact time than drainage time. Therefore, the film drainage and contact times can be considered as one of the rate determining steps of the coalescence process. There are many mathematical models for calculating contact and drainage times[48]. Their applicability depends greatly on the dispersion properties (fluids, drop sizes, deformability of particles and mobility of interfaces) and flow characteristics.

4.3. Bubble-droplet interactions

Interactions between gas bubbles and liquid droplets requires the presence of at least three phases – two immiscible liquids and a gas. In flotation units, the gas is dispersed in order to remove the droplets or particles suspended in water. Like the coalescence process, the interactions of gas bubbles and droplets can also be divided into three separate parts: **encounter** (collision), **film drainage** and **rupture** or **detachment** (Figure 4-2).

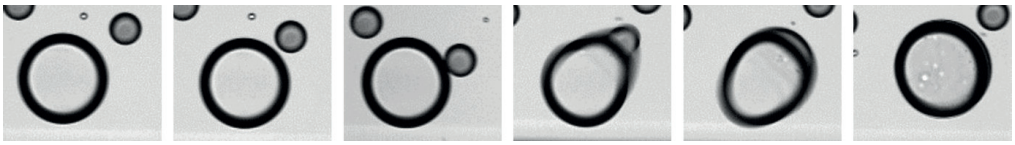

Figure 4-2 Snapshots of a droplet spreading around a bubble. From left to right: approach (first two pictures), contact, thin film breakage, spreading and an oil-coated bubble.

A collision between a droplet and a bubble can occur through couple of different mechanisms[58]. The first is due to gravity action and the density difference between the bubble and the droplet. The less dense bubble will rise faster than the oil drop with higher density. The latter will appear to fall on the surface of the bubble and follow the water streams around it, resulting in quite low encounter efficiency. In the interception mechanism, the movement of fluid particles is due to an external flow, thus the densities do not play a significant role. However, during gas flotation both mechanisms frequently occur simultaneously. In general, a bubble rises 10 to 100 times faster than an oil droplet. Inertial impact happens when the droplet's inertia is high enough for it to deviate from the water streamlines, created by a bubble. This can take place, for instance, during centrifugal flotation. The last mechanism describes the behaviour of bubbles and droplets in turbulent eddies. Both gas and oil (in most cases) have lower density than the continuous water phase, so the bubbles and drops tend to locate themselves in the centre of a turbulent eddy. Consequently, this mechanism has a very high encounter efficiency.

Once encountered, a thin liquid film is created between the drop and the gas bubble, and needs to be drained before the oil droplet can attach to the gas bubble. The rate of drainage is determined by the same surface forces as described in the section above. The resulting attachment is governed by the spreading (S_{ow}) and entry coefficients (E_{ow}) defined as[59]:

$$S_{ow} = \gamma_{wg} - \gamma_{ow} - \gamma_{og} \quad (2)$$

$$E_{ow} = \gamma_{wg} + \gamma_{ow} - \gamma_{og} \quad (3)$$

where γ_{wg} is the surface tension of water against gas phase, γ_{ow} is the interfacial tension between oil and water, and γ_{og} is the surface tension of oil against gas. If the value of the spreading coefficient is positive, the spreading of oil on gas (i.e. removing water-gas interface) will be favourable from a thermodynamic point of view. A negative entry coefficient means that the oil droplet will not be able to enter the bubble surface, which can occur in systems

with high surfactant concentrations. In gas flotation the spreading coefficient should always be above zero.

The possible outcome of droplet-bubble encounter also greatly depends on their size ratio. Some possible configurations of droplet-bubble attachment are depicted in Figure 4-3.

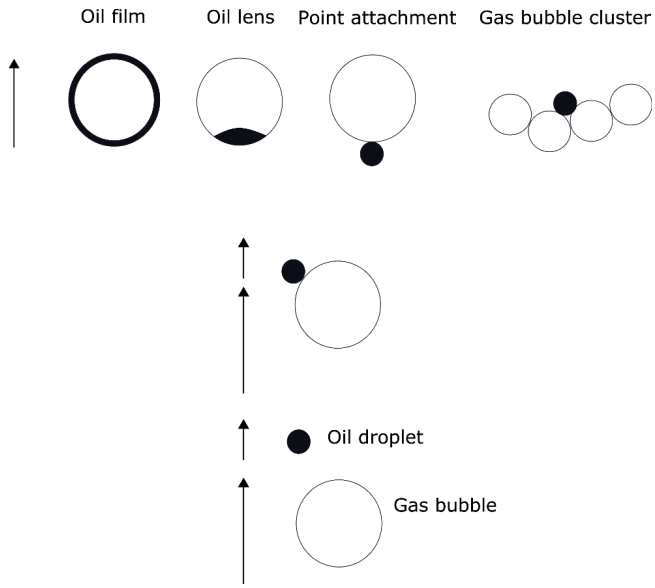

Figure 4-3 Mechanisms of oil droplet encounter and capture by gas bubbles.

Full encapsulation occurs when a droplet, upon contact with a gas bubble, spreads around it and forms an oil film on the surface of the bubble. This provides the most stable bond between the oil and gas, and minimizes the detachment probability. In addition, other droplets are likely to coalesce with an oil-coated bubble. If the droplet is too small for full encapsulation, the oil can form a lens inside the bubble, however this aggregate is less resistant against turbulence, often present in a flotation unit. When the spreading coefficient is negative, or the drop is significantly smaller than the gas bubble, the drop can attach to the surface of the bubble or become entrapped in the hydrodynamic wake of a rising bubble. This, however, provides a very weak bond between the bubble and the drop, and can very likely result in detachment. Another mechanism occurs when bubble clusters, stable against coalescence, form a “pillow” that physically lifts dispersed droplets. In the dissolved gas flotation, gas bubbles can also nucleate on the surface or within the droplets. This, however,

requires a significant pressure drop, and at the same time much finer gas bubbles are produced, which can aid in the separation process[60].

Like the coalescence process, the efficiency of the bubble-droplet aggregation is determined by the contact and drainage (induction) times. If the average contact time is shorter than the time needed for the film to drain, the oil drop will not attach itself to the gas bubble. This will reduce the performance of gas flotation. The rupture time, or in this case coverage time, is expected to be more significant, compared to the coalescence process[58].

4.4. Fundamental aspects of produced water treatment

In general, the coalescence of crude oil drops proceeds in a similar fashion as described above. When the droplets collide, a thin film is formed. It must be drained in order for the droplets to merge together. As the process often occurs in high-salinity water, the electrostatic repulsion is rather insignificant. However, certain components of crude oil are surface-active and can diffuse to the oil-water interface. These molecules can affect the coalescence process in various ways, for instance by slowing down the drainage through the Marangoni effect or changing the viscoelastic properties of the interface. The changes in the water pH and temperature may result in diffusion of different components to the oil-water interface or even their partitioning to the water phase[61]. The type of the water-soluble components strongly depends on the crude oil[30]. Besides, the stability of drops against coalescence may be further affected by the presence of other dissolved and dispersed components in the produced water[62], such as small particles, low-molecular organic species, multivalent inorganic ions or production chemicals[63]. It should also be noted that the crude oil droplets in the produced water stream are exposed to some level of turbulence, which may induce their break-up.

The interactions between gas bubbles and oil droplets may be affected in the same way. The crude oil composition plays an important role in the film thinning rate[64]. Moreover, the adsorption of the surface-active compounds at the oil-water interface influences the film drainage and oil attachment to bubbles. The high salinity does not only reduce the electrostatic repulsion, but also decreases the coalescence between bubbles[65]. At the same time, the dissolved components present in the water phase will adsorb at the air-water interface, causing additional changes to the system. The adsorption at the bubble surface will

be affected by the water composition and the type of the adsorbed molecules[29]. As a result, bubbles may be more or less prone to coalesce with each other. A different size distribution of bubbles can greatly impact the bubble-droplet interactions. Overall, the underlying mechanisms of the gas flotation process were shown to have an effect on the oil removal efficiency[66], however still require more fundamental understanding.

4.5. Methodology for studying fundamental interactions

Several techniques can be utilized to study the interfacial behaviour of droplets and bubbles. Many of them are well established and have been used for decades, while some are relatively new and not yet very widespread. Their applicability and usefulness often depend on the studied system and the expected information from the experiments.

One of the most common method of assessing dispersion stability is **microscopy**. A sample of a previously prepared dispersion is put on a glass slide or in a cuvette, and analysed with a microscope. A camera connected to the microscope is used to capture the images of the dispersed particles. Later, these pictures can be processed with an image analysis software to obtain average drop sizes or drop size distributions. Due to its simplicity and versatility, this method is used quite often to analyse drop size distributions of both oil-in-water[67] and water-in-oil[68] emulsions in petroleum-related research. This, however, provides only the information after the process, for example after the addition of a de-emulsifier, and gives no insight about the *in-situ* de-emulsification process. Optical analysis can also be used to study the behaviour of dispersed phases in bubble columns[69-70]. Since the volumes and bubble sizes are usually much larger, a microscope is not necessary, and the pictures can be taken with a simple camera.

The measurements of drop size distributions were improved with the introduction of **light scattering techniques**. They work on the principle that particles of different sizes scatter light at specific angles. The intensity of the scattered light can later be transformed into a size distribution by using the Fraunhofer Approximation or Mie Theory. Contrary to microscopy systems, light scattering instruments can be coupled to a flow system (for example, a stirred tank) and allow to directly follow the dynamic changes of drop sizes during the experiment. As a result, the system can be characterized not only by the size distributions, but also the kinetics of the coalescence and breakage phenomena. Recently, light scattering methods are

used for studying the effect of various parameters on the oil droplet size distribution in water, such as mixing time and speed[71-72], volume fraction of the dispersed phase[73], presence of EOR chemicals[67] and water composition[74]. Nevertheless, that type of instrumentation describes the bulk behaviour of dispersions and gives little information about the individual drop behaviour.

Surface force apparatus (SFA) is a group of extremely sensitive instruments, designed to measure interaction forces at very small distances (sub-nanometre). They can be used to measure all kinds of fundamental interactions between surfaces, such as van der Waals attraction, electrostatic and steric repulsion, capillary and adhesion forces or hydrophobic interactions[75]. One example from the SFA group of instruments is atomic force microscope (AFM). It scans a surface with a sharp, flexible cantilever, which movement is detected and converted into the force of interaction. It allows measurements of not only the mechanical properties of a surface, but also the interaction forces between a surface and the cantilever tip. The precision of the instrument is high enough to measure the forces in the Ångström range. Among other things, it was used for the measurement of the van der Waals forces[76] and hydrophobic interactions between surfaces in water phase[77-78].

Interfacial properties of single drops or bubbles can be studied with **drop tensiometers**, like pendant drop or spinning drop tensiometer. Both techniques rely on the video analysis of the drop shape. In the pendant drop method, a drop is suspended from a capillary, immersed in a bulk phase. The deformation of the drop depends on its weight and interfacial tension (IFT). With the known volume and densities of both phases, the dedicated software can convert the drop shape into a value of interfacial tension through Young-Laplace equation. In addition, one can introduce oscillations to the drop volume, which allows measurement of the viscoelastic properties of the interface. In spinning drop tensiometry, a drop is suspended in the centre of a rotating capillary as a result of the centrifugal force. The elongation of the drop is determined by the interfacial tension, rotation speed and physical properties of the phases. By knowing the last two, the IFT can be calculated with Vonnegut or Young-Laplace approach. The spinning drop tensiometers are used for measuring extremely low values of the interfacial tension (below 1 mN/m), whereas pendant drop tensiometers are more precise in the higher ranges of the IFT. Both methods are often employed in petroleum research[79-82], however they

can only be used to study the interfacial behaviour of single drops and not interactions between them.

A setup similar to the pendant drop apparatus may be used to follow the **interactions between a droplet and an interface**, both in liquid-liquid[83-84] and gas-liquid systems[85]. The droplet is generated through a capillary and once released, rises (or falls) to an interface. After sufficient time (i.e. drainage time), the thin film breaks and the droplet merges with an interface. The entire experiment can be recorded with a camera, which allows to determine the drainage time. Further modification of this setup included adding another capillary to generate two similar drops simultaneously, and following their coalescence[86]. Such a setup can be utilized for conducting coalescence experiments between two droplets[87], bubbles[88] or a droplet and a bubble[64]. While the aforementioned techniques allow investigating interactions between single drops in a highly controlled way, the experimental environment is quite static. As a consequence, the time scale of the results may differ significantly from a process occurring in dynamic flow conditions.

Recently, a new **microfluidic** methodology has been proposed as an alternative tool to study the emulsion stability. This will be described in detail in the following chapter.

5. Microfluidics

In the past several years, miniaturization of processes related to the biological and chemical research fields has become increasingly popular. The obvious advantages of smaller footprint and cost of instrumentation, together with the ability to study the fundamental, but equally important aspects of certain processes, are just some qualities sought after by researchers both in the academic and industrial circles. For more than 20 years now **microfluidics** has played a key role in the popularization of microstructured devices.

Microfluidics deals with the control of fluids in channels with at least one dimension in the micrometre size range. The flow in the channels can be manipulated and monitored with internal sensors and valves or by external auxiliary equipment. Additionally, microfluidics is also concerned with the development of microsystems, composed of small channels and miniaturized, integrated devices. The possibility of incorporating various tools in one device gave rise to the name 'Lab-on-a-Chip' (LOC). At the same time, it is possible to couple microfluidic devices with more conventional techniques, for instance spectroscopy or chromatography instrumentation. Depending on the application, microfluidic devices can be made out of glass, silicon, polymers, paper or even metals with the use of various manufacturing techniques, e.g. etching, deposition, injection moulding or lately also 3D printing[89].

Microfluidic devices introduced several improvements, compared to the conventional bench instruments, such as:

- High heat and mass transfer rates, thanks to the increased area-to-volume ratio;
- Significantly reduced sample and waste volumes;
- Decreased analysis time and cost per sample; increased reproducibility;
- Possibility of visualization of the desired phenomena;
- Less troublesome at demanding experimental conditions (high pressure, high temperature).

At first, the application of microfluidics was limited to the chemistry field, where the low volumes of the required reagents, shorter reaction time and high sensitivity were seen as great improvements over the conventional methods[90]. However, lately researchers in other disciplines, such as biomedicine, cytology, nanotechnology and surface science, discovered

that the microfluidic technology can be utilized in their respective fields as well. Both the benefits of using microfluidics and the recent progress in the device manufacturing process were crucial in the process of popularizing the technique.

One of the subcategories of microfluidics is droplet-based microfluidics. It is concerned with creating discrete volumes of one or more phases in another, granted their mutual immiscibility (Figure 5-1).

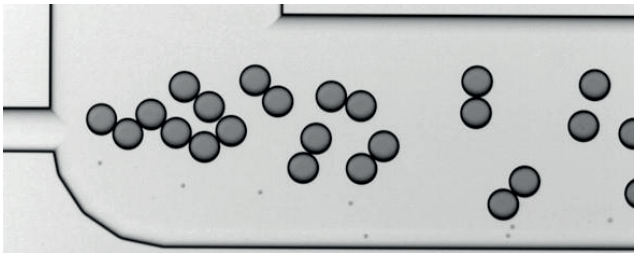

Figure 5-1 Illustration of oil droplets in a continuous water phase.

Droplet microfluidics offers certain advantages that are beneficial to several research fields. The flowing dispersed drops can easily be manipulated inside the microchannels, for instance through sorting, merging, splitting, mixing or trapping[91]. Small volumes of drops, together with the characteristic for microfluidics enhanced mass and heat transfer, and mixing within the drop, make it attractive for chemical analysis and reactions[92]. These features are also utilized in applications related to emulsion science[93], where quick diffusion of surface-active molecules to the interface allows working in quasi-equilibrium conditions within very short timescales. In addition, the continuous generation of monodisperse droplets allows parallelization and high-throughput analyses.

5.1. Microfluidics in emulsion science

The application of droplet-based microfluidics for investigation of dispersions is quite recent. However, being a very versatile method and offering high degree of control over dispersions at a high rate, it became an important tool for conducting systematic studies on emulsions. Due to the miniaturization aspects and the development of high-speed imaging, it is possible to probe the behaviour of micron-sized droplets and on a very short timescale, which is often the case in many industrial applications. In addition, the number of generated droplets per unit time allows obtaining statistically relevant results faster than the standard methodology.

The microfluidic studies on emulsions can be generally divided into three separate categories: emulsification, destabilization and probing interfacial properties[93].

In conventional methods, a dispersion is created through adding energy (e.g. mechanical mixing or turbulence during flow) to the system, composed of at least two immiscible fluids. In microfluidics, the droplets are most commonly created as a result of shear stress exerted by the flow of the carrier fluid. The flow characteristics and fluid properties are often described with a dimensionless capillary number (Equation 4):

$$Ca = \frac{\mu v}{\gamma}, \tag{4}$$

where μ is the viscosity of the continuous phase, v is the linear velocity and γ is the interfacial tension between both phases. In microfluidics, the value of capillary number ranges between 10^{-3} and 10^{1} [94]. There are three main channel geometries that are used to generate droplets[94]: cross-flow, flow focusing and co-flow (Figure 5-2).

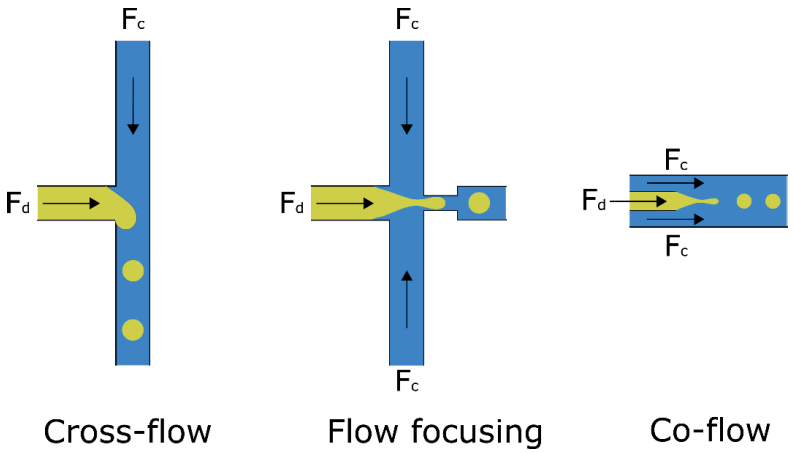

Figure 5-2 Main methods of droplet generation in microfluidic channels. F_c and F_d are the flow rates of the continuous and dispersed phases, respectively. In most cases F_c is higher than F_d.

In the cross-flow regime, droplets are created in a perpendicular T-junction, where the two phases meet. The flow-focusing method for droplet generation relies on squeezing the dispersed phase by two counter-flowing streams of the continuous phase. In the co-flow design, all phases flow in the same direction and droplets are formed through either dripping or jetting regimes. All of the mentioned geometries ensure high monodispersity of the produced droplets. The size and droplet production rate is mostly controlled by the flow rates

of the phases, however other parameters, such as physicochemical and interfacial properties of the phases or channel dimensions also play a role[95]. Consequently, the number of produced droplets may vary between a few to tens of thousands per second.

As discussed before, one of the main destabilization mechanisms of emulsions is coalescence. This phenomenon has been the topic of many microfluidic-based studies, which underlines the progress of microfluidics in this field. Generally, droplets can be merged with passive or active approaches. Passive fusion occurs through collisions, caused by the droplet velocity differences. These can be the result of either drop size differences[96], channel restrictions[97] or simply local velocity gradients in the channels, induced by collisions or other coalescing drops[93]. Active merging is most commonly obtained by subjecting drops to an electric field. The so-called electrocoalescence can provide precise and highly controllable fusion between droplets and has been widely investigated with regard to many various aspects of the process, such as strength[98] and type[99] of the electric field, electrode design[100] or drop size[101]. Interestingly, electric field in digital microfluidics is used for very precise control of the movement of drops inside the channels in order to mix, separate or store them[102]. Other types of active fusion include localized heating[103] or changing the quality of a solvent[104]. The coalescence in both water-in-oil[105-106] and oil-in-water[107-108] systems has been quite extensively investigated with microfluidic systems. Moreover, microfluidics was used for determining the stability of gas bubbles in the continuous water phase[109-110]. Merging of drops was commonly described by parameters such as coalescence frequency, rate and time[95, 111-112]. However, due to the *quasi* two-dimensional nature of channels, the droplets are often squeezed between the top and bottom part of the channel, and consequently the timescale of the studied events may differ significantly from real processes[113]. Regardless of that, the observed trends should remain similar.

The interfacial properties of dispersions are extremely important for understanding their stability. Due to the high area-to-volume ratio in microfluidic systems, the interfacial equilibrium is achieved much faster, compared to the conventional methods. This is of importance for evaluating the interfacial tension and rheology, both of which depend on the interfacial mass transfer kinetics. Microfluidic tools proved to be useful in that regard as well[114-117].

Altogether, droplet microfluidics has recently emerged as a tool for systematic studies of interfacial properties and behaviour of dispersions, both foams and emulsions. Many researchers, however, focused on the work with model systems. They are often too simplified to be related to real-life, industrial applications, for example in the petroleum industry.

5.2. Petroleum-related applications of microfluidics

As it was mentioned before, crude oil is an extremely complex fluid, frequently with an origin-specific composition and complicated interfacial behaviour. For this reason, it may be difficult to draw general conclusions from even very extensive research with many crude oil samples, and it is often necessary to perform experiments on a specific sample. A simple and fast tool with small footprint, such as microfluidics, can be of interest for many analytical and research applications within the petroleum industry[118]. In recent years, one could observe an increasing number of research papers and technological solutions, reported in this field[119-121]. The literature reported to this date was published mostly in the last ten years and focuses around three main aspects of crude oil-related research: **fluid analysis**, **oil recovery** and **fundamental aspects of separation processes**.

Based on the advantageous features of microfluidics, like low amounts of sample and waste, quick measurement times and high repeatability, it is potentially a good candidate to become an alternative or even replace some of the conventional methods for analysing petroleum fluids. First, microfluidic systems were applied in connection to PVT (pressure-volume-temperature) and VLE (vapour-liquid equilibrium) measurements[122-123], important for knowing the phase behaviour of produced fluids. With these methods, it was possible to reduce the long equilibration time from hours to minutes, due to the efficient mass transfer rate. A similar solution was also used for measuring gas-oil ratio (GOR) of petroleum samples[124], where it ensured accurate measurements at quickly reached equilibria. Other examples include measurements of pressure-temperature phase diagrams[125], and dew[126] or bubble points[127]. Other parameters that were studied with microfluidics were diffusivity and miscibility, both being of importance to oil recovery processes. For instance, during heavy oil recovery a solvent can be injected in order to reduce the viscosity of the oil thus improving the recovery. This process will depend on the diffusion rate of the solvent to bitumen. This can be studied with a microfluidic setup presented by Fadaei et al.[128]. Optionally, carbon dioxide can be used for the viscosity-reducing effect. Its diffusion in bitumen[129] and

minimum miscibility pressure[130] was also studied with miniaturized systems. Finally, one of the most important aspects during crude oil production is precipitation. Most commonly, this occurs due to changes in the pressure, temperature or fluid composition. The information about the extent and conditions facilitating precipitation in the produced fluids is vital for flow assurance. Compared to the time- and reagent-consuming conventional protocols, the microfluidic precipitation of asphaltenes is fast, economic and repeatable[131-132]. The deposition of asphaltenes in porous media can also be investigated through microfluidic means[133]. Moreover, changes in the temperature may cause precipitation and agglomeration of wax in crude oils. For this reason, crude oils are often characterized, among other things, by the wax appearance temperature (WAT). Molla et al.[134] presented a microfluidic, pressure-based technique for measuring WAT and the results were comparable with the industry-standard method of cross-polar microscopy. The new method had a smaller footprint and was operator-independent, which are great improvements. Other petroleum-related examples involved extraction of certain fractions of crude oil with hexane[135] or assessing the boron concentration in the produced water samples[136].

Due to the transparent fabrication materials and channel sizes, microfluidics became a useful tool for visual investigation of oil recovery processes. The pore sizes inside the reservoirs are often of similar scale to what can be fabricated in microfluidics. Moreover, as argued by Lifton[120], the new fabrication methods, like 3D printing, can provide an inexpensive and quick way to reproduce very complex real-life reservoirs. For these reasons, the microfluidic technique is a promising new methodology for studying pore-scale phenomena that occurs during recovery processes. In addition, easier cleaning and re-use possibilities makes it a viable candidate for screening tests. The so-called Reservoir-on-a-chip is quite widely used to study common oil recovery techniques, such as water/surfactant[137-138], polymer[139] or foam flooding[140-141]. Furthermore, research on heavy oil extraction can be assisted with microfluidics. Detailed and systematic studies on alkaline flooding or steam-assisted gravity drainage (SAGD) were reported by several research groups[142-144]. Microfluidic-based investigations can also provide proof-of-concept for new, promising ideas to improve oil extraction. Examples may include nanofluid flooding[145] or nanoparticle-stabilized foams for enhanced oil recovery[146].

The fundamental aspects of petroleum-related separation are a significantly less explored topic within microfluidic research. Only a couple of papers reported the use of actual crude oil products in their separation-oriented studies. Mostowfi et al.[147] developed a microfluidic technique for assessing the stability of thin films in emulsions, prepared with diluted bitumen. Among other things, their system was used for systematic studies on the effect of the de-emulsifier concentration on the thin film stability. Another example was the work of Morin et al.[148], who introduced a method to study the viscoelastic properties of the crude oil-brine interface. In addition to different crude oil and water compositions, they were also able to vary aging times and flow conditions during the measurement. A recent paper from Nowbahar et al.[149] focused on the coalescence of water droplets dispersed in diluted bitumen. They followed the destabilization kinetics of the water-in-oil-emulsion upon addition of different de-emulsifiers. Other authors presented solutions that could also be applied in the petroleum research, however the reported work involved only model components. This included studying phenomena such as gas-liquid separation[150], CO_2 absorption[151-152], liquid-liquid extraction[153] and coalescence of oil drops in water[95, 111]. The latter contribution constituted the foundation for part of the work presented in this thesis.

6. Experimental techniques

6.1. Microfluidics

One of the deliverables of this project was to design and assemble a microfluidic platform in the Ugelstad Laboratory. In addition to the experimental work, related to studying fundamental aspects of separation, the setup should also allow working with other projects that are in line with the research scope of the group. First, a thorough literature review was performed in order to identify the required parts for the new setup. It was revealed that the entire platform can be divided into four main components: an **inverted microscope**, a **high-speed camera** with an appropriate light source, a **flow setup** and **microfluidic chips** with all the necessary parts providing a fluidic interface between the flow setup and the chips. Inverted microscopes are often used in microfluidics, as the space above the observed element is occupied by the tubing, which can obscure the field of view. High-speed imaging (>1000 frames per second) is frequently required to visualize the fast-occurring phenomena inside the microfluidic chip. This is a consequence of very small channels. The flow of the fluids in the channels has to be easily controlled and monitored by the flow setup with precise syringe pumps and pressure or temperature sensors. In our case the equipment had other, more strict requirements. In addition to supplying a pulseless flow in low flow rates and high pressures (>20 bar), it also had to be chemically resistant against various organic solvents. The smallest, but extremely important part of the microfluidic platform are the chips, where the phenomena takes place. The main criteria for them was the pressure and chemical resistance, which limited the possible fabrication material to glass.

The major parts of the setup were ordered and delivered within 8 months. After assembly, the first tests with simple drop generation were performed. Figure 6-1 illustrates the initial layout of the setup (A), the design of the chip for achieving droplet generation (B) and a snapshot of from one of the experiments involving formation of xylene drops in water (C).

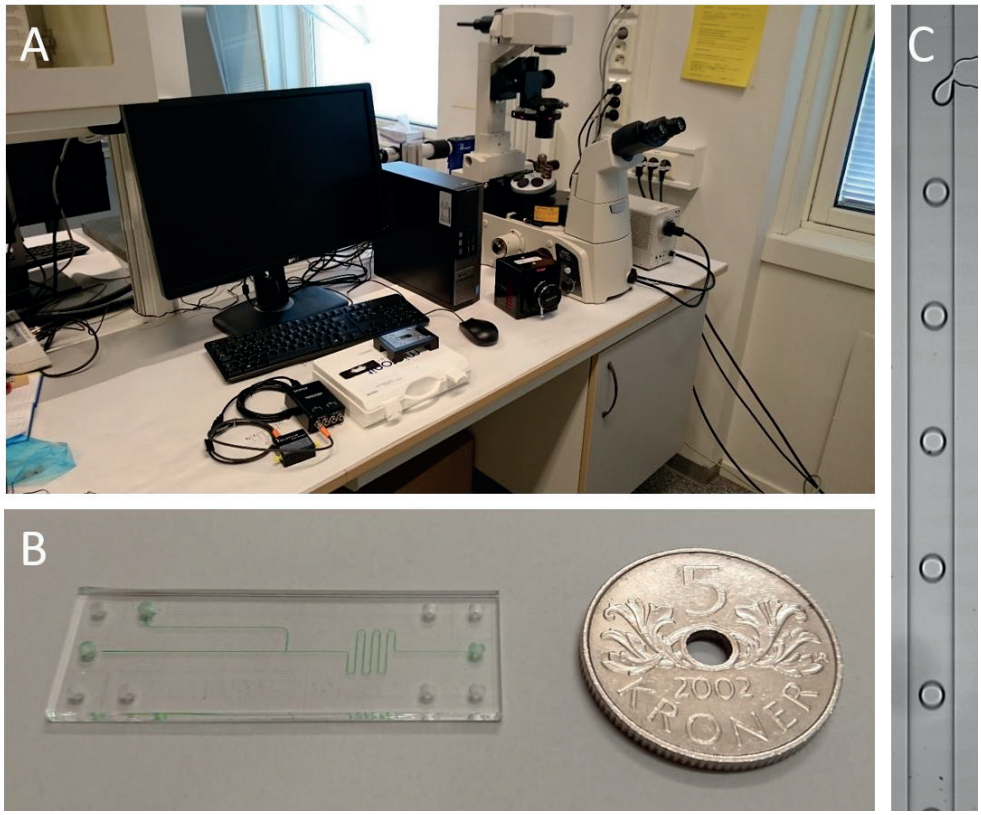

Figure 6-1 Early design of the microfluidic platform (A), chip type and size, compared to a five kroner coin (B), and 60 µm xylene drops generated in MQ water (C).

In general, the platform and the method performed well under high pressure, however more experience was necessary to address several issues, occurring during trial runs. A research stay in a well-established microfluidic laboratory was organized in the end of the first year of the PhD project to get acquainted with other relevant equipment and learn the required procedures. This took place over a period of one month in the Food Process Engineering group at Wageningen University and Research in the Netherlands. It resulted in much needed development of laboratory practices related to microfluidics. After further adjustments and expansions of the microfluidic platform, and subsequent delivery of the custom-designed microfluidic chips, the first repeatable experiments were performed. This coincided with the midpoint of the PhD project.

The current configuration of the setup makes it a universal tool for studying various phenomena. Figure 6-2 depicts the recent layout of the setup. The inverted microscope

(Nikon Ti-U [1]) with the connected high-speed camera (Photron AX100 [2]) and a LED light source allow observing the events inside the chip at extremely high frame rate speeds (up to 500 000 frames per second). The flow setup (Cetoni Qmix [3]) ensures a stable flow of fluids to a chip, placed in a chip holder (Micronit Microtechnologies [4]) and on the microscopic stage. The computer-controlled software [5] grants the possibility of both control and observation of the experiment. Other equipment, not shown in Figure 6-2, allows measuring the flow of the phases or the use gases during the experiment. At the time of finalizing this thesis, the design and fabrication of a heated setup is under way.

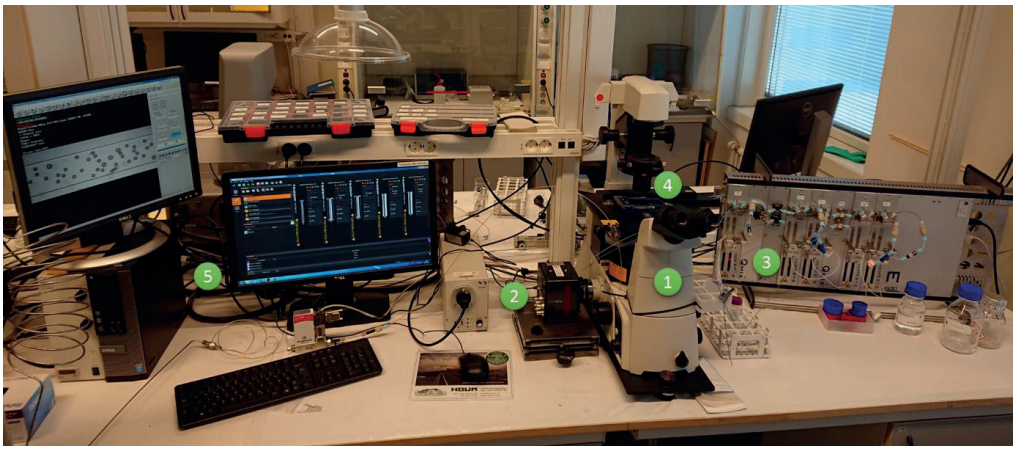

Figure 6-2 The Universal Microfluidic Platform in the Ugelstad Laboratory.

As mentioned earlier, one of the main requirements was the flexibility of the platform, so that by simply changing the chip, one could perform entirely different experiments. This feature was used during the work for the present thesis, where several chip designs were used to study various aspects of the produced water treatment.

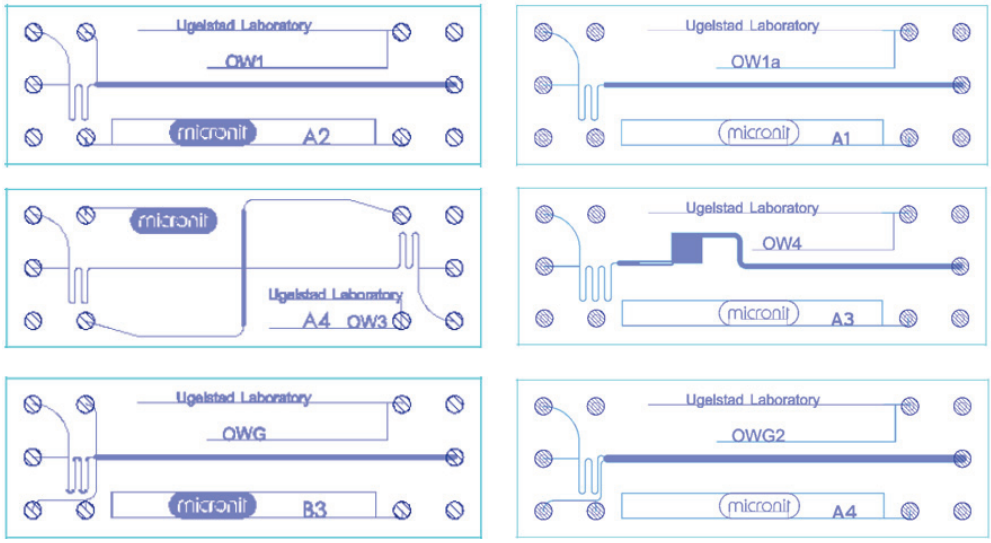

Figure 6-3 Overview of the chip designs used during tests and experiments for the present work.

The top two chips in Figure 6-3 (OW1 and OW1a) were used to determine the coalescence frequency of oil drops. They consisted of a T-junction for droplet generation, a meandering channel and a wider chamber, where the drops could collide and undergo coalescence. Unlike OW1a, the OW1 design had an additional inlet for the continuous phase in the beginning of the coalescence chamber. The chips in the middle (OW3 and OW4) were designed to measure the coalescence time between drops. OW3 included two T-junctions on both sides of a larger coalescence chamber. After passing the meandering channels, the droplet underwent head-on collisions that enabled recording of the entire coalescence process (collision, drainage and merging of drops). The OW4 design consisted of only one T-junction, but after certain length, the droplets were split into two smaller channels and delivered into a square channel. Slower and diagonal flow in the square channel assisted in successful recording of the entire process of merging. The last two chips were utilized for simultaneous generation of oil drops (upper T-junction) and gas bubbles (lower T-junction) in the continuous water phase. Both met in a wider chamber, where the oil drops could spread over the surface of the gas bubbles. It should be noted that the OW1, OW1a and OW3 designs were based on the work of Krebs et al.[111-112]. All chips were used during the PhD project, but some work has not yet been published or needs further development. Specific details on the dimensions of the channels, experimental and cleaning procedures can be found in the respective papers.

6.1.1. Microfluidic coalescence of model oils and crude oils

The coalescence between oil drops, as a function of various parameters, was studied in Papers 2 and 3. Most of the results presented in both papers relied on the use of the chips OW1 and OW1a for obtaining coalescence frequencies. Hence, the setup and method were relatively similar. Both methods were described in detail in the manuscripts. The configuration of the setup is depicted in Figure 6-4.

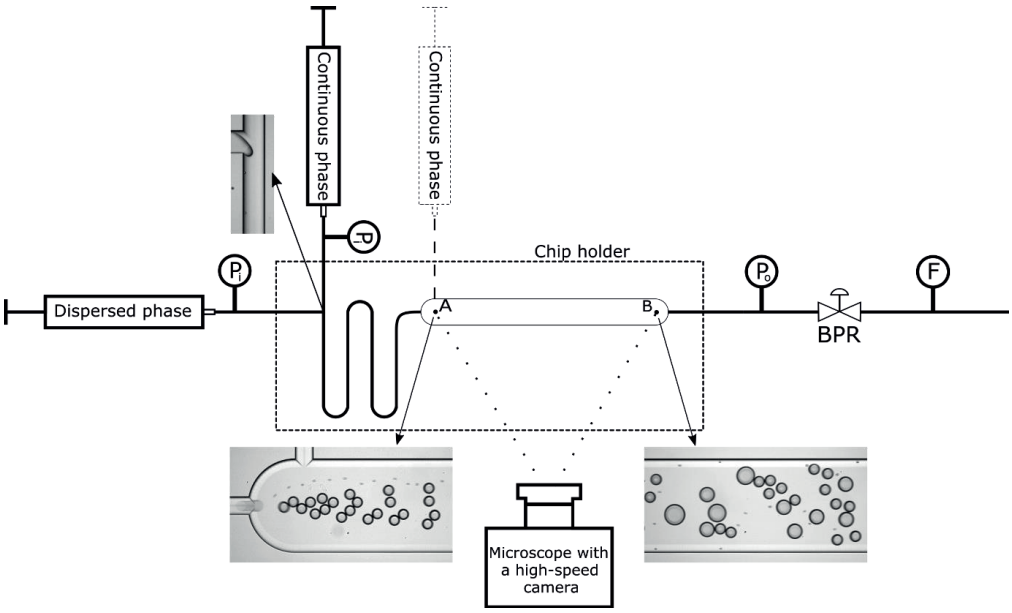

Figure 6-4 Microfluidic setup for coalescence studies.

The flow rates of the continuous and dispersed phases were controlled by the syringe pumps, fitted with glass or stainless-steel syringes. In most cases, the drop sizes were around 50-60 µm. The system pressure was controlled by a back-pressure regulator (BPR) and monitored by pressure sensors at the inlet (P_i) and outlet (P_o) of the chip holder. The total flow was measured with a flowmeter (F). By varying both the continuous and dispersed phase compositions, different coalescence behaviour was discovered. To analyse it, two sets of images were recorded over a period of 1-1.5 seconds at 8 500 frames per second (fps). The inlet (A in Figure 6-4) was recorded in order to retrieve the initial size and number of droplets. Afterwards, a recording was taken further down the chamber (B in Figure 6-4) for the analysis of coalescence events. When the model oils (xylene, heptane) were used, the location of the second point was moved towards the middle of the channel due to extensive

coalescence. Next, the recorded images were processed with the ImageJ software, first to convert to a binary mask and then to retrieve the areas and centre of mass coordinates of the detected drops within part of an image (Figure 6-5).

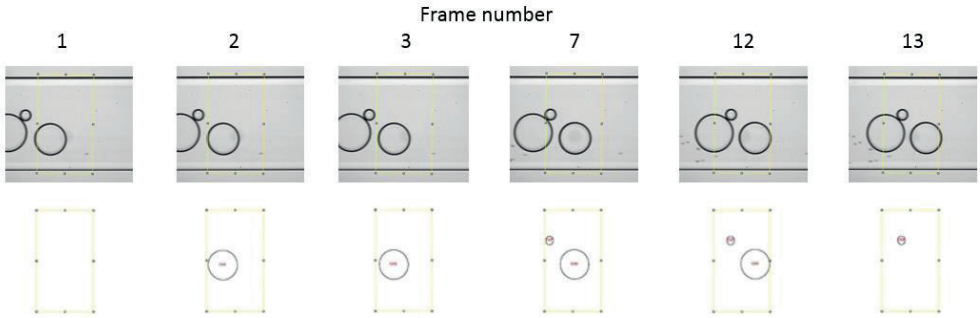

Figure 6-5 Selected recorded frames (top) and frames after processing with ImageJ software.

The drops were usually smaller than the detection box (yellow frames in Figure 6-5), therefore a single drop was detected several times over a number of consecutive frames (bigger drop in frames 2 to 12 in Figure 6-5). The areas of the drops were found to increase linearly with the number of coalescence events and, based on this, were sorted into several size classes. The changes of X,Y coordinates of the droplets between the frames were used to calculate their velocity. This, together with the width of the detection box and the average drop diameter in each of the size classes allowed estimating the actual number of observed drops of different sizes. The ratio between the initial and final number of drops (N_i and N_f, respectively) gave the mean relative size of a droplet and the average number of coalescence events ((N_{in}/N_f) -1). The coalescence frequency was obtained from Equation 5:

$$f = \frac{\frac{N_{in}}{N_f} - 1}{t_{res}}, \tag{5}$$

where the t_{res} is the residence time, calculated by dividing the coalescence channel length by the average drop velocity. Statistical analysis (t-Student, α=0.05) was performed for all results to determine whether the differences between the data sets were statistically significant or not.

6.1.2. Microfluidic method for studying spreading of crude oil on gas bubbles

Another protocol was developed to study the fundamental aspects of gas flotation. The experimental method, used in Paper 4, was analogous to the coalescence determination, with only few modifications (Figure 6-6).

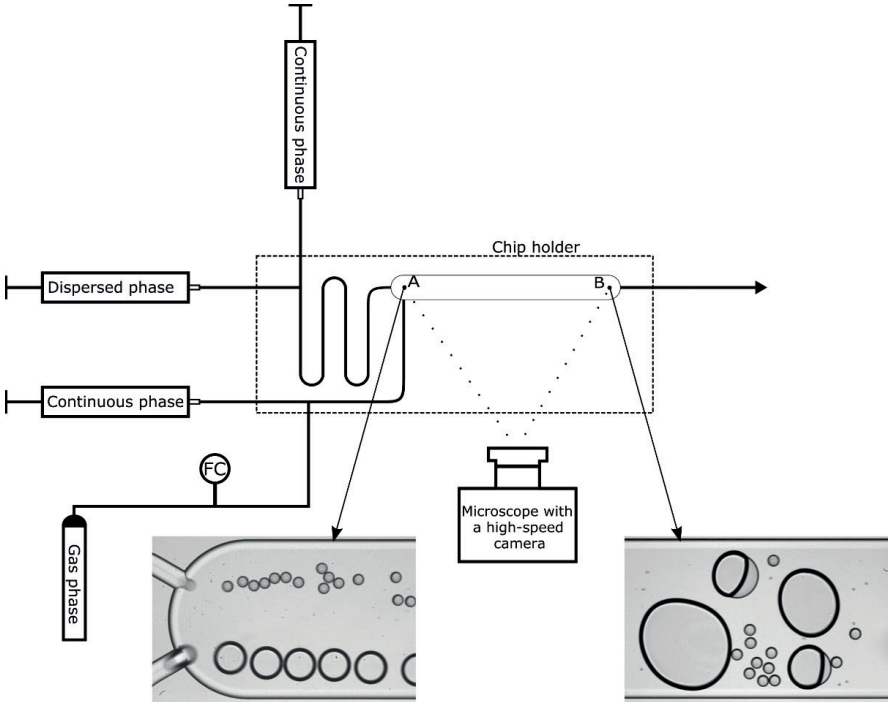

Figure 6-6 Setup used for studying the fundamental aspects of gas flotation.

In addition to the T-junction for droplet generation, another was added to simultaneously generate gas bubbles. The flow of the water and oil phases was controlled by the syringe pumps, while the flow of gas was regulated by a gas flow controller. After passing through the entire channel, some drops spread on the surface of the gas bubbles. Notably, the coalescence between drops was negligible.

Similarly to the coalescence method, two sets of approx. 16 000 images (at 8 500 fps) were recorded in the beginning and end of the wide channel (points A and B in Figure 6-6, respectively). The former was used to retrieve the initial number of generated drops, whereas the latter provided the information on the remaining droplets that did not spread on the gas bubbles. The gas bubbles at the end of the channel were significantly larger than the oil drops.

Based on that, the parameters in the image analysis tool were set so that only the objects below a certain size were detected and counted. This effectively excluded the detection of gas bubbles, as shown in Figure 6-7.

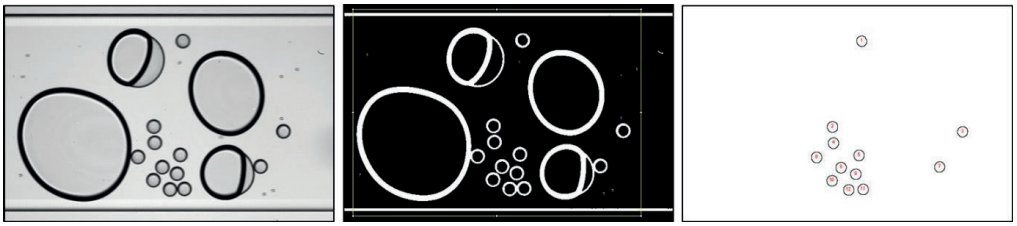

Figure 6-7 Raw and processed images from microfluidic flotation experiments. From left to right: frame with both oil (smaller) droplets and (bigger) gas bubbles; the same frame converted to a binary mask and lastly the objects detected by the image processing tool.

The ratio of drops detected at the end of the channel to those in the beginning (i.e. removal efficiency) served as a comparison parameter between all experimental conditions.

6.2. Crude oil characterization

Six crude oils, denoted A to F, were obtained from the industrial partners in the SUBPRO project and characterized as received. The in-house characterization included measurements of the density, viscosity, total acid and base numbers (TAN and TBN, respectively), water content, SARA and wax content. The separated SARA fractions were sent to the Oil and Gas Institute in Cracow (Poland) to analyse the elemental composition (C, H, N, O and S content). The interfacial tension of crude oils was measured against different water phases and by using different techniques (pendant drop, spinning drop and du Noüy ring method).

6.3. Produced water preparation and characterization

The synthetic produced water in Paper 1 was prepared by mixing 50/50 (v/v) brines and crude oils. The two brines contained pure NaCl or NaCl with the addition of $CaCl_2$ to study the effect of calcium ions. The ionic strength was kept constant for both solutions. The brines were adjusted to three different pH levels. After mixing and two hours of gravity separation, the water was extracted and analysed for pH, total organic carbon, oil concentration and drop size distribution. In Paper 2, the NaCl brine was either used as is or degassed by ultrasonication to remove the dissolved atmospheric gases. In the remaining papers, the

water phase generally consisted of two brines at three pH levels. During some measurements, the brines contained certain dissolved components (4-heptylbenzoic acid, Fluka acids or water-soluble crude oil components). The details on the respective experimental procedures can be found in the papers.

7. Main results

***Paper 1*: Influence of the Crude Oil and Water Compositions on the Quality of Synthetic Produced Water**

The first paper focused on the characteristics of crude oils and evaluating the quality of the water phase after mixing it with crude oils. Overall, the report underlined the complexity of the composition of produced water and its dependence on the oil properties.

Five crude oils were analysed with respect to the density, viscosity, total acid and base numbers, SARA composition, water content and interfacial tension. In addition, crude oils and their SARA fractions were analysed for the content of carbon, hydrogen, nitrogen, oxygen and sulphur. Subsequently, the crude oils were mixed with two types of brine (with and without divalent ions) and at three pH levels. After mixing and a period of gravity separation, the volume of the free water phase was recorded. The water was sampled and analysed for the dispersed oil concentration, droplet size distribution, total organic carbon (TOC) content and pH value.

The crude oils were divided into two groups: light (API 35-38°) and heavier oils (19-23°). Most of the physical and chemical parameters reflected that division (Table 7-1). What is more, the elemental analysis revealed that on average, the lighter oils were more saturated, whereas heavier crude oils had higher content of nitrogen and sulphur in the most polar fractions.

Table 7-1 Physicochemical properties and compositions of crude oils.

Crude oil		A	B	C	D	E
API gravity [°]		19.2	35.8	23.0	36.3	37.9
Density at 20°C [g/cm^3]		0.935	0.841	0.911	0.839	0.831
Viscosity at 20°C [mPa*s]		354.4	14.2	74.4	10.3	8.3
TAN [mg KOH/g oil]		2.2	<0.1	2.7	0.2	0.5
TBN [mg KOH/g oil]		2.8	1.0	1.1	1.1	0.4
SARA	Saturates [% (w/w)]	50.6	84.0	64.9	71.5	74.8
	Aromatics [% (w/w)]	31.2	13.4	26.3	23.1	23.2
	Resins [% (w/w)]	15.7	2.3	8.4	5.1	1.9
	Asphaltenes [% (w/w)]	2.5	0.3	0.4	0.3	0.1
Water content [ppm]		590.9	85.4	535.8	202.4	333.4
IFT [mN/m]	Na-Brine (pH 6)	20.4 ±0.6	20.5 ±0.2	22.2 ±0.6	19.0 ±0.5	19.9 ±0.1
	NaCa-Brine (pH 6)	18.6 ±0.8	19.9 ±0.2	18.9 ±0.7	16.2 ±0.4	17.4 ±0.4

The analysis of the synthetic produced water provided further observations. It was found that the amount of the separated water increased with the initial pH of the aqueous phase in all cases. Moreover, at the highest pH the presence of calcium stabilized emulsions and resulted in less water breaking out. This was attributed to strengthening of the interfacial film by complexes of calcium and naphthenic acids.

The total organic carbon content was highly dependent on the oil type, whereas the water pH affected the amount of dissolved organics only slightly. The highest TOC values were found in the water from oils with considerably higher presence of oxygen in the asphaltenes. This suggested the improved water-solubility of the smallest compounds in that fraction. The biggest changes in pH after mixing were observed for the initial pH 10, and that agreed with the previously reported higher water-solubility of acidic species in crude oils. The total oil concentration was the highest for the two heavier oils (between 100 and 500 ppm), while remaining at a similar level for the light oils (typically below 100 ppm). The density difference between the water and oil phases could have played a significant role here, as the water

phases were sampled after a period of gravity separation. Droplet size distributions and Sauter mean diameters were calculated from the image analysis of microscopic pictures. Representative images of droplets made from heavier and light oil are shown in Figure 7-1.

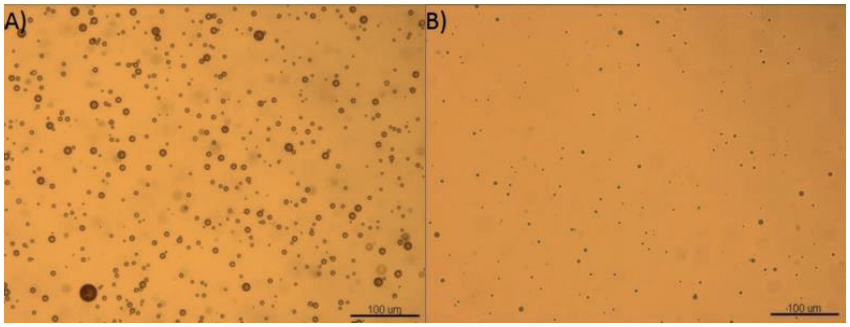

Figure 7-1 Microscopic pictures of dispersed crude oil droplets in water from heavier (left) and light (right) crude oils.

In general, larger drops were detected for the two heavier crude oils and smaller ones for the light oils. This was also reflected in the size distributions. The increased viscosity most likely contributed to the wider distributions of the heavier crude oil, with a substantial volume contribution from droplets larger than 10 µm. In the case of light oils, the distributions were less polydisperse and hardly any drops above 10 µm in diameter were detected.

***Paper 2*: The Effect of Dissolved Gas on Coalescence of Oil Drops Studied with Microfluidics**

This paper reported our first research, performed with microfluidic methodology and used for evaluating emulsion stability. In it, we investigated the influence of the dissolved atmospheric gases on the coalescence of oils with different hydrophobicity and at elevated system pressures.

Previous reports uncovered that the removal of dissolved gas from liquids can lead to the formation of kinetically stable surfactant-free oil-in-water emulsions. This was mostly attributed to the decreased "hydrophobic interactions" between surfaces in water phase. Later, it was suggested that these interactions are in fact a combination of long-ranged attractive forces, caused by the preferential adsorption of nanobubbles at hydrophobic surfaces, and truly hydrophobic interactions at short range.

The glass microfluidic chip consisted of a T-junction, where the water and oil phases met, and where droplets were generated. Later, the droplets entered a wider chamber, where they could collide with each other and possibly undergo coalescence. A recording was made at the end of the coalescence chamber to quantify the extent of droplet growth with image analysis tools. The results were reported as coalescence frequencies, which described how often did the droplet coalesce.

With the use of microfluidics, we were able to probe the coalescence behaviour of heptane (most hydrophobic) and xylene (less hydrophobic) droplets in standard and degassed brine. It was found that the coalescence frequency decreased by ca. 25-30% upon removal of dissolved gas from the water phase and led to smaller droplets at the end of the channel (Figure 7-2).

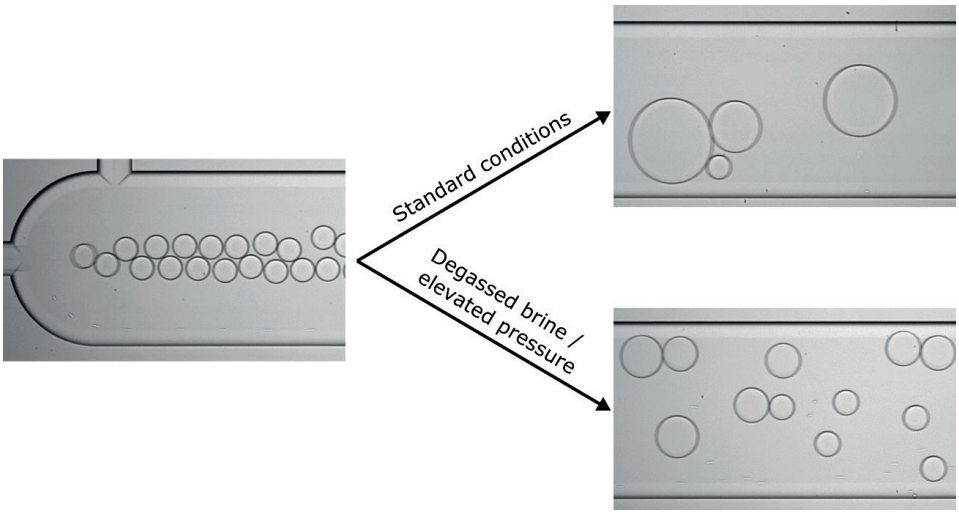

Figure 7-2 Snapshots of the beginning (left) and the end of the channel with the dissolved gas present (upper right) and absent (lower right) in the system.

What is more, when the pressure was increased, the coalescence frequencies in both brines were the same for xylene, whereas slightly lower values were obtained in the degassed brine for heptane. Increased system pressure probably resulted in the enhanced solubility in both liquids, and this most likely led to less nucleation of dissolved gas at the surfaces, which reduced the attractive forces. In addition, the gas molecules had probably higher affinity to the more hydrophobic heptane, which could explain the difference in coalescence behaviour observed in the standard brine at higher system pressure.

Finally, the coalescence of a diluted crude oil with dynamic interfacial behaviour was also studied (Figure 7-3).

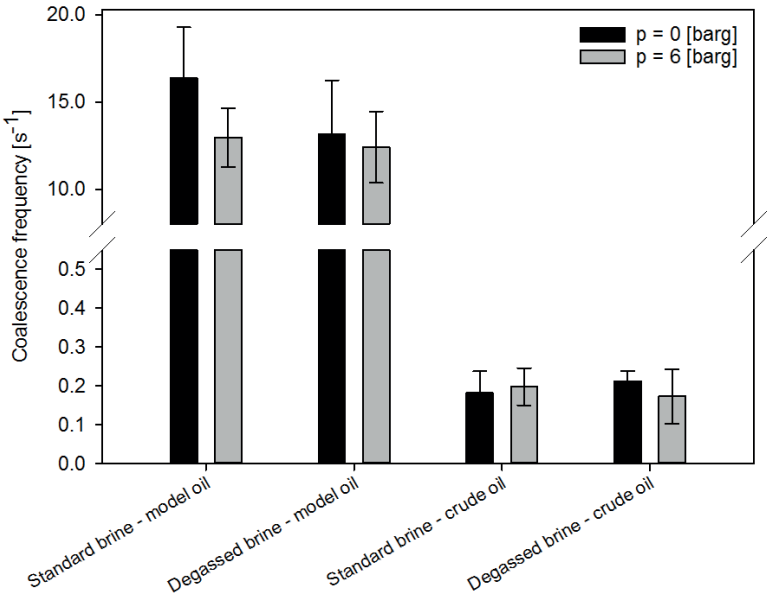

Figure 7-3 Coalescence frequencies of a model and diluted crude oils in stanard and degassed conditions.

First, the coalescence frequency was reduced by a factor of 100 when compared to a model oil. Unlike the model oil, the removal of dissolved gas and the increased system pressure had no effect on the coalescence of the diluted crude oil. The merging between crude oil drops was inhibited by the crude oil-indigenous surfactants, namely resins, asphaltenes and naphthenic acids that influence the interfacial properties of crude oils. The lack of response to the presence or absence of the dissolved gas molecules was probably also a result of the presence of the surface-active components. It probably decreased the hydrophobicity of drops and most likely limited the adsorption of dissolved gas at their vicinity.

***Paper 3*: Microfluidic Tools for Studying Coalescence of Crude Oil Droplets in Produced Water**

Following the work with model fluids, this paper focused on applying the developed microfluidic method to study the coalescence of crude oil droplets in various conditions. Coalescence between oil drops is one of the main mechanisms of droplet growth and is important during the gravity-based methods of the produced water treatment.

The experimental setup was essentially the same as in the previous report: glass microfluidic chip with a T-junction for droplet generation, which led to a wider channel, where the coalescence took place. Six crude oils, diluted with xylene, were used as the dispersed phases in the first part of the paper, whereas the second part was conducted with three non-diluted crude oils with addition of an oil-soluble surfactant. All values were reported as coalescence frequencies.

The coalescence of diluted crude oils was highly oil and water type-dependent. Less stable emulsions were generally observed for the lighter crude oils and when the water pH was lower, whereas not a lot of coalescence took place at high pH. This was attributed to the higher interfacial activity of the acidic species compared to the basic ones. In addition, at the highest pH the presence of calcium increased coalescence, most likely due to complexing and removal from the interface of some of the dissociated naphthenic acids. Interestingly, the coalescence frequencies highly depended on the weight fractions of the most polar crude oil components: resins and asphaltenes (Figure 7-4). This agreed with their previously reported role in the interfacial behaviour of crude oils.

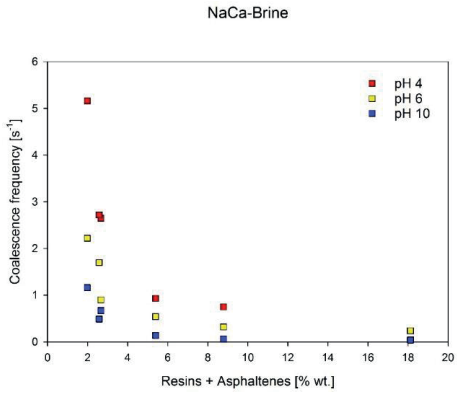

Figure 7-4 Coalescence frequencies of diluted crude oils plotted against the sum of resins and asphaltenes of respective crude oils.

The coalescence frequencies of the non-diluted crude oils were significantly lower than for the diluted ones. However, the effect of the water composition remained similar. Furthermore, the influence of the dissolved components in the water phase was also studied. Crude oils reacted uniquely to their presence and these effects had a reflection in the oil compositions. What is more, there was hardly any difference in the coalescence behaviour between systems with model naphthenic acids and dissolved water-soluble crude oil components (Figure 7-5). This implied that the role of other than acidic species in the coalescence between crude oil drops was rather insignificant.

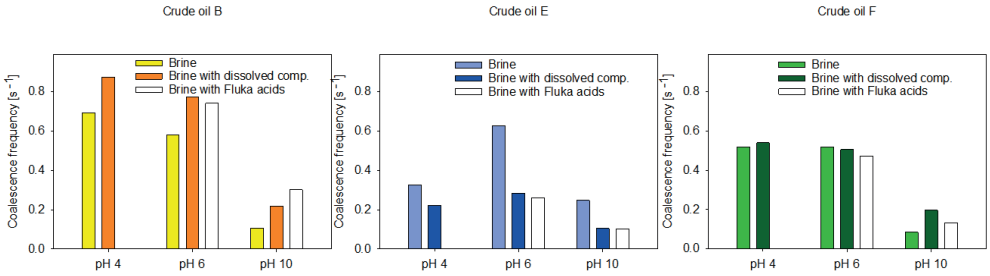

Figure 7-5 Coalescence frequencies of different crude oil in brine with dissolved crude oil components (darker bars) and naphthenic acids (white bars).

Finally, we investigated the effect of the system pressure on the coalescence. It was revealed that in the range of 0 to 40 bar(g), the coalescence frequencies remained unchanged. The most probable cause behind that was the lack of the lightest components in the system, as the oils were stored in ambient conditions.

***Paper 4*: Removal of Crude Oil Droplets through Spreading on Gas Bubbles Studied with Microfluidics**

In Paper 4, a novel microfluidic method was developed to study the removal of crude oil through spreading on the surfaces of gas bubbles. This process is relevant to the gas flotation treatment of the produced water.

The newly developed technique relies on the simultaneous generation of gas bubbles and oil droplets at two T-junctions. Later, the fluid particles meet in a wide channel, where they can get in contact. Droplets were removed through spreading over the surface of gas bubbles (Figure 7-6). The initial number of droplets was recovered through a recording of the inlet of the channel, whereas the remaining drop number was counted at the outlet. Therefore, the results were presented as the removal efficiencies of crude oil drops after passing through the channel.

Figure 7-6 Images of bubbles and droplets entering the channel (left) and oil-coated bubbles at the end of the channel (right). Frames of the spreading of oil on a gas bubble are shown in the middle.

The developed method allowed us to systematically study the effect of the oil, water and gas phases. The highest removal efficiencies were observed at low or neutral pH. This was most likely due to the reduced interfacial activity of acidic species in that pH range. Notably, the lowest removal efficiency was obtained for the most viscous oil, which agreed with the previously reported effect of the viscosity on the coverage time. By reducing the salinity, the electrostatic repulsion increased. This had a negative effect on the removal efficiency. The increase of the droplet number caused a reduction of the removal efficiency. At the same time, the smallest droplets were removed more efficiently. The latter effect was attributed to the reduced drainage time of the thin film between drops and bubbles. Its thickness was probably lower for the smaller droplets.

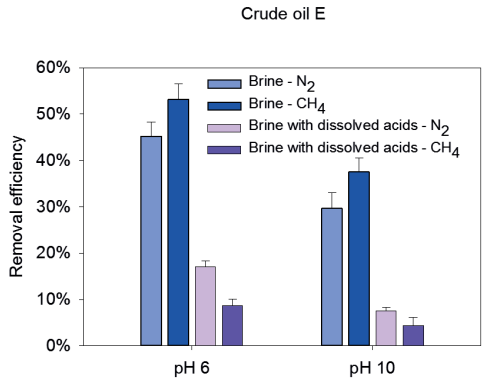

Figure 7-7 Percentage of removed crude oil E droplets in brines with or without dissolved components, and while using nitrogen or methane.

Addition of the naphthenic acids to the water phase greatly reduced the spreading of oil on bubbles (light blue and light purple bars in Figure 7-7). While the acidic species might have had a mixed effect on the coalescence between oil drops (as shown in Paper 3), they significantly improved the stability of gas bubbles, which altogether led to increased repulsive interactions between bubbles and drops. Using methane instead of nitrogen improved the bubble-droplet interactions, leading to more oil being removed (bright and dark blue bars in Figure 7-7). Crude oil droplets most likely had a higher affinity to the hydrocarbon gas, which could have decreased the induction time and increased the attraction between the two fluid particles.

Concluding remarks and future work

This thesis revolves around the fundamental aspects of produced water generated during the production of crude oil. Produced water quality is an important issue for both technical and environmental reasons. Nowadays, treatment of the produced water is a vital process, as its global production is three times higher than the volume of the extracted crude oil. The treatment processes of produced fluids have to be thoroughly designed and investigated to ensure high separation efficiency. This includes not only process parameters, such as recycle ratio or residence time, but also fundamental phenomena, like droplet coalescence or the interactions between oil drops and gas bubbles. Systematic studies on the effect of different parameters on these processes will improve the fundamental understanding of the produced water treatment and should also contribute to the enhanced separation performance. Remarkably, only a handful of research tools is available for that sort of experiments.

The microfluidic methodology developed during this PhD will be improved and used by a Postdoc following this project. The coalescence method, used in **Paper 2** and **Paper 3**, can be applied for further studies on the effect of various parameters on the merging process. This can include production chemicals (both oil- and water-soluble) or more complex water composition. The method for the assessment of coalescence time, presented in **Paper 2**, could also be improved. When ready, this approach can also be used for the measurement of the induction time between bubbles and droplets, which interactions were studied in **Paper 4**. The microfluidic platform should also have better screening capabilities, allowing for instantaneous control over, for instance, the water pH or the concentration of certain component by simply adjusting the flow rate of the pumps. The design and construction process of a setup with temperature control is currently under way. This will expand the application range of the platform. Finally, other separation processes, like extraction or filtration, can also be miniaturized and simulated inside microfluidics chips.

My project has initiated the work with microfluidics in our laboratory group. Since then, couple of other projects have either started or plan to include some microfluidic experiments in their research. It is my personal belief that microfluidics, with its many interesting features, can play an important role in the field of the produced water research. At the same time, I also hope that it will be a valuable addition to the broad range of experimental methods, available at the Ugelstad Laboratory.

References

1. Speight, J. G., Exploration, Recovery, and Transportation. In *An Introduction to Petroleum Technology, Economics, and Politics*, John Wiley & Sons, Inc.: 2011; pp 65-101.
2. Jewell, D. M.; Albaugh, E. W.; Davis, B. E.; Ruberto, R. G., Integration of Chromatographic and Spectroscopic Techniques for the Characterization of Residual Oils. *Industrial & Engineering Chemistry Fundamentals* **1974,** *13* (3), 278-282.
3. Kaur, G.; Mandal, A. K.; Nihlani, M. C.; Lal, B., Control of sulfidogenic bacteria in produced water from the Kathloni oilfield in northeast India. *Int. Biodeterior. Biodegrad.* **2009,** *63* (2), 151-155.
4. Dudášová, D. Characterization of solid particle suspensions with organic coatings in oilfield produced water. Norwegian University of Science and Technology, Trondheim, Norway, 2008.
5. Fakhru'l-Razi, A.; Pendashteh, A.; Abdullah, L. C.; Biak, D. R.; Madaeni, S. S.; Abidin, Z. Z., Review of technologies for oil and gas produced water treatment. *J. Hazard. Mater.* **2009,** *170* (2-3), 530-51.
6. Igunnu, E. T.; Chen, G. Z., Produced water treatment technologies. *International Journal of Low-Carbon Technologies* **2014,** *9* (3), 157-177.
7. Sharp, J. H., Total organic carbon in seawater — comparison of measurements using persulfate oxidation and high temperature combustion. *Mar. Chem.* **1973,** *1* (3), 211-229.
8. Hansen, B. R.; Davies, S. H., Review of potential technologies for the removal of dissolved components from produced water. *Chem. Eng. Res. Des.* **1994,** *72* (A2), 176-188.
9. Tibbetts, P. J. C.; Buchanan, I. T.; Gawel, L. J.; Large, R., A Comprehensive Determination of Produced Water Composition. In *Produced Water: Technological/Environmental Issues and Solutions*, Ray, J. P.; Engelhardt, F. R., Eds. Springer US: Boston, MA, 1992; pp 97-112.
10. Bader, M. S. H., Sulfate scale problems in oil fields water injection operations. *Desalination* **2006,** *201* (1), 100-105.
11. Puntervold, T.; Austad, T., Injection of seawater and mixtures with produced water into North Sea chalk formation: Impact of fluid–rock interactions on wettability and scale formation. *Journal of Petroleum Science and Engineering* **2008,** *63* (1), 23-33.
12. Wang, X.; Alvarado, V., Effects of Aqueous-Phase Salinity on Water-in-Crude Oil Emulsion Stability. *J. Dispersion Sci. Technol.* **2012,** *33* (2), 165-170.
13. Perles, C. E.; Volpe, P. L. O.; Bombard, A. J. F., Study of the Cation and Salinity Effect on Electrocoalescence of Water/Crude Oil Emulsions. *Energy Fuels* **2012,** *26* (11), 6914-6924.
14. Azetsu-Scott, K.; Yeats, P.; Wohlgeschaffen, G.; Dalziel, J.; Niven, S.; Lee, K., Precipitation of heavy metals in produced water: Influence on contaminant transport and toxicity. *Mar. Environ. Res.* **2007,** *63* (2), 146-167.
15. Kralova, I.; Sjöblom, J.; Øye, G.; Simon, S.; Grimes, B. A.; Paso, K., Heavy Crude Oils/Particle Stabilized Emulsions. *Adv. Colloid Interface Sci.* **2011,** *169* (2), 106-127.
16. Deng, S.; Yu, G.; Chen, Z.; Wu, D.; Xia, F.; Jiang, N., Characterization of suspended solids in produced water in Daqing oilfield. *Colloids Surf. Physicochem. Eng. Aspects* **2009,** *332* (1), 63-69.
17. Veil, J. A.; Puder, M. G.; Elcock, D.; Redweik, R. J., Jr. *A white paper describing produced water from production of crude oil, natural gas, and coal bed methane*; Argonne National Laboratory for the U.S. Department of Energy, National Energy Technology Laboratory: 2004.
18. Arthur, J. D.; Langhus, B. G.; Patel, C. *Technical Summary of Oil & Gas Produced Water Treatment Technologies*; ALL Consulting, LLC.: 2005.
19. Mansfield, G. E. In *Corrugated Plate Interceptors*, American Institute of Chemical Engineers, National Meeting, 1987.
20. van den Broek, W. M. G. T.; Plat, R.; van der Zande, M. J., Comparison of Plate Separator, Centrifuge and Hydrocyclone. Society of Petroleum Engineers: 1998.
21. Young, G. A. B.; Wakley, W. D.; Taggart, D. L.; Andrews, S. L.; Worrell, J. R., Oil-water separation using hydrocyclones: An experimental search for optimum dimensions. *Journal of Petroleum Science and Engineering* **1994,** *11* (1), 37-50.

22. *Technical Assessment of Produced Water Treatment Technologies*; Colorado School of Mines: Golden, CO, 2009.
23. Moosai, R.; Dawe, R. A., Gas attachment of oil droplets for gas flotation for oily wastewater cleanup. *Sep. Purif. Technol.* **2003,** *33* (3), 303-314.
24. Discharges, spills and emissions from offshore oil and gas installations. OSPAR, Ed. 2010.
25. Røe Utvik, T. I., Chemical characterisation of produced water from four offshore oil production platforms in the North Sea. *Chemosphere* **1999,** *39* (15), 2593-2606.
26. Stanford, L. A.; Kim, S.; Klein, G. C.; Smith, D. F.; Rodgers, R. P.; Marshall, A. G., Identification of Water-Soluble Heavy Crude Oil Organic-Acids, Bases, and Neutrals by Electrospray Ionization and Field Desorption Ionization Fourier Transform Ion Cyclotron Resonance Mass Spectrometry. *Environ. Sci. Technol.* **2007,** *41* (8), 2696-2702.
27. *Environmental Report 2017*; Norsk olje & gass: 2017.
28. Endo, S.; Pfennigsdorff, A.; Goss, K.-U., Salting-Out Effect in Aqueous NaCl Solutions: Trends with Size and Polarity of Solute Molecules. *Environ. Sci. Technol.* **2012,** *46* (3), 1496-1503.
29. Eftekhardadkhah, M.; Øye, G., Dynamic Adsorption of Organic Compounds Dissolved in Synthetic Produced Water at Air Bubbles: The Influence of the Ionic Composition of Aqueous Solutions. *Energy Fuels* **2013,** *27* (9), 5128-5134.
30. Eftekhardadkhah, M.; Reynders, P.; Øye, G., Dynamic adsorption of water soluble crude oil components at air bubbles. *Chem. Eng. Sci.* **2013,** *101*, 359-365.
31. Eftekhardadkhah, M.; Kløcker, K. N.; Trapnes, H. H.; Gaweł, B.; Øye, G., Composition and Dynamic Adsorption of Crude Oil Components Dissolved in Synthetic Produced Water at Different pH Values. *Ind. Eng. Chem. Res.* **2016,** *55* (11), 3084-3090.
32. Bertheussen, A.; Simon, S.; Sjöblom, J., Equilibrium Partitioning of Naphthenic Acid Mixture Part 1: Commercial Naphthenic Acid Mixture. *Manuscript in preparation*.
33. OLF *2007 Environmental Report*; 2007.
34. Bringedal, B.; Ingebretsen, T.; Haugen, K., Subsea Separation and Reinjection of Produced Water. In *Offshore Technology Conference*, Offshore Technology Conference: Houston, Texas, 1999.
35. Knowles, D. W.; Boytim, R. G., Brine Handling And Disposal By Reinjection. Society of Petroleum Engineers: 1999.
36. Paige, R. W.; Murray, L. R., Re-injection of produced water - Field experience and current understanding. Society of Petroleum Engineers: 1994.
37. Vance, I.; Thrasher, D. R., Reservoir Souring: Mechanisms and Prevention. In *Petroleum Microbiology*, American Society of Microbiology: 2005.
38. Mueller, J.; Cen, Y.; Davis, R. H., Crossflow microfiltration of oily water. *J. Membr. Sci.* **1997,** *129* (2), 221-235.
39. Arnold, K.; Stewart, M.; Stewart, M. I.; Stewart, M. I., *Surface Production Operations: Design of Oil-Handling Systems and Facilities*. Second ed.; Gulf Professional Publishing: Woburn, 1999.
40. Rawlins, C. H., Sand Management Methodologies for Sustained Facilities Operations. Society of Petroleum Engineers: 2013.
41. Judd, S.; Qiblawey, H.; Al-Marri, M.; Clarkin, C.; Watson, S.; Ahmed, A.; Bach, S., The size and performance of offshore produced water oil-removal technologies for reinjection. *Sep. Purif. Technol.* **2014,** *134*, 241-246.
42. Saththasivam, J.; Loganathan, K.; Sarp, S., An overview of oil–water separation using gas flotation systems. *Chemosphere* **2016,** *144*, 671-680.
43. Weschenfelder, S. E.; Louvisse, A. M. T.; Borges, C. P.; Meabe, E.; Izquierdo, J.; Campos, J. C., Evaluation of ceramic membranes for oilfield produced water treatment aiming reinjection in offshore units. *Journal of Petroleum Science and Engineering* **2015,** *131*, 51-57.
44. Ebrahimi, M.; Ashaghi, K. S.; Engel, L.; Willershausen, D.; Mund, P.; Bolduan, P.; Czermak, P., Characterization and application of different ceramic membranes for the oil-field produced water treatment. *Desalination* **2009,** *245* (1), 533-540.

45. Ruud, T.; Idrac, A.; McKenzie, L. J.; Høy, S. H., All Subsea: A Vision for the Future of Subsea Processing. Offshore Technology Conference: 2015.
46. Tadros, T. F., Emulsion Formation, Stability, and Rheology. In *Emulsion Formation and Stability*, Wiley-VCH Verlag GmbH & Co. KGaA: 2013; pp 1-75.
47. Shinnar, R.; Church, J. M., Statistical Theories of Turbulence in Predicting Particle Size in Agitated Dispersions. *Industrial & Engineering Chemistry* **1960,** *52* (3), 253-256.
48. Liao, Y.; Lucas, D., A literature review on mechanisms and models for the coalescence process of fluid particles. *Chem. Eng. Sci.* **2010,** *65* (10), 2851-2864.
49. Marinova, K. G.; Alargova, R. G.; Denkov, N. D.; Velev, O. D.; Petsev, D. N.; Ivanov, I. B.; Borwankar, R. P., Charging of Oil−Water Interfaces Due to Spontaneous Adsorption of Hydroxyl Ions. *Langmuir* **1996,** *12* (8), 2045-2051.
50. Saulnier, P.; Lachaise, J.; Morel, G.; Graciaa, A., Zeta Potential of Air Bubbles in Surfactant Solutions. *J. Colloid Interface Sci.* **1996,** *182* (2), 395-399.
51. Danov, K. D., Effect of Surfactants on Drop Stability and Thin Film Drainage. In *Fluid Mechanics of Surfactant and Polymer Solutions*, Starov, V.; Ivanov, I., Eds. Springer Vienna: Vienna, 2004; pp 1-38.
52. Maldonado-Valderrama, J.; Martín-Rodriguez, A.; Gálvez-Ruiz, M. J.; Miller, R.; Langevin, D.; Cabrerizo-Vílchez, M. A., Foams and emulsions of β-casein examined by interfacial rheology. *Colloids Surf. Physicochem. Eng. Aspects* **2008,** *323* (1), 116-122.
53. Ninham, B. W.; Lo Nostro, P., *Molecular Forces and Self Assembly in Colloid, Nano Sciences and Biology*. 1 ed.; Cambridge University Press: Cambridge, 2010.
54. Karaman, M. E.; Ninham, B. W.; Pashley, R. M., Effects of Dissolved Gas on Emulsions, Emulsion Polymerization, and Surfactant Aggregation. *The Journal of Physical Chemistry* **1996,** *100* (38), 15503-15507.
55. Pashley, R. M., Effect of Degassing on the Formation and Stability of Surfactant-Free Emulsions and Fine Teflon Dispersions. *The Journal of Physical Chemistry B* **2003,** *107* (7), 1714-1720.
56. Chesters, A. K., The modelling of coalescence processes in fluid-liquid dispersions: a review of current understanding. *Chem. Eng. Res. Des.* **1991,** *69* (A4), 259-270.
57. Chen, J.-D., A model of coalescence between two equal-sized spherical drops or bubbles. *J. Colloid Interface Sci.* **1985,** *107* (1), 209-220.
58. Niewiadomski, M.; Nguyen, A. V.; Hupka, J.; Nalaskowski, J.; Miller, J. D., Air bubble and oil droplet interactions in centrifugal fields during air-sparged hydrocyclone flotation. *Int. J. Environ. Pollut.* **2007,** *30* (2), 313-331.
59. Bergeron, V.; Cooper, P.; Fischer, C.; Giermanska-Kahn, J.; Langevin, D.; Pouchelon, A., Polydimethylsiloxane (PDMS)-based antifoams. *Colloids Surf. Physicochem. Eng. Aspects* **1997,** *122* (1), 103-120.
60. Al-Shamrani, A. A.; James, A.; Xiao, H., Separation of oil from water by dissolved air flotation. *Colloids Surf. Physicochem. Eng. Aspects* **2002,** *209* (1), 15-26.
61. Hutin, A.; Argillier, J.-F.; Langevin, D., Mass Transfer between Crude Oil and Water. Part 1: Effect of Oil Components. *Energy Fuels* **2014,** *28* (12), 7331-7336.
62. Dickhout, J. M.; Moreno, J.; Biesheuvel, P. M.; Boels, L.; Lammertink, R. G. H.; de Vos, W. M., Produced water treatment by membranes: A review from a colloidal perspective. *J. Colloid Interface Sci.* **2017,** *487*, 523-534.
63. Zangaeva, E. Produced water challenges. Influence of production chemicals on flocculation. Master thesis, University of Stavanger, Stavanger, Norway, 2010.
64. Eftekhardadkhah, M.; Øye, G., Induction and Coverage Times for Crude Oil Droplets Spreading on Air Bubbles. *Environ. Sci. Technol.* **2013,** *47* (24), 14154-14160.
65. Craig, V. S. J.; Henry, C. L., Specific Ion Effects at the Air–Water Interface: Experimental Studies. In *Specific Ion Effects*, WORLD SCIENTIFIC: 2011; pp 191-214.

66. Eftekhardadkhah, M.; Aanesen, S. V.; Rabe, K.; Øye, G., Oil Removal from Produced Water during Laboratory- and Pilot-Scale Gas Flotation: The Influence of Interfacial Adsorption and Induction Times. *Energy Fuels* **2015,** *29* (11), 7734-7740.
67. Deng, S.; Bai, R.; Chen, J. P.; Yu, G.; Jiang, Z.; Zhou, F., Effects of alkaline/surfactant/polymer on stability of oil droplets in produced water from ASP flooding. *Colloids Surf. Physicochem. Eng. Aspects* **2002,** *211* (2), 275-284.
68. Gafonova, O. V.; Yarranton, H. W., The Stabilization of Water-in-Hydrocarbon Emulsions by Asphaltenes and Resins. *J. Colloid Interface Sci.* **2001,** *241* (2), 469-478.
69. Prince, M. J.; Blanch, H. W., Bubble coalescence and break-up in air-sparged bubble columns. *AlChE J.* **1990,** *36* (10), 1485-1499.
70. Mitre, J. F.; Takahashi, R. S. M.; Ribeiro, C. P.; Lage, P. L. C., Analysis of breakage and coalescence models for bubble columns. *Chem. Eng. Sci.* **2010,** *65* (23), 6089-6100.
71. Angle, C. W.; Hamza, H. A., Drop sizes during turbulent mixing of toluene–heavy oil fractions in water. *AlChE J.* **2006,** *52* (7), 2639-2650.
72. Angle, C. W.; Hamza, H. A.; Dabros, T., Size distributions and stability of toluene diluted heavy oil emulsions. *AlChE J.* **2006,** *52* (3), 1257-1266.
73. Angle, C. W.; Dabros, T.; Hamza, H. A., Predicting sizes of toluene-diluted heavy oil emulsions in turbulent flow. Part 1—Application of two adsorption kinetic models for σE in two size predictive models. *Chem. Eng. Sci.* **2006,** *61* (22), 7309-7324.
74. Angle, C. W.; Hamza, H. A., Effects of sand and process water pH on toluene diluted heavy oil in water emulsions in turbulent flow. *AlChE J.* **2009,** *55* (1), 232-242.
75. Hiemenz, P. C.; Rajagopalan, R., *Principles of Colloid and Surface Chemistry*. Third ed.; CRC Press: 1997.
76. Hutter, J. L.; Bechhoefer, J., Measurement and manipulation of van der Waals forces in atomic-force microscopy. *Journal of Vacuum Science & Technology B: Microelectronics and Nanometer Structures Processing, Measurement, and Phenomena* **1994,** *12* (3), 2251-2253.
77. Ishida, N.; Sakamoto, M.; Miyahara, M.; Higashitani, K., Attraction between Hydrophobic Surfaces with and without Gas Phase. *Langmuir* **2000,** *16* (13), 5681-5687.
78. Christenson, H. K.; Claesson, P. M., Direct measurements of the force between hydrophobic surfaces in water. *Adv. Colloid Interface Sci.* **2001,** *91* (3), 391-436.
79. Rane, J. P.; Harbottle, D.; Pauchard, V.; Couzis, A.; Banerjee, S., Adsorption Kinetics of Asphaltenes at the Oil–Water Interface and Nanoaggregation in the Bulk. *Langmuir* **2012,** *28* (26), 9986-9995.
80. Moeini, F.; Hemmati-Sarapardeh, A.; Ghazanfari, M.-H.; Masihi, M.; Ayatollahi, S., Toward mechanistic understanding of heavy crude oil/brine interfacial tension: The roles of salinity, temperature and pressure. *Fluid Phase Equilib.* **2014,** *375*, 191-200.
81. Ye, Z.; Zhang, F.; Han, L.; Luo, P.; Yang, J.; Chen, H., The effect of temperature on the interfacial tension between crude oil and gemini surfactant solution. *Colloids Surf. Physicochem. Eng. Aspects* **2008,** *322* (1), 138-141.
82. Tichelkamp, T.; Vu, Y.; Nourani, M.; Øye, G., Interfacial Tension between Low Salinity Solutions of Sulfonate Surfactants and Crude and Model Oils. *Energy Fuels* **2014,** *28* (4), 2408-2414.
83. Kourio, M. J.; Gourdon, C.; Casamatta, G., Study of drop-interface coalescence: Drainage time measurement. *Chemical Engineering & Technology* **1994,** *17* (4), 249-254.
84. He, Y.; Howes, T.; Litster, J. D.; Ko, G. H., Experimental study of drop-interface coalescence in the presence of polymer stabilisers. *Colloids Surf. Physicochem. Eng. Aspects* **2002,** *207* (1), 89-104.
85. chakibi, h.; Henaut, I.; Salonen, A.; Langevin, D.; Argillier, J.-F., Role of bubble-drop interactions and salt addition in flotation performance. *Energy & Fuels* **2018**.
86. Won, J. Y.; Krägel, J.; Makievski, A. V.; Javadi, A.; Gochev, G.; Loglio, G.; Pandolfini, P.; Leser, M. E.; Gehin-Delval, C.; Miller, R., Drop and bubble micro manipulator (DBMM)—A unique tool for mimicking processes in foams and emulsions. *Colloids Surf. Physicochem. Eng. Aspects* **2014,** *441*, 807-814.

87. Gaweł, B.; Lesaint, C.; Bandyopadhyay, S.; Øye, G., Role of Physicochemical and Interfacial Properties on the Binary Coalescence of Crude Oil Drops in Synthetic Produced Water. *Energy Fuels* **2015,** *29* (2), 512-519.
88. Bournival, G.; de Oliveira e Souza, L.; Ata, S.; Wanless, E. J., Effect of alcohol frothing agents on the coalescence of bubbles coated with hydrophobized silica particles. *Chem. Eng. Sci.* **2015,** *131*, 1-11.
89. Ren, K.; Zhou, J.; Wu, H., Materials for Microfluidic Chip Fabrication. *Acc. Chem. Res.* **2013,** *46* (11), 2396-2406.
90. Whitesides, G. M., The origins and the future of microfluidics. *Nature* **2006,** *442* (7101), 368-373.
91. Shang, L.; Cheng, Y.; Zhao, Y., Emerging Droplet Microfluidics. *Chem. Rev.* **2017,** *117* (12), 7964-8040.
92. Mashaghi, S.; Abbaspourrad, A.; Weitz, D. A.; van Oijen, A. M., Droplet microfluidics: A tool for biology, chemistry and nanotechnology. *TrAC, Trends Anal. Chem.* **2016,** *82*, 118-125.
93. Bremond, N.; Bibette, J., Exploring emulsion science with microfluidics. *Soft Matter* **2012,** *8* (41), 10549-10559.
94. Baroud, C. N.; Gallaire, F.; Dangla, R., Dynamics of microfluidic droplets. *Lab Chip* **2010,** *10* (16), 2032-2045.
95. Krebs, T.; Schroën, C. G. P. H.; Boom, R. M., Coalescence kinetics of oil-in-water emulsions studied with microfluidics. *Fuel* **2013,** *106*, 327-334.
96. Mazutis, L.; Baret, J.-C.; Treacy, P.; Skhiri, Y.; Araghi, A. F.; Ryckelynck, M.; Taly, V.; Griffiths, A. D., Multi-step microfluidic droplet processing: kinetic analysis of an in vitro translated enzyme. *Lab Chip* **2009,** *9* (20), 2902-2908.
97. Niu, X.; Gulati, S.; Edel, J. B.; deMello, A. J., Pillar-induced droplet merging in microfluidic circuits. *Lab Chip* **2008,** *8* (11), 1837-1841.
98. Zagnoni, M.; Cooper, J. M., On-chip electrocoalescence of microdroplets as a function of voltage, frequency and droplet size. *Lab Chip* **2009,** *9* (18), 2652-2658.
99. Priest, C.; Herminghaus, S.; Seemann, R., Controlled electrocoalescence in microfluidics: Targeting a single lamella. *Appl. Phys. Lett.* **2006,** *89* (13), 134101.
100. Guzman, A. R.; Kim, H. S.; de Figueiredo, P.; Han, A., A three-dimensional electrode for highly efficient electrocoalescence-based droplet merging. *Biomed. Microdevices* **2015,** *17* (2), 35.
101. Ahn, K.; Agresti, J.; Chong, H.; Marquez, M.; Weitz, D. A., Electrocoalescence of drops synchronized by size-dependent flow in microfluidic channels. *Appl. Phys. Lett.* **2006,** *88* (26), 264105.
102. Freire, S. L. S., Perspectives on digital microfluidics. *Sensors and Actuators A: Physical* **2016,** *250*, 15-28.
103. Fradet, E.; Bayer, C.; Hollfelder, F.; Baroud, C. N., Measuring Fast and Slow Enzyme Kinetics in Stationary Droplets. *Anal. Chem.* **2015,** *87* (23), 11915-11922.
104. Thiam, A. R.; Bremond, N.; Bibette, J., From Stability to Permeability of Adhesive Emulsion Bilayers. *Langmuir* **2012,** *28* (15), 6291-6298.
105. Bremond, N.; Thiam, A. R.; Bibette, J., Decompressing Emulsion Droplets Favors Coalescence. *Phys. Rev. Lett.* **2008,** *100* (2).
106. Lee, M.; Collins, J. W.; Aubrecht, D. M.; Sperling, R. A.; Solomon, L.; Ha, J. W.; Yi, G. R.; Weitz, D. A.; Manoharan, V. N., Synchronized reinjection and coalescence of droplets in microfluidics. *Lab Chip* **2014,** *14* (3), 509-13.
107. Mazutis, L.; Griffiths, A. D., Selective droplet coalescence using microfluidic systems. *Lab Chip* **2012,** *12* (10), 1800-6.
108. Muijlwijk, K.; Colijn, I.; Harsono, H.; Krebs, T.; Berton-Carabin, C.; Schroën, K., Coalescence of protein-stabilised emulsions studied with microfluidics. *Food Hydrocolloids* **2017,** *70*, 96-104.
109. Yang, L.; Wang, K.; Tan, J.; Lu, Y.; Luo, G., Experimental study of microbubble coalescence in a T-junction microfluidic device. *Microfluid. Nanofluid.* **2012,** *12* (5), 715-722.

110. Wang, J.; Tan, S. H.; Nguyen, A. V.; Evans, G. M.; Nguyen, N.-T., A Microfluidic Method for Investigating Ion-Specific Bubble Coalescence in Salt Solutions. *Langmuir* **2016,** *32* (44), 11520-11524.
111. Krebs, T.; Schroen, K.; Boom, R., A microfluidic method to study demulsification kinetics. *Lab Chip* **2012,** *12* (6), 1060-1070.
112. Krebs, T.; Schroën, K.; Boom, R., Coalescence dynamics of surfactant-stabilized emulsions studied with microfluidics. *Soft Matter* **2012,** *8* (41), 10650-10657.
113. Chen, D.; Cardinaels, R.; Moldenaers, P., Effect of Confinement on Droplet Coalescence in Shear Flow. *Langmuir* **2009,** *25* (22), 12885-12893.
114. Martin, J. D.; Marhefka, J. N.; Migler, K. B.; Hudson, S. D., Interfacial Rheology Through Microfluidics. *Adv. Mater.* **2011,** *23* (3), 426-432.
115. Zhao, C.-X.; Rondeau, E.; Cooper-White, J. J.; Middelberg, A. P. J., Microfluidic Elucidation of the Effects of Interfacial Rheology on Droplet Deformation. *Industrial & Engineering Chemistry Research* **2012,** *51* (4), 2021-2029.
116. Muijlwijk, K.; Hinderink, E.; Ershov, D.; Berton-Carabin, C.; Schroën, K., Interfacial tension measured at high expansion rates and within milliseconds using microfluidics. *J. Colloid Interface Sci.* **2016,** *470*, 71-79.
117. Honaker, L. W.; Lagerwall, J. P. F.; Jampani, V. S. R., Microfluidic Tensiometry Technique for the Characterization of the Interfacial Tension between Immiscible Liquids. *Langmuir* **2018,** *34* (7), 2403-2409.
118. Mohanty, K. K.; Saputelli, L. A., Application of "Lab-on-a-chip" Technology to The Upstream Petroleum Industry. Society of Petroleum Engineers: 2001.
119. Sinton, D., Energy: the microfluidic frontier. *Lab Chip* **2014,** *14* (17), 3127-3134.
120. Lifton, V. A., Microfluidics: an enabling screening technology for enhanced oil recovery (EOR). *Lab Chip* **2016,** *16* (10), 1777-1796.
121. Bao, B.; Riordon, J.; Mostowfi, F.; Sinton, D., Microfluidic and nanofluidic phase behaviour characterization for industrial CO2, oil and gas. *Lab Chip* **2017,** *17* (16), 2740-2759.
122. Mostowfi, F.; Molla, S.; Tabeling, P., Determining phase diagrams of gas-liquid systems using a microfluidic PVT. *Lab on a Chip - Miniaturisation for Chemistry and Biology* **2012,** *12* (21), 4381-4387.
123. Luther, S. K.; Stehle, S.; Weihs, K.; Will, S.; Braeuer, A., Determination of Vapor–Liquid Equilibrium Data in Microfluidic Segmented Flows at Elevated Pressures Using Raman Spectroscopy. *Anal. Chem.* **2015,** *87* (16), 8165-8172.
124. Fisher, R.; Shah, M. K.; Eskin, D.; Schmidt, K.; Singh, A.; Molla, S.; Mostowfi, F., Equilibrium gas-oil ratio measurements using a microfluidic technique. *Lab Chip* **2013,** *13* (13), 2623-33.
125. Bao, B.; Riordon, J.; Xu, Y.; Li, H.; Sinton, D., Direct Measurement of the Fluid Phase Diagram. *Anal. Chem.* **2016,** *88* (14), 6986-6989.
126. Song, W.; Fadaei, H.; Sinton, D., Determination of Dew Point Conditions for CO2 with Impurities Using Microfluidics. *Environ. Sci. Technol.* **2014,** *48* (6), 3567-3574.
127. Sullivan, M. T.; Angelescu, D. E., Microfluidic Bubble Point Measurement Using Thermal Nucleation. *Energy Fuels* **2016,** *30* (4), 2655-2661.
128. Fadaei, H.; Shaw, J. M.; Sinton, D., Bitumen–Toluene Mutual Diffusion Coefficients Using Microfluidics. *Energy Fuels* **2013,** *27* (4), 2042-2048.
129. Fadaei, H.; Scarff, B.; Sinton, D., Rapid Microfluidics-Based Measurement of CO2 Diffusivity in Bitumen. *Energy Fuels* **2011,** *25* (10), 4829-4835.
130. Nguyen, P.; Mohaddes, D.; Riordon, J.; Fadaei, H.; Lele, P.; Sinton, D., Fast fluorescence-based microfluidic method for measuring minimum miscibility pressure of CO2 in crude oils. *Anal. Chem.* **2015,** *87* (6), 3160-4.
131. Schneider, M. H.; Sieben, V. J.; Kharrat, A. M.; Mostowfi, F., Measurement of Asphaltenes Using Optical Spectroscopy on a Microfluidic Platform. *Anal. Chem.* **2013,** *85* (10), 5153-5160.

132. Sieben, V. J.; Tharanivasan, A. K.; Andersen, S. I.; Mostowfi, F., Microfluidic Approach for Evaluating the Solubility of Crude Oil Asphaltenes. *Energy Fuels* **2016,** *30* (3), 1933-1946.
133. Hu, C.; Morris, J. E.; Hartman, R. L., Microfluidic investigation of the deposition of asphaltenes in porous media. *Lab Chip* **2014,** *14* (12), 2014-2022.
134. Molla, S.; Magro, L.; Mostowfi, F., Microfluidic technique for measuring wax appearance temperature of reservoir fluids. *Lab Chip* **2016,** *16* (19), 3795-3803.
135. Bowden, S. A.; Monaghan, P. B.; Wilson, R.; Parnell, J.; Cooper, J. M., The liquid-liquid diffusive extraction of hydrocarbons from a North Sea oil using a microfluidic format. *Lab Chip* **2006,** *6* (6), 740-743.
136. Floquet, C. F. A.; Sieben, V. J.; MacKay, B. A.; Mostowfi, F., Determination of boron concentration in oilfield water with a microfluidic ion exchange resin instrument. *Talanta* **2016,** *154*, 304-311.
137. He, K.; Xu, L.; Gao, Y.; Neeves, K. B.; Yin, X.; Bai, B.; Ma, Y.; Smith, J., Validating Surfactant Performance in the Eagle Ford Shale: A Correlation between the Reservoir-on-a-Chip Approach and Enhanced Well Productivity. In *SPE Improved Oil Recovery Symposium*, Society of Petroleum Engineers: Tulsa, Oklahoma, USA, 2014.
138. Howe, A. M.; Clarke, A.; Mitchell, J.; Staniland, J.; Hawkes, L.; Whalan, C., Visualising surfactant enhanced oil recovery. *Colloids Surf. Physicochem. Eng. Aspects* **2015,** *480*, 449-461.
139. Howe, A. M.; Clarke, A.; Giernalczyk, D., Flow of concentrated viscoelastic polymer solutions in porous media: effect of MW and concentration on elastic turbulence onset in various geometries. *Soft Matter* **2015,** *11* (32), 6419-6431.
140. Ma, K.; Liontas, R.; Conn, C. A.; Hirasaki, G. J.; Biswal, S. L., Visualization of improved sweep with foam in heterogeneous porous media using microfluidics. *Soft Matter* **2012,** *8* (41), 10669-10675.
141. Conn, C. A.; Ma, K.; Hirasaki, G. J.; Biswal, S. L., Visualizing oil displacement with foam in a microfluidic device with permeability contrast. *Lab Chip* **2014,** *14* (20), 3968-3977.
142. Dong, M.; Liu, Q.; Li, A., Displacement mechanisms of enhanced heavy oil recovery by alkaline flooding in a micromodel. *Particuology* **2012,** *10* (3), 298-305.
143. de Haas, T. W.; Fadaei, H.; Guerrero, U.; Sinton, D., Steam-on-a-chip for oil recovery: the role of alkaline additives in steam assisted gravity drainage. *Lab Chip* **2013,** *13* (19), 3832-3839.
144. Xu, L.; Abedini, A.; Qi, Z.; Kim, M.; Guerrero, A.; Sinton, D., Pore-scale analysis of steam-solvent coinjection: azeotropic temperature, dilution and asphaltene deposition. *Fuel* **2018,** *220*, 151-158.
145. Xu, K.; Zhu, P.; Huh, C.; Balhoff, M. T., Microfluidic Investigation of Nanoparticles' Role in Mobilizing Trapped Oil Droplets in Porous Media. *Langmuir* **2015,** *31* (51), 13673-13679.
146. Nguyen, P.; Fadaei, H.; Sinton, D., Pore-Scale Assessment of Nanoparticle-Stabilized CO2 Foam for Enhanced Oil Recovery. *Energy Fuels* **2014,** *28* (10), 6221-6227.
147. Mostowfi, F.; Czarnecki, J.; Masliyah, J.; Bhattacharjee, S., A microfluidic electrochemical detection technique for assessing stability of thin films and emulsions. *J. Colloid Interface Sci.* **2008,** *317* (2), 593-603.
148. Morin, B.; Liu, Y.; Alvarado, V.; Oakey, J., A microfluidic flow focusing platform to screen the evolution of crude oil-brine interfacial elasticity. *Lab Chip* **2016,** *16* (16), 3074-3081.
149. Nowbahar, A.; Whitaker, K. A.; Schmitt, A. K.; Kuo, T.-C., Mechanistic Study of Water Droplet Coalescence and Flocculation in Diluted Bitumen Emulsions with Additives Using Microfluidics. *Energy Fuels* **2017**.
150. Lam, K. F.; Sorensen, E.; Gavriilidis, A., Review on gas–liquid separations in microchannel devices. *Chem. Eng. Res. Des.* **2013,** *91* (10), 1941-1953.
151. Yue, J.; Chen, G.; Yuan, Q.; Luo, L.; Gonthier, Y., Hydrodynamics and mass transfer characteristics in gas–liquid flow through a rectangular microchannel. *Chem. Eng. Sci.* **2007,** *62* (7), 2096-2108.

152. Constantinou, A.; Barrass, S.; Gavriilidis, A., CO2 Absorption in Polytetrafluoroethylene Membrane Microstructured Contactor Using Aqueous Solutions of Amines. *Industrial & Engineering Chemistry Research* **2014,** *53* (22), 9236-9242.
153. Ciceri, D.; Perera, J. M.; Stevens, G. W., A study of molecular diffusion across a water/oil interface in a Y–Y shaped microfluidic device. *Microfluid. Nanofluid.* **2011,** *11* (5), 593-600.

Paper 1

Influence of the Crude Oil and Water Compositions on the Quality of Synthetic Produced Water

energy&fuels

Article

pubs.acs.org/EF

Influence of the Crude Oil and Water Compositions on the Quality of Synthetic Produced Water

Marcin Dudek,[†] Eugénie Kancir,[‡] and Gisle Øye*[,†]

[†]Ugelstad Laboratory, Department of Chemical Engineering, Norwegian University of Science and Technology (NTNU), Sem Sælandsvei 4, 7491 Trondheim, Norway

[‡]National Graduate School of Engineering (ENSICAEN), 6 Boulevard Maréchal Juin, 14000 Caen, France

Supporting Information

ABSTRACT: Produced water originates from crude oil production. It is a mixture of organic and inorganic compounds, and its composition is highly oilfield-dependent. The present study was carried out to increase the understanding of the effects of the relationships between the crude oil properties and the composition of the aqueous phase on the quality of the produced water. Brines with different compositions and pH levels were mixed with five crude oils. Initially, the physicochemical properties and compositions of the crude oils were determined, and the qualities of samples of synthetic produced water were described by parameters such as the total oil concentration, total organic carbon content, pH, drop size distribution, and Sauter mean diameter. Analysis of the characterization data revealed that the crude oils fell into two categories: light and heavier oils. Most parameters such as density, viscosity, total acid number (TAN), and composition reflected this division. A similar pattern was sustained for the water-quality analyses. Water produced with heavier crude oils generally contained higher concentrations of emulsified oil with the largest and most polydisperse droplets. Light oils had a tendency to create water-in-oil emulsions between the oil and water phases, which impeded the phase separation, resulting in less free water. The Sauter mean drop diameters were found to increase with the pH of the water phase. However, the presence of calcium at the highest pH decreased the droplet size and the amount of free water, compared to the results obtained using brine without divalent ions, in agreement with the interfacial role of naphthenic acids in crude oil emulsions. The results showed the significance of both the water and oil compositions on the quality of the produced water, which can lead to an improved fundamental understanding of the process for treating produced water.

INTRODUCTION

During the production of crude oil and gas, the largest byproduct of the extraction process is produced water. The water cut depends on the location of the reservoir and the age of the production wells and can vary from a few percent in the beginning of the exploitation of a reservoir to more than 95% in the last phases of production. Global estimates state that, for every barrel of crude oil, three barrels of water are produced.[1]

There are two main pathways for the disposal of produced water. One is discharge of the water into the sea. Before the water can be discharged, however, it needs to undergo treatment processes to reach a certain quality level, specified by local environmental regulations. Depending on the location, the maximum average oil-in-water (OIW) content for disposal is between 30 and 40 ppm.[2] The second disposal option, reinjection, can be carried out by pumping the water into a disposal or production reservoir. The latter is more desirable from technological and economic points of view, as it can sustain the production pressure of the reservoir.[3] The reinjection of produced water is also likely to be the preferred method of handling the water in subsea production and processing facilities. However, the process also carries several risks, for instance, reservoir souring or formation damage due to reduced injectivity. Furthermore, emulsified oil droplets and suspended solid particles in the produced water can block the pores in the reservoir and decrease the permeability of the formation. This means that the requirements for the quality of the produced water are strict for both the discharge and reinjection options.[4]

Methods for the treatment of produced water can be divided into three types. The primary separation relies on the bulk phase separation of gas, crude oil, and water, using a conventional or modified gravity separator. In this step, the OIW concentration in the outlet water can range from 100 to 1000 ppm.[5] The secondary treatment usually consists of hydrocyclones or gas flotation units. Both of these technologies are capable of lowering the oil-in-water concentration below the discharge limit.[6−8] A tertiary treatment (or water-polishing step) can be performed to reduce the concentration of dissolved components through media filtration or adsorption processes.[6,9,10] Novel techniques such as ultrafiltration,[11] nanofiltration and reverse osmosis,[12,13] and biological treatment[1,14] are also considered to be promising water-polishing methods.

Produced water contains dissolved salts, dispersed solids, and dissolved and dispersed crude oil components, as well as traces of heavy metals and radioactive materials.[9] Additionally, chemicals added during different stages of production affect the quality and properties of the produced water.[15,16] The composition of the produced water is field-dependent, as the

Received: December 12, 2016
Revised: March 2, 2017
Published: March 7, 2017

DOI: 10.1021/acs.energyfuels.6b03297
Energy Fuels 2017, 31, 3708−3716

location of the reservoir determines its conditions (pressure, temperature), reservoir rock, and type of the produced oil. The conditions of the reservoir mostly affect the water solubilities of salts dissolved from the rock formation, gases, and indigenous crude oil compounds. In addition, the conditions of the reservoir also change as oil production proceeds, especially when seawater is injected or enhanced oil recovery techniques are employed.

The chemical composition of the crude oil has an effect on the quality of the produced water, with respect to both dispersed and dissolved components. Typically, crude oil is characterized by physical properties, such as density and viscosity, and chemical properties, such as total acid and base numbers and SARA (saturates, aromatics, resins, asphaltenes) composition. The interfacial activities of the components in crude oils are affected by these parameters and can lead to increased emulsion stability and problems with separation.[17,18] It has been shown that the interfacial properties can influence the coalescence of oil droplets[19] and the stability of oil-in-water emulsions.[20,21] Once in contact with an aqueous phase, water-soluble hydrocarbons in the crude oil partition into the water phase,[22−24] adsorb at gas−water interfaces, and influence the efficiency of oil removal by gas flotation.[25,26] The characteristics of the produced water also depend on properties such as pH,[27,28] ionic strength,[29] and the presence of divalent ions.[30]

The aim of this work was to investigate the effect of the water and crude oil properties on the quality of produced water. First, the physicochemical and interfacial properties of five crude oils were studied. Then, the oils were mixed with water with different pH values and ionic compositions. After separation of the mixtures, the quality of the synthetic produced water (i.e., free water) was determined in terms of the total organic carbon, pH, total oil concentration, and drop size distribution of the dispersed oil. The preparation conditions were kept the same for all of the samples to enhance the influence of the crude oil properties and water composition on the quality of the synthetic produced water.

MATERIALS AND METHODS

Crude Oil Characterization. *Crude Oils.* Five dead (i.e., stored at ambient pressure and temperature) crude oils from the Norwegian Continental Shelf were analyzed and used as received.

Density Measurements. The densities of the crude oils were measured at 20 °C, using a DMA 5000 laboratory density meter (Anton Paar, Graz, Austria).

Viscosity Measurements. The viscosities of the crude oils were measured at 20 °C, using an MCR 301 laboratory rheometer (Anton Paar, Graz, Austria) with a cylindrical geometry (CC-27).

Measurements of Total Acid and Base Numbers. Analysis of the total acidic number (TAN) was performed according to the ASTM method D664-95.[31] The total base number (TBN) was evaluated by a method similar to that presented by Dubey and Doe.[32] Both methods were described in detail previously.[33] In short, TAN was determined by titrating a solution of crude oil in a 100:99:1 (v/v) toluene/isopropanol/water mixture with a 0.1 M solution of tetrabutylammonium hydroxide in a 10:1 mixture of isopropanol and methanol (Sigma-Aldrich). To measure the TBN, a solution of crude oil dissolved in methylisobutyl ketone was titrated with a 0.025 M solution of perchloric acid in acetic acid. In both cases, the titration was controlled with a Titrando unit (Metrohm, Herisau, Switzerland), connected to a 6.0229.100 LL solvotrode.

High-Performance Liquid Chromatography (HPLC) Fractionation. The procedure for the fractionation of the crude oils into saturates, aromatics, resins, and asphaltenes (SARA) was previously reported by Hannisdal et al.[34] Specifically, 4 g of crude oil was dissolved in 160 mL of *n*-hexane (CHROMANORM for HPLC, VWR). The solutions were mixed overnight and then filtered with a 0.45-μm membrane filter (Millipore HVLP) to isolate the asphaltene fraction. An HPLC system with two columns (unbonded silica and amino) was used to fractionate the filtered maltenes into saturate, aromatic, and resin fractions. After controlled evaporation of the solvent in a N_2 atmosphere, the weight percentages of the fractions were determined gravimetrically.

Interfacial Tension Measurements. Measurements of the interfacial tension (IFT) were performed using a pendant drop tensiometer (PAT-1M, Sinterface Technologies, Berlin, Germany). Images of a crude oil drop immersed in a brine solution were recorded over time. The measurements lasted until near-equilibrium values were reached. This usually took less than 7 h for the light oils, whereas it often exceeded 16 h for the heavier crude oils (an example of the evolution of the dynamic interfacial tension is shown in Figure S1 of the Supporting Information). Values for the interfacial tension were calculated by fitting the drop profiles to the Young−Laplace equation. The reported IFT values are averages of at least two measurements. All measurements were performed at room temperature (22 °C).

Elemental Composition Analysis. The contents of carbon, hydrogen, nitrogen, oxygen, and sulfur were determined for the crude oils and each of their SARA fractions. The analyses were performed using an EA 1108 elemental analyzer (Fisons Instruments) at the Oil and Gas Institute−National Research Institute in Krakow, Poland.

Water Content. The amounts of water in the as-received crude oils were analyzed by Karl Fischer titration, using a KF Coulometer 831 (Metrohm, Herisau, Switzerland).

Preparation and Characterization of Synthetic Produced Water. *Brine Solutions.* Two types of brines were used during this study to simulate high-salinity conditions and to study the influence of divalent ions on the quality of the produced water. The first contained only NaCl (Emsure, Merck Millipore) and is referred to as Na-Brine. The other was a mixture of NaCl and $CaCl_2{\cdot}2H_2O$ (p.a., Sigma-Aldrich) with a molar ratio of sodium to calcium equal to 35:1 and is referred to as NaCa-Brine. The ionic strength was kept the same in both brines (I = 0.59 M). The salt concentrations were similar to seawater conditions, but the produced waters from the Norwegian Continental Shelf were reported to be of comparable salinity.[35] The solutions were adjusted to pH 3 and 10, using solutions of dilute HCl (AnalaR, VWR) and dissolved NaOH (AnalaR, VWR). The natural pH of the brines ranged from 5.9 to 6.4 and is later referred to as pH 6. Deionized water (Millipore Simplicity Systems, Darmstadt, Germany) was used to prepare all solutions.

Preparation of Produced Water. To prepare each sample of produced water, 100 mL of brine and 100 mL of crudeoil were poured into a 250 mL aspirator bottle and mixed for 8 min at 20000 rpm, using an Ultra-Turrax S25N-10G homogenizer (IKA, Königswinter, Germany). The samples were left to phase separate for 2 h, before the water phase was collected through the bottom outlet of the aspirator bottle. The amount of free water obtained after 2 h was recorded. From the collected water phase (later referred to as the synthetic produced water), the drop size distribution, total oil concentration, and pH of this synthetic produced water were determined. Each sample was prepared and analyzed at least three times. All of the steps were performed at room temperature (22 °C).

Drop Size Measurements. The drop sizes in the water phase were analyzed within 5 min after sampling using a Nikon LV 100D microscope. Between 10 and 12 pictures were captured per sample, and Image-Pro Plus 5.0 software was used to determine drop size distributions and Sauter mean diameters, which were calculated as

$$d_{32} = \frac{\sum d_i^3}{\sum d_i^2} \quad (1)$$

where d_{32} is the Sauter mean diameter and d_i is the diameter of drop i, detected by the software. Only drops with diameters of less than 30 μm were considered.

DOI: 10.1021/acs.energyfuels.6b03297
Energy Fuels 2017, 31, 3708−3716

Table 1. Physicochemical Properties and Compositions of Crude Oils

	crude oils				
	A	B	C	D	E
API gravity (deg)	19.2	35.8	23.0	36.3	37.9
density at 20 °C (g/cm^3)	0.935	0.841	0.911	0.839	0.831
viscosity at 20 °C (mPa s)	354.4	14.2	74.4	10.3	8.3
TAN (mg of KOH/g of oil)	2.2	<0.1	2.7	0.2	0.5
TBN (mg of KOH/g of oil)	2.8	1.0	1.1	1.1	0.4
SARA composition [% (w/w)]					
saturates	50.6	84.0	64.9	71.5	74.8
aromatics	31.2	13.4	26.3	23.1	23.2
resins	15.7	2.3	8.4	5.1	1.9
asphaltenes	2.5	0.3	0.4	0.3	0.1
water content (ppm)	590.9	85.4	535.8	202.4	333.4
IFT at pH 6 (mN/m)					
Na-Brine	20.4 ± 0.6	20.5 ± 0.2	22.2 ± 0.6	19.0 ± 0.5	19.9 ± 0.1
NaCa-Brine	18.6 ± 0.8	19.9 ± 0.2	18.9 ± 0.7	16.2 ± 0.4	17.4 ± 0.4

Total Oil Concentration. An appropriate amount of methylene chloride (HiPerSolv CHROMANORM for HPLC, VWR) was added to the water phase, and the mixture was shaken to extract the dispersed and dissolved crude oil components into the organic phase. The two phases were then separated in a separation funnel. The organic phase was collected, and UV analysis was performed to determine the amount of oil using a UV−vis spectrophotometer (UV-2401PC, Shimadzu, Kyoto, Japan). Calibration curves, prepared individually for each crude oil, were used to calculate the oil concentration from the absorbance at 259 nm.

pH Measurements. The pH values of the water phases were measured using a pH meter (SevenEasy pH, Mettler-Toledo, Greifensee, Switzerland). Prior to the measurements, the oil drops were removed by centrifugation (Heraeus Multifuge X3R, Thermo Scientific, Waltham, MA).

Total Organic Carbon (TOC) Analysis. Approximately 50 mL of brine and 50 mL of crude oil were poured into Schott bottles and put on a vertical shaker (200 rpm) for 24 h to saturate the water phase with the water-soluble oil components. Subsequently, the aqueous phase was sampled, centrifuged (Heraeus Multifuge X3R, Thermo Scientific, Waltham, MA), and acidified to pH < 2 with sulfuric acid (95−97% p.a., Sigma-Aldrich). TOC analyses were then performed using a TOC-L$_{CPH}$ Analyzer (Shimadzu, Kyoto, Japan). These analyses were performed at GIG Research Institute in Katowice, Poland.

RESULTS AND DISCUSSION

Crude Oil Characterization. The physicochemical properties and compositions of the crude oils are presented in Table 1. Based on the API gravities, the crude oils were divided into light oils, with API values of ca. 36−38 (B, D, and E), and heavier oils, with API values of 19.2 and 23 (A and C). The heavier oils were characterized by significantly lower contents of the saturate fraction and higher TANs (greater than 2 mg of KOH/g of oil) than the other oils. Furthermore, their substantial contents of polar components (resins and asphaltenes) provided higher densities and viscosities. The light oils consisted of low amounts of acidic and basic components. In addition, they had similar values of density and viscosity; the lowest water contents; and some variations in the saturate, aromatic, and resin contents.

More detailed insight into the compositions of the crude oils was provided by the elemental analysis of all of the fractions, as previously demonstrated by Gaweł et al.[33] The C/H atomic ratios of the crude oils are shown in Figure 1. The division into light and heavier crude oils can also be noticed here, as crude oils A and C had higher C/H ratios (0.62 and 0.59, respectively) than the remaining crude oils (ca. 0.55). The C/H atomic ratios in the saturate fractions were slightly higher for the heavier crude oils (0.52−0.53) than for the light oils (ca. 0.5). The saturate fractions are usually expected to contain straight-chain, branched, and cyclic aliphatic hydrocarbons, but this could suggest that the heavier crude oils also contained some compounds with unsaturated moieties. The fractions of aromatics and resins had C/H ratios of comparable values for most of the oils, which indicated similar aromacities with analogous extents of methylene moieties in the two fractions. The greatest variation was observed for the asphaltenes. Crude oils A and C had the highest aromaticities in this fraction, whereas the aromaticities were lower for the lighter crudes. The surprisingly low value for crude oil E might be due to oxidation of the sample (see below).

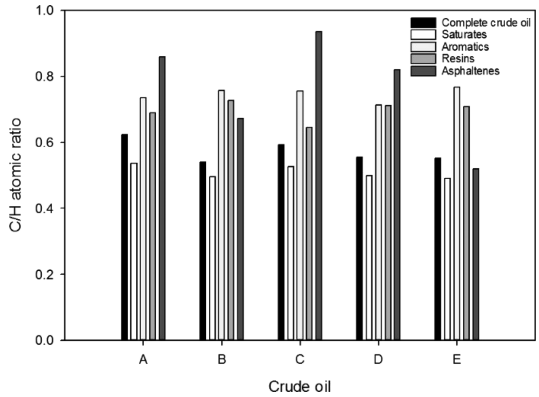

Figure 1. C/H atomic ratios of the crude oils and their fractions.

Figure 2 shows the amounts of nitrogen, oxygen, and sulfur in the complete crude oils and their SARA fractions. The amount of nitrogen in crude oil D was considerably higher than the amounts in the rest of the oils (Figure 2A). No nitrogen was detected in the saturate fractions of the crude oils, whereas the aromatic and resin fractions contained similar amounts of nitrogen. The asphaltene fractions contained the highest nitrogen amounts for crude oils A and C. For the lighter oils, however, the highest nitrogen content was seen in the resin fraction. The oxygen contents were similar in all of the crude

DOI: 10.1021/acs.energyfuels.6b03297
Energy Fuels 2017, 31, 3708−3716

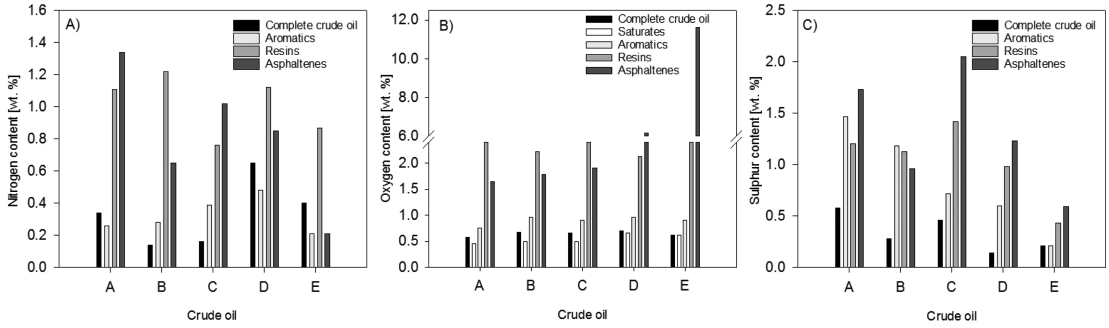

Figure 2. (A) Nitrogen, (B) oxygen, and (C) sulfur contents of complete crude oils and their SARA fractions.

oils (Figure 2B). Furthermore, the saturate and aromatic fractions had comparable and relatively low amounts of oxygen, whereas the two most polar fractions contained significantly more of this element. Most of the light crude oils had higher amounts of oxygen in the asphaltene fractions than in the resin fractions, which agrees with the observations made by Gawel et al.[33] The crude oils with the highest viscosities (A and C) tended to have larger amounts of sulfur (Figure 2C). This trend was also seen in the SARA fractions, where all of the fractions of the heavier crudes contained more sulfur, with the exception of crude oil B, which had a very high content of sulfur in the aromatics fraction. Similarly to nitrogen, no sulfur was detected in the saturate fractions of any of the crude oils.

The IFT values of the crude oils varied from 19 to 20.5 mN/m for Na-Brine and from 16.2 to 19.9 mN/m for NaCa-Brine. The lowering of the IFT when calcium was present in the aqueous phase suggested that the acidic components play some role in the interfacial properties, as dissociated acids can form complexes with Ca^{2+}.[36,37] However, no quantitative relationships were found between the IFT and the TAN. Asphaltenes are also known to reduce the IFT.[38] An interesting observation in this respect is that slightly lower interfacial tension values were obtained for the two crude oils (D and E) with the highest contents of nitrogen. These crude oils also had significantly higher contents of oxygen in their asphaltene fractions. An inverse dependence was observed for sulfur, as crude oils A−C had the highest values of the IFT. These observations were in agreement with previous findings.[39]

Separation. Figure 3 shows that the total amounts of free water observed after 2 h of gravity separation varied between the samples but generally increased when the initial pH of the Na-Brine increased. A similar trend was noticed for NaCa-Brine (Figure S2, Supporting Information). The amounts of water recovered were higher for the samples with heavier crudes than for the samples prepared from the lighter crude oils at the two lowest pHs. This was likely due to the formation of stable water-in-oil emulsion layers that reduced the amounts of water recovered in the latter samples; however, the size distributions of the water drops might have also played a role. A similar trend was not seen at the highest pH, where the difference in the amounts of recovered water varied less between the samples. Furthermore, whereas the amount of recovered water was more or less independent of the ionic composition at the lowest pHs, the amount of recovered water decreased in the presence of calcium ions at pH 10, as seen in Table 2. The reduction ranged from a few percent (crude oils A and D) to almost 30% (crude oils C and E).

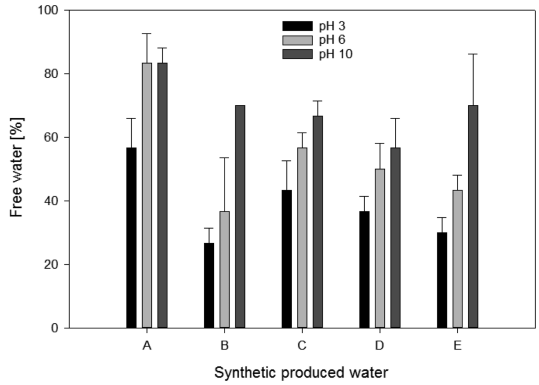

Figure 3. Percentages of free water observed 2 h after mixing the crude oils with Na-Brine at various pH values.

Table 2. Amounts of Water Recovered after Mixing Crude Oils and Brines at pH 10

	recovered water (%)	
crude oil	Na-Brine	NaCa-Brine
A	83.3 ± 4.7	76.7 ± 4.7
B	70.0 ± 0	56.7 ± 17
C	66.7 ± 4.7	43.3 ± 4.7
D	56.7 ± 9.4	46.7 ± 9.4
E	70.0 ± 16.3	46.7 ± 12.5

The higher water-in-oil emulsion stability for the systems with the lighter crude oils was explained by the high saturate and low aromatic contents in these oils. This can facilitate increased interfacial activity, as well as the aggregation of asphaltenes, resulting in rigid interfacial layers that enhance the emulsion stability.[19,38,40] It was also argued by other authors that wax particles, often found in light crude oils, can increase the emulsion stability.[41] The pH of the aqueous phase can also influence the rigidity or viscoelasticity of interfacial films and, thereby, the emulsion stability. At low pH, competitive adsorption of protonated naphthenic acids and molecules of resins and asphaltenes was reported to form rigid interfacial layers that oppose the coalescence of crude oil drops.[42] Increased pH causes dissociation of the naphthenic acids, which enhances their interfacial activity and their water solubility. The replacement of molecules causing interfacial rigidity by

DOI: 10.1021/acs.energyfuels.6b03297
Energy Fuels 2017, 31, 3708−3716

dissociated naphthenic acids has been proposed as a reason for decreased emulsion stability.[42] Furthermore, the partitioning of naphthenic acids into the aqueous phase has also been found to reduce interfacial film stability.[43] Here, the presence of divalent ions increased the emulsion stability at the highest pH. This indicates that sufficient dissociated acids at the interface underwent complexation with calcium and strengthened the interfacial film. As mentioned above, another contributing factor for the differences in the stabilities of the water-in-oil emulsions might have been the size distributions of the water droplets. Crude oils with higher viscosities require longer mixing times, in comparison with less viscous oils, to reach comparable water droplet size distribution.[44] As the mixing time here was constant for all of the samples, it is possible that large enough water droplets were present in the heavier crude oils to give higher amounts of recovered water as a result of faster sedimentation.

Quality of the Produced Water. The total organic carbon content, representing the water-soluble crude oil components, in the synthetic produced water from NaCa-Brine varied from about 20 to 70 ppm between the samples, as can be seen in Figure 4. Similar trends, with slightly lower TOC values, were

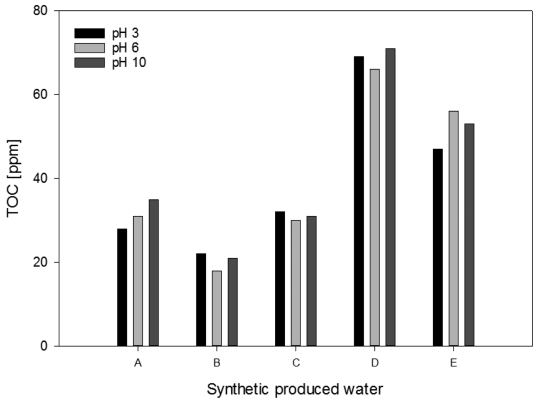

Figure 4. Total organic carbon contents of water samples produced with different crude oils (NaCa-Brine).

observed in the samples from the Na-Brine (Figure S3, Supporting Information). The highest values of TOC were found in the synthetic produced water prepared from crude oils D and E. Notably, these crude oils stood out with considerably higher oxygen contents in the asphaltene fractions than the other oils. This could suggest improved water solubility of the smallest compounds in the asphaltene fractions.[21] Similar observations were made previously,[45] where the amount of oxygen in the asphaltene fraction was found to affect its water solubility.

The composition of the crude oil was also found to have an impact on the pH of the synthetic produced water (Figure 5). When the initial pH of the brine was 3, most of the samples displayed a slight increase in the pH. For the produced water from crude oil A, however, the pH was noticeably higher. The significantly higher TBN in the corresponding crude oil might promote more extensive partitioning of the basic components into the aqueous phase. When the initial pH of the brine was 6, the produced-water samples experienced either a small decline or a small increase in the final pH value. However, in this pH range, even the smallest concentration of dissociated species can cause a noticeable change in the pH. The effect of dissolved CO_2 would also be most noticeable in this range. All water samples experienced a considerable decrease in pH (down to 6−7) when the brine was initially at pH 10. This agrees with the higher water solubility of the acidic components in the crude oils.[27] It is worth pointing out that the water produced with crude oil C showed a lower pH value than the other samples with brines at pH 6 and 10, corresponding to a high TAN value for this crude oil. Overall, these results show that the type of compounds that partitioned into the aqueous phase depended on the initial pH of the brine for all of the crude oils. When the pH was low, the solubility of the basic components increased, whereas the brines with higher pH levels raised the water solubilities of the molecules with acidic groups. The results also resembled those from a study on the mass transfer between crude oil and water performed by Hutin et al.[24] The authors introduced a model for quantifying the effects of the partitioning of acidic and basic components from the oil phase on the final pH of the aqueous phase. Generally, the results indicated that acidic components were more water-soluble in the tested pH range and were in agreement with the mentioned paper. Even when the TAN values of the crude oils were low (0.5 mg of KOH/g of oil or less), the final pH of aqueous phase dropped from 10 to 6−7. Similar observations were not made for the TBN values. At the low initial pH, only crude oil A had significant partitioning of basic components into the aqueous phase. This crude oil not only had the highest TBN value, but also contained the highest amount of asphaltenes and resins. Furthermore, it had the highest nitrogen content in the asphaltene fraction, which could explain the increase in pH.

As seen in Figure 6, a marked difference in the oil-in-water concentration was observed between the produced waters from the light and heavier oils. The water from the heavier crude oils usually contained between 100 and 500 ppm of oil, whereas the light crude oils gave water with less than 100 ppm of oil. The increased amount of oil in the produced water from the heaviest crude oils was seen only at high pH when calcium was present. Both of these crude oils had significantly higher TAN values, traditionally used as an indicator of the content of naphthenic acids. As discussed previously, increased pH causes dissociation of the naphthenic acids and their enhanced interfacial activity. The presence of calcium enabled the formation of complexes, which could accumulate at the oil/water interface and stabilize the system. The relatively high standard deviations in the produced-water samples from the heavier oils (A and C) were due to difficulties when sampling the water phase after separation. The viscous crude oils tended to get stuck in the outlet and distorted the oil-in-water concentration results.

Representative microscopy images of selected produced-water samples are shown in Figure 7. The produced-water sample prepared from heavy crude oil A (Figure 7A) contained more and larger drops than the sample produced from light crude oil E (Figure 7B). This also represented the major difference between the produced-water samples from the heavy and light crude oils.

The corresponding drop size distributions are shown in Figure 8. The drop size distribution in the synthetic produced water from crude oil A was broad. Even though the overall number of drops larger than 10 μm was low (less than 10% of the total number of detected drops), these drops made a considerable contribution to the volume distribution (ca. 50%).

DOI: 10.1021/acs.energyfuels.6b03297
Energy Fuels 2017, 31, 3708−3716

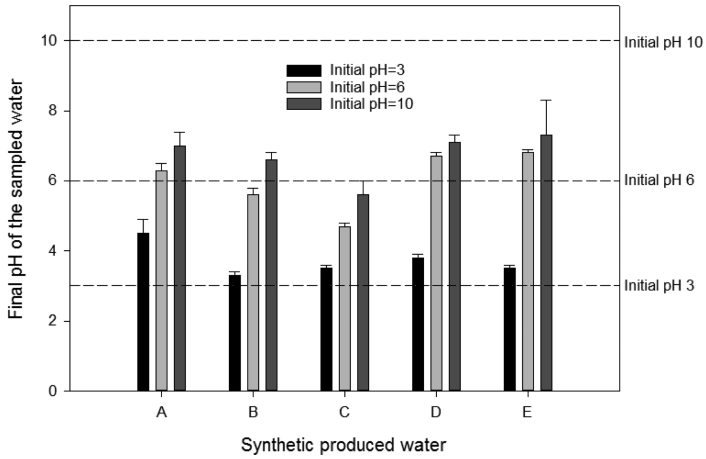

Figure 5. pH values of the synthetic produced waters prepared using Na-Brine at different initial brine pH values, as indicated by the dotted lines.

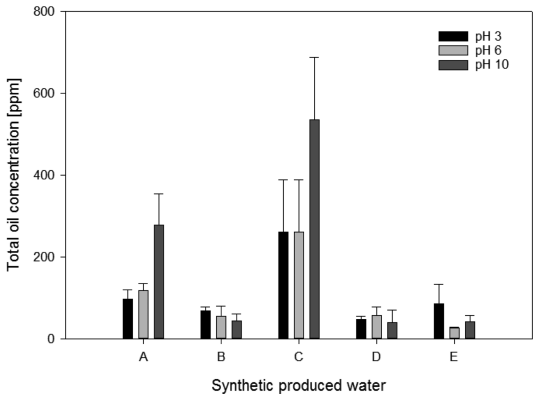

Figure 6. Total oil concentrations in the synthetic produced-water samples prepared using NaCa-Brine at different initial brine pH values.

The water samples produced from crude oil E had a narrower size distribution, where the great majority of drops (number-wise, more than 70%) were smaller than or equal to 5 μm. Furthermore, the volume contribution of drops larger than 10 μm was negligible. The increased polydispersity in the emulsions when the viscosity of the dispersed phase was higher agrees with other reports,[20,46] even though the measurements were done after 2 h of gravity separation. When the viscosity of the dispersed phase increases, the drop breakage regime can shift from bursting to stretching, which can lead to broadening of the size distribution,[46] as observed in this study. Additionally, the increased contents of polar components in oils A and C could have played a role in the stabilization of larger crude oil droplets in the water phase.

The Sauter mean diameters of the oil drops were generally lowest in the synthetic water produced at low pH and increased with pH, as seen in Figure 9. This trend was less clear for the samples prepared with NaCa-Brine (Figure S4, Supporting Information). The average Sauter diameter of drops in the produced water from the heaviest crude oils (A and C) was 20−50% larger than those in the samples prepared with the light oils. Higher creaming velocities of drops created with the light crude oils (due to the higher density difference between the dispersed and continuous phases) could have contributed

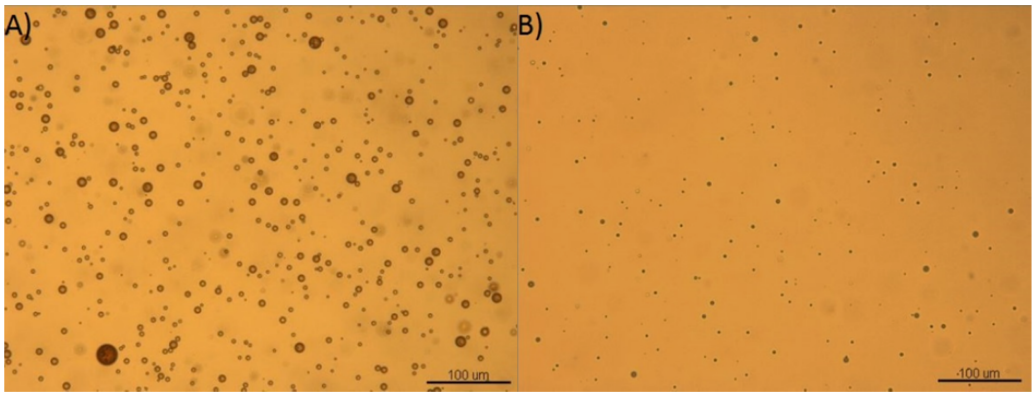

Figure 7. Pictures of dispersed droplets in water from (left) crude oil A and (right) crude oil E in Na-Brine at pH 6.

DOI: 10.1021/acs.energyfuels.6b03297
Energy Fuels 2017, 31, 3708−3716

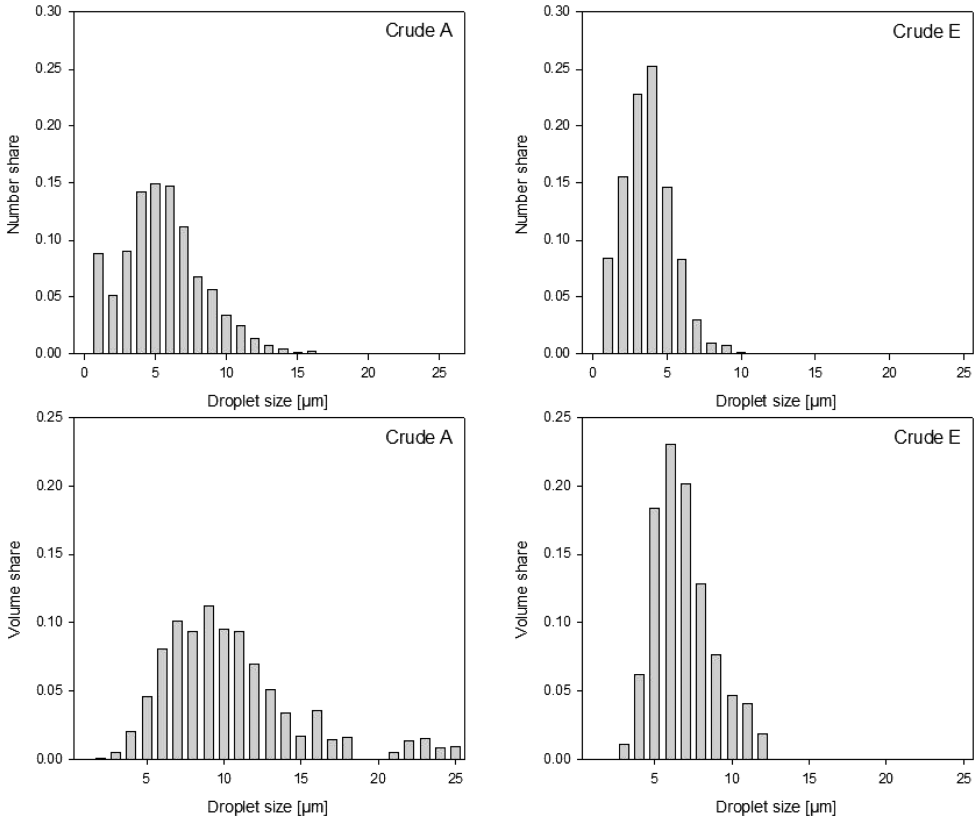

Figure 8. (Left) Number and (right) volume size distributions of oil drops for crude oils A and E in Na-Brine (pH 6).

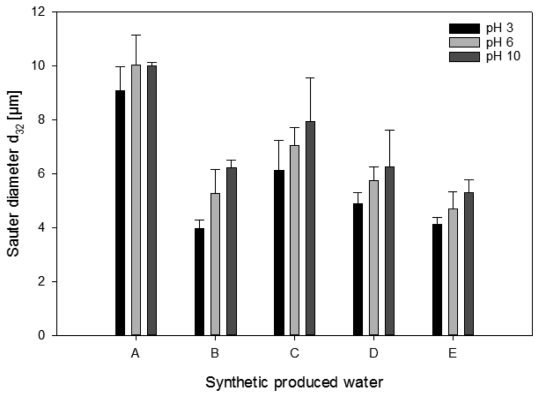

Figure 9. Sauter mean diameters in the synthetic produced-water samples prepared from Na-Brine.

to that difference. Furthermore, as mentioned previously, at higher pH levels naphthenic acids are deprotonated and govern the interfacial activity of the crude oils, resulting in significantly lower values of IFT (Figure S5, Supporting Information). The less clear trend with NaCa-Brine could be further evidence for the role of calcium in the rigidity of the interfacial film. Most samples with calcium experienced a drop of the Sauter mean diameter between pH 6 and 10. Moreover, when comparing the Sauter mean diameter values between the brines at pH 10, for most of the oils, one could notice smaller droplets when calcium was in the system. Possibly, the accumulation of the hydrophobic complexes of calcium at the oil/water interface negatively influenced the coalescence, resulting in smaller drops.

CONCLUSIONS

The influence of the properties of crude oils and water composition on the quality of synthetic produced water was studied. The quality of the synthetic produced-water samples was found to be highly dependent on the composition and properties of the crude oils. The light crude oils gave higher water quality in terms of the total oil concentration, even though the amount of free water obtained from the samples was significantly lower. Additionally, the initial pH was of importance to the properties of the synthetic produced water. The amount of free water was lowest at low pH and increased with increasing pH. In addition, the size of the emulsified droplets increased with the initial pH of the brines. The effect of calcium was mostly seen at the highest pH, where it created complexes with dissociated naphthenic acid molecules and stabilized emulsions. The results indicate the complexity of crude-oil emulsions and the severity of the separation issues that can occur during the treatment of produced water. The

DOI: 10.1021/acs.energyfuels.6b03297
Energy Fuels 2017, 31, 3708−3716

interfacially active components found in crude oils can experience different behaviors, for example, increased water solubility or interfacial rigidity that can affect phenomena such as creaming and coalescence and, in the end, lead to differences in the quality of the produced water.

■ ASSOCIATED CONTENT

Supporting Information

The Supporting Information is available free of charge on the ACS Publications website at DOI: 10.1021/acs.energyfuels.6b03297.

Dynamic interfacial tensions between crude oils A and B and Brine-Na at pH 6 (Figure S1), percentages of free water observed 2 h after mixing the crude oils with NaCa-Brine at various pH values (Figure S2), total organic carbon contents of water samples produced with different crude oils (NaCa-Brine; Figure S3), Sauter mean diameters in synthetic produced-water samples prepared from NaCa-Brine (Figure S4), and interfacial tensions of crude oils in (left) Na-Brine and (right) NaCa-Brine (Figure S5) (PDF)

■ AUTHOR INFORMATION

Corresponding Author

*Tel.: +47 735 94 135. E-mail: gisle.oye@ntnu.no.

ORCID

Marcin Dudek: 0000-0001-6444-7109

Gisle Øye: 0000-0002-6391-3750

Notes

The authors declare no competing financial interest.

■ ACKNOWLEDGMENTS

This work was carried out as a part of SUBPRO, a Centre for Innovation-based Research within subsea production and processing. The authors gratefully acknowledge financial support from SUBPRO, which is financed by the Research Council of Norway, NTNU, and major industrial partners (ABB, Aker Solutions, DNV GL, ENGIE, Lundin, Shell, and Statoil). We additionally thank ENGIE, Shell, and Statoil for providing us with crude oil samples.

■ REFERENCES

(1) Fakhru'l-Razi, A.; Pendashteh, A.; Abdullah, L. C.; Biak, D. R.; Madaeni, S. S.; Abidin, Z. Z. Review of technologies for oil and gas produced water treatment. *J. Hazard. Mater.* **2009**, *170* (2−3), 530−51.

(2) Igunnu, E. T.; Chen, G. Z. Produced water treatment technologies. *Int. J. Low-Carbon Technol.* **2014**, *9* (3), 157−177.

(3) Muggeridge, A.; Cockin, A.; Webb, K.; Frampton, H.; Collins, I.; Moulds, T.; Salino, P. Recovery rates, enhanced oil recovery and technological limits. *Philos. Trans. R. Soc., A* **2014**, *372* (2006), 20120320.

(4) Paige, R. W.; Sweeney, F. M. Produced Water Re-Injection: Understanding the Problems. Presented at the *Water Management Offshore Conference*, Aberdeen, U.K., 1993.

(5) Arthur, J. D.; Langhus, B. G.; Patel, C. *Technical Summary of Oil & Gas Produced Water Treatment Technologies*; ALL Consulting, LLC: Tulsa, OK, 2005.

(6) *Technical Assessment of Produced Water Treatment Technologies*; RPSEA Project 07122-12; Colorado School of Mines: Golden, CO, 2009.

(7) Rawlins, C. H. Flotation of Fine Oil Droplets in Petroleum Production Circuits. In *Recent Advances in Mineral Processing Plant Design*; Malhotra, D., Taylor, P. R., Spiller, E., LeVier, M., Eds.; Society for Mining, Metallurgy & Exploration (SME): Englewood, CO, 2009; pp 232−246.

(8) Saththasivam, J.; Loganathan, K.; Sarp, S. An overview of oil−water separation using gas flotation systems. *Chemosphere* **2016**, *144*, 671−680.

(9) Hansen, B. R.; Davies, S. H. Review of potential technologies for the removal of dissolved components from produced water. *Chem. Eng. Res. Des.* **1994**, *72* (A2), 176−188.

(10) Dastgheib, S. A.; Knutson, C.; Yang, Y.; Salih, H. H. Treatment of produced water from an oilfield and selected coal mines in the Illinois Basin. *Int. J. Greenhouse Gas Control* **2016**, *54* (Part 2), 513−523.

(11) Li, Y. S.; Yan, L.; Xiang, C. B.; Hong, L. J. Treatment of oily wastewater by organic−inorganic composite tubular ultrafiltration (UF) membranes. *Desalination* **2006**, *196* (1), 76−83.

(12) Xu, P.; Drewes, J. E. Viability of nanofiltration and ultra-low pressure reverse osmosis membranes for multi-beneficial use of methane produced water. *Sep. Purif. Technol.* **2006**, *52* (1), 67−76.

(13) Piemonte, V.; Prisciandaro, M.; Mascis, L.; Di Paola, L.; Barba, D. Reverse osmosis membranes for treatment of produced water: a process analysis. *Desalin. Water Treat.* **2015**, *55* (3), 565−574.

(14) Berdugo-Clavijo, C.; Gieg, L. M. Conversion of crude oil to methane by a microbial consortium enriched from oil reservoir production waters. *Front. Microbiol.* **2014**, *5*, 197.

(15) Veil, J. A.; Puder, M. G.; Elcock, D.; Redweik, R. J., Jr. *A White Paper Describing Produced Water from Production of Crude Oil, Natural Gas, and Coal Bed Methane*; Argonne National Laboratory: Argonne, IL, 2004.

(16) Dickhout, J. M.; Moreno, J.; Biesheuvel, P. M.; Boels, L.; Lammertink, R. G. H.; de Vos, W. M. Produced water treatment by membranes: A review from a colloidal perspective. *J. Colloid Interface Sci.* **2017**, *487*, 523−534.

(17) Sjöblom, J.; Aske, N.; Harald Auflem, I.; Brandal, Ø.; Erik Havre, T.; Sæther, Ø.; Westvik, A.; Eng Johnsen, E.; Kallevik, H. Our current understanding of water-in-crude oil emulsions.: Recent characterization techniques and high pressure performance. *Adv. Colloid Interface Sci.* **2003**, *100−102*, 399−473.

(18) Zolfaghari, R.; Fakhru'l-Razi, A.; Abdullah, L. C.; Elnashaie, S. S. E. H.; Pendashteh, A. Demulsification techniques of water-in-oil and oil-in-water emulsions in petroleum industry. *Sep. Purif. Technol.* **2016**, *170*, 377−407.

(19) Gaweł, B.; Lesaint, C.; Bandyopadhyay, S.; Øye, G. Role of Physicochemical and Interfacial Properties on the Binary Coalescence of Crude Oil Drops in Synthetic Produced Water. *Energy Fuels* **2015**, *29* (2), 512−519.

(20) Silset, A.; Flåten, G. R.; Helness, H.; Melin, E.; Øye, G.; Sjöblom, J. A Multivariate Analysis on the Influence of Indigenous Crude Oil Components on the Quality of Produced Water. Comparison Between Bench and Rig Scale Experiments. *J. Dispersion Sci. Technol.* **2010**, *31* (3), 392−408.

(21) Poteau, S.; Argillier, J.-F.; Langevin, D.; Pincet, F.; Perez, E. Influence of pH on Stability and Dynamic Properties of Asphaltenes and Other Amphiphilic Molecules at the Oil−Water Interface†. *Energy Fuels* **2005**, *19* (4), 1337−1341.

(22) Faksness, L.-G.; Grini, P. G.; Daling, P. S. Partitioning of semi-soluble organic compounds between the water phase and oil droplets in produced water. *Mar. Pollut. Bull.* **2004**, *48* (7−8), 731−742.

(23) Stanford, L. A.; Kim, S.; Klein, G. C.; Smith, D. F.; Rodgers, R. P.; Marshall, A. G. Identification of Water-Soluble Heavy Crude Oil Organic-Acids, Bases, and Neutrals by Electrospray Ionization and Field Desorption Ionization Fourier Transform Ion Cyclotron Resonance Mass Spectrometry. *Environ. Sci. Technol.* **2007**, *41* (8), 2696−2702.

(24) Hutin, A.; Argillier, J.-F.; Langevin, D. Mass Transfer between Crude Oil and Water. Part 1: Effect of Oil Components. *Energy Fuels* **2014**, *28* (12), 7331−7336.

(25) Eftekhardadkhah, M.; Øye, G. Induction and Coverage Times for Crude Oil Droplets Spreading on Air Bubbles. *Environ. Sci. Technol.* **2013**, *47* (24), 14154−14160.
(26) Eftekhardadkhah, M.; Aanesen, S. V.; Rabe, K.; Øye, G. Oil Removal from Produced Water during Laboratory- and Pilot-Scale Gas Flotation: The Influence of Interfacial Adsorption and Induction Times. *Energy Fuels* **2015**, *29* (11), 7734−7740.
(27) Havre, T. E.; Sjöblom, J.; Vindstad, J. E. Oil/Water-Partitioning and Interfacial Behavior of Naphthenic Acids. *J. Dispersion Sci. Technol.* **2003**, *24* (6), 789−801.
(28) Hutin, A.; Argillier, J.-F.; Langevin, D. Influence of pH on Oil-Water Interfacial Tension and Mass Transfer for Asphaltenes Model Oils. Comparison with Crude Oil Behavior. *Oil Gas Sci. Technol.* **2016**, *71* (4), 58.
(29) Nour, A. H.; Yunus, R. M. Stability Investigation of Water-in-Crude Oil Emulsion. *J. Appl. Sci.* **2006**, *6* (14), 2895−2900.
(30) Brandal, Ø.; Hanneseth, A. M. D.; Hemmingsen, P. V.; Sjöblom, J.; Kim, S.; Rodgers, R. P.; Marshall, A. G. Isolation and Characterization of Naphthenic Acids from a Metal Naphthenate Deposit: Molecular Properties at Oil-Water and Air-Water Interfaces. *J. Dispersion Sci. Technol.* **2006**, *27* (3), 295−305.
(31) *ASTM D664-95: Standard Test Method for Acid Number of Petroleum Products by Potentiometric Titration*; ASTM International: West Conshohocken, PA, 2001.
(32) Dubey, S. T.; Doe, P. H. Base Number and Wetting Properties of Crude Oils. *SPE Reservoir Eng.* **1993**, *8*, 195−200.
(33) Gaweł, B.; Eftekhardadkhah, M.; Øye, G. Elemental Composition and Fourier Transform Infrared Spectroscopy Analysis of Crude Oils and Their Fractions. *Energy Fuels* **2014**, *28* (2), 997−1003.
(34) Hannisdal, A.; Hemmingsen, P. V.; Sjöblom, J. Group-Type Analysis of Heavy Crude Oils Using Vibrational Spectroscopy in Combination with Multivariate Analysis. *Ind. Eng. Chem. Res.* **2005**, *44* (5), 1349−1357.
(35) *Produced Water: Technological/Environmental Issues and Solutions*; Ray, J. P., Engelhardt, F. R., Eds.; Environmental Science Research; Springer: San Diego, CA, 1992; Vol. *46*.
(36) Tichelkamp, T.; Teigen, E.; Nourani, M.; Øye, G. Systematic study of the effect of electrolyte composition on interfacial tensions between surfactant solutions and crude oils. *Chem. Eng. Sci.* **2015**, *132*, 244−249.
(37) Farooq, U.; Simon, S.; Tweheyo, M. T.; Øye, G.; Sjöblom, J. Interfacial Tension Measurements Between Oil Fractions of a Crude Oil and Aqueous Solutions with Different Ionic Composition and pH. *J. Dispersion Sci. Technol.* **2013**, *34* (5), 701−708.
(38) Langevin, D.; Argillier, J.-F. Interfacial behavior of asphaltenes. *Adv. Colloid Interface Sci.* **2016**, *233*, 83−93.
(39) Eftekhardadkhah, M.; Øye, G. Correlations between crude oil composition and produced water quality: A multivariate analysis approach. *Ind. Eng. Chem. Res.* **2013**, *52* (48), 17315−17321.
(40) Spiecker, P. M.; Gawrys, K. L.; Kilpatrick, P. K. Aggregation and solubility behavior of asphaltenes and their subfractions. *J. Colloid Interface Sci.* **2003**, *267* (1), 178−193.
(41) Stockwell, A.; Taylor, A. S.; Thompson, D. G., The Rheological Properties of Water-in-Crude-Oil Emulsions. In *Surfactants in Solution*'; Mittal, K. L., Bothorel, P., Eds.; Springer: Boston, MA, 1986; Vol. *6*, pp 1617−1632.
(42) Arla, D.; Flesisnki, L.; Bouriat, P.; Dicharry, C. Influence of Alkaline pH on the Rheology of Water/Acidic Crude Oil Interface. *Energy Fuels* **2011**, *25* (3), 1118−1126.
(43) Brandal, Ø.; Sjöblom, J. Interfacial Behavior of Naphthenic Acids and Multivalent Cations in Systems with Oil and Water. II: Formation and Stability of Metal Naphthenate Films at Oil-Water Interfaces. *J. Dispersion Sci. Technol.* **2005**, *26* (1), 53−58.
(44) Clark, P. E.; Pilehvari, A. Characterization of crude oil-in-water emulsions. *J. Pet. Sci. Eng.* **1993**, *9* (3), 165−181.
(45) Eftekhardadkhah, M.; Kløcker, K. N.; Trapnes, H. H.; Gaweł, B.; Øye, G. Composition and Dynamic Adsorption of Crude Oil Components Dissolved in Synthetic Produced Water at Different pH Values. *Ind. Eng. Chem. Res.* **2016**, *55* (11), 3084−3090.
(46) Calabrese, R. V.; Chang, T. P. K.; Dang, P. T. Drop breakup in turbulent stirred-tank contactors. Part I: Effect of dispersed-phase viscosity. *AIChE J.* **1986**, *32* (4), 657−666.

DOI: 10.1021/acs.energyfuels.6b03297
Energy Fuels 2017, 31, 3708−3716

Paper 2

The Effect of Dissolved Gas on Coalescence of Oil Drops Studied with Microfluidics

Journal of Colloid and Interface Science 528 (2018) 166–173

Contents lists available at ScienceDirect

Journal of Colloid and Interface Science

journal homepage: www.elsevier.com/locate/jcis

The effect of dissolved gas on coalescence of oil drops studied with microfluidics

Marcin Dudek [a], Kelly Muijlwijk [b], Karin Schroën [c], Gisle Øye [a,*]

[a] Ugelstad Laboratory, Department of Chemical Engineering, Norwegian University of Science and Technology (NTNU), Trondheim, Norway
[b] FrieslandCampina, Wageningen, The Netherlands
[c] Food Process Engineering Group, Wageningen University and Research Centre (WUR), Wageningen, The Netherlands

GRAPHICAL ABSTRACT

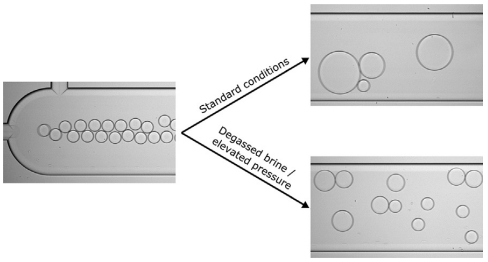

ARTICLE INFO

Article history:
Received 19 February 2018
Revised 22 May 2018
Accepted 22 May 2018
Available online 23 May 2018

Keywords:
Microfluidics
Coalescence
Emulsion stability
Dissolved gases
Hydrophobic interaction

ABSTRACT

Hypothesis: In literature it is stated that the stability of oil-in-water emulsions could be enhanced by decreasing the so-called "hydrophobic interactions" between surfaces through removal of dissolved atmospheric gases. Since the effect of the dissolved gases depends on the hydrophobicity of the oil phase, as well as the system pressure, we vary this effect systematically and monitor droplet coalescence in a tailor-made microfluidic device.

Experiments: The coalescence of oil drops in standard and degassed conditions was studied by direct observation using a microfluidic setup. Two model oils (heptane and xylene) were used to represent different hydrophobicity of the dispersed phases, together with an oil with dynamic interfacial behaviour (diluted crude oil). In addition, the effect of the volume fraction, droplet size and degassing method was studied.

Findings: At ambient pressure, the degassing of the continuous phase reduced the extent of coalescence for the model oils, which is in agreement with other reports. No effect of the dissolved gases was found on the drop formation process. At elevated pressures, the dissolved gases influenced only the most hydrophobic oil (heptane), while causing no effect in the other systems. The coalescence frequencies decreased upon the reduction of the drop sizes, which was justified with the theory for two interacting spheres.

1. Introduction

Emulsions are kinetically stabilized systems of dispersed drops that, given sufficient time, will phase-separate. Coalescence is one

* Corresponding author.
E-mail address: gisle.oye@chemeng.ntnu.no (G. Øye).

https://doi.org/10.1016/j.jcis.2018.05.083
0021-9797/

of the main processes that governs emulsion stability, and is important in various applications, including petroleum, pharmaceutical and food industry. Liao and Lucas [1] presented a literature review of coalescence theories, and most widely used is probably the film drainage model proposed by Shinnar and Church [2]. In this model, the coalescence process is divided into three steps: (1) approach of droplets leading to thin film formation, (2) film drainage and (3) film rupture, leading to coalescence. The film thickness and drainage process are governed by droplet features, fluid characteristics, interfacial properties and flow aspects [3]. These factors will give rise to interaction forces acting across the thin film between droplets, of which the attractive interactions are generally considered to be the result of van der Waals forces, whereas the repulsive interactions originate from overlapping electrical double layers or steric (often polymer-induced) repulsion.

However, additional attractive interactions that cannot be explained by van der Waals interactions, have long been observed between hydrophobic surfaces in aqueous solutions [4,5]. In an early review, Christenson and Claesson [6] put these 'hydrophobic interactions' into the following categories:

(1) Strong, short-range attractive interactions between stable surfaces. These interactions were found between very hydrophobic surfaces and occur in a similar range as the van der Waal attraction (i.e. up to 20 nm), but are stronger.
(2) Attractive interactions of variable strength and range in the presence of bubbles. These ranged from 25 to 250 nm and originated from the presence of nanobubbles near the vicinity of hydrophobic surfaces.
(3) Very long-ranged attractive interactions that decay exponentially. These interactions are most elusive and difficult to explain, in regard to both the origin and magnitude of the attraction, but are commonly observed in systems with mobile hydrophobic groups.

More recently, it has been suggested that the 'hydrophobic interactions' may be a combination of long-ranged attraction (likely originating from bridging bubbles) that are not directly related to the hydrophobicity of the surfaces, and truly hydrophobic interactions at short range (separation distances <10–20 nm) [7,8].

It is clear that the origin of these interactions is not well understood, although interesting results were reported. The presence of dissolved atmospheric gases (typically 1 mM at standard conditions) affects the hydrophobic interactions considerably [7,9,10], and numerous papers have demonstrated the importance of dissolved gas for particle aggregation [11,12], emulsion stability [9,13,14] and surface tension [15]. Conversely, degassing improved removal of hydrophobic contaminants from water [16]. The effect of dissolved gases was also studied in reverse osmosis desalination process at laboratory [17] and pilot scale [18], and in both cases degassing improved process performance. The influence of dissolved gas on formation and stability of emulsion droplets has only been studied at ambient pressure.

Recently, microfluidics have become popular tools to investigate emulsions [19–21], including coalescence of drops in both oil-in-water [22,23] and water-in-oil systems [24,25]. Krebs et al. used it to quantify coalescence of oil droplets, leading to coalescence time distributions as function of the droplet velocity and size [26], and surfactant concentration [27]. Microfluidic tools are well fitted to study emulsion stability in more extreme conditions, i.e. high temperature [28–30], g-force [31], but also elevated pressure. Still, emulsion behaviour in microfluidics at pressurized conditions has scarcely been reported [32], while, to the best of our knowledge, no one has studied the effect of dissolved gas on emulsion stability at elevated pressures.

The objective of this work was to study the effect of dissolved gas on the droplet coalescence at elevated pressure. Microfluidic methods were developed to provide insight into the stability of oil-in-water emulsions through direct observations at high frame rates. The influence of droplet size and dispersed phase volume fraction were investigated using two pure model oils, heptane and xylene. Furthermore, diluted crude oil with dynamic interfacial behaviour was used. The results of triplicate measurements (>1000 droplets each) were reported as coalescence frequency values, in combination with drop size distributions.

2. Experimental

2.1. Materials

Heptane (Chromasolv for HPLC, Sigma-Aldrich, USA) and xylene (isomeric mixture for analysis, Merck, Germany) were used as received. The crude oil was produced at the Norwegian Continental Shelf, and diluted to 25 wt.% in a mixture of heptane and xylene (later referred to as HX) with mass ratio 71.5:28.5, which corresponded to a saturated to aromatic ratio in the crude oil (characteristics were reported elsewhere: crude oil D in [33]). The basic physical parameters of the oil phases used here are listed in Table 1.

Densities of oil phases were measured with a DMA 5000 laboratory density meter (Anton Paar, Austria). Viscosity was obtained by using a MCR 301 laboratory rheometer (Anton Paar, Austria) with cylindrical geometry (CC-27). The interfacial tension (IFT) between model oil and water phases were measured with Du Noüy ring tensiometer (Sigma 70, KSV, Finland), while the IFT of brine and diluted crude oil was measured with a pendant drop tensiometer (PAT-1M, Sinterface Technologies, Germany).

3.5 wt.% sodium chloride (for analysis, Merck Millipore, USA) was dissolved in deionized water (resistivity > 18.2 MΩ cm, Millipore Simplicity Systems, Germany) to make standard brine solutions, referred to as Std-Brine. For degassing of brine, an ultrasonic bath (Bransonic CPXH2800-E, Emerson, USA) was used for 15 min (further referred to as Deg-Brine). To compare the efficiency of degassing by ultrasonication, a series of experiments was also performed with conventionally degassed brines (vacuum < 25 mmHg).

The dissolved gas from the brine and one of the model oils (xylene) was also removed through repeated freezing and thawing procedure. The samples were put in Schlenk tubes and sealed in nitrogen atmosphere to avoid condensation of oxygen. Next, they were frozen by immersing the tubes into liquid nitrogen. Once frozen, the samples were put under vacuum (ca. 10^{-4} bar) for 15 min. Afterwards, the sealed tubes were warmed under tepid water in order to thaw the liquid inside. The procedure was repeated until the bubbles stopped appearing in the solution (min. 3 times).

3. Methods

3.1. Microfluidic chips

Custom-designed glass microfluidic chips, Fig. 1, were provided by Micronit Microtechnologies B.V. (The Netherlands) and their design was similar to those used by Krebs et al. [27]. The inlet channels, leading to a *T*-junction where the droplets were created, were 100 μm wide. After passing a meandering channel, the droplets entered a coalescence chamber with a width of 500 μm, where they could undergo coalescence. The length of the coalescence chamber was approximately 33 mm and led to the outlet of the chip. The chips had an additional inlet for the continuous phase, located at the beginning of the coalescence channel. This

Table 1
Physical properties of the dispersed phases.

Dispersed phase		Heptane	Xylene	Heptane/xylene (HX)	Crude oil in HX
Density @20 °C [g/ml]		0.684	0.867	0.736	0.761
Viscosity @20 °C [mPa s]		0.550	0.541	0.548	0.597
Interfacial tension [mN/m]	Standard brine	47.4 ± 0.1	38.2 ± 0.1	42.2 ± 0.5	13.7 ± 0.2
	Degassed brine	47.3 ± 0.3	38.0 ± 0.1	41.1 ± 0.9	13.5 ± 0.7

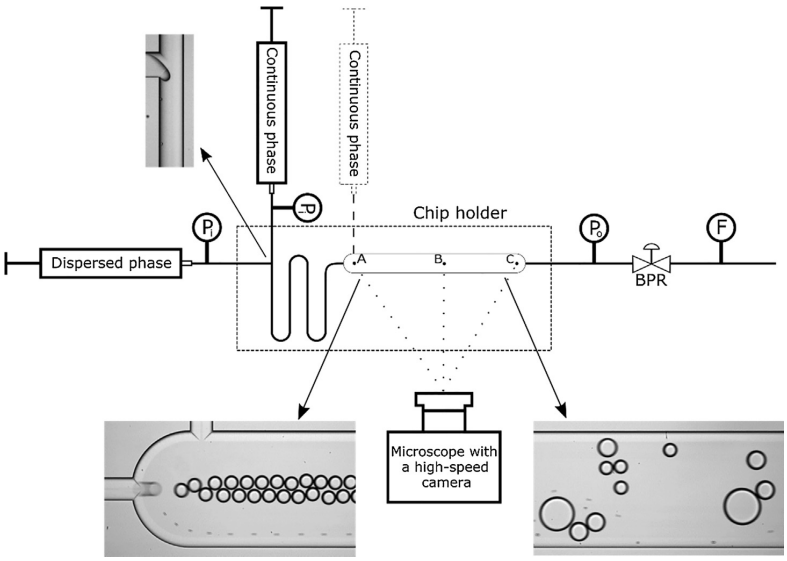

Fig. 1. The microfluidic setup with the design of the chip. The pressure was controlled by a backpressure regulator (BPR) and was measured at the inlet (P_i) and outlet (P_o) by the pressure sensors. The total flow was measured by a Coriolis force flowmeter. A, B and C illustrate the recording points during the experiments.

allowed for variation in the volume fraction of the dispersed phase. Unless otherwise stated, the additional inlet was blocked during the experiments. All channels had the same depth (45 μm). The microfluidic chips were placed in a chip holder (Fluidic Connect PRO, Micronit Microtechnologies B.V., The Netherlands) and connected to the flow setup with PEEK tubing (inner diameter 250 μm, Sigma-Aldrich, USA) and FFKM ferrules (Fluidic PRO Ferrules, Micronit Microtechnologies B.V., The Netherlands). After the experiments, the chips were first sonicated in deionized (DI) water, then isopropanol, followed by sonication in DI water again. Each step lasted 15 min. For the chips used in the diluted crude oil experiments, a mixture of toluene and acetone (3:1 v/v) was used instead of DI water in the first sonication step. Afterwards, the chips were dried with compressed air and baked in an ashing furnace for 6 h at 475 °C. Shortly before the experiments, the chips were treated with low-pressure oxygen plasma for 10 min (Zepto, Diener electronic GmbH, Germany).

3.2. Microfluidic setup

The flow rate and the pressure were controlled with the flow setup depicted in Fig. 1. The liquids were pumped with syringe pumps (neMESYS mid-pressure module V3, Cetoni GmbH, Germany), fitted with stainless steel syringes. Generally, the droplet diameter exceeded the height of the channel slightly leading to a somewhat flattened shape that always deviated less than 10% of the hydraulic diameter. Therefore, the measured diameters are directly reported. Generally, the droplet size was controlled by the flow rate of the continuous phase, with a small dependency on the dispersed phase as also reported by other authors [22]. The flow rate of the dispersed phase governed the number of droplets. The ratio between the continuous and dispersed phase flow rates was kept constant at 1:8, except when the additional inlet for the continuous phase was used. All experimental conditions are presented in Table 2 and experiments at each condition were repeated 3 times.

The pressure of each liquid before the inlet (P_i) and combined liquids at the outlet (P_o) was monitored with pressure sensors (Qmix P, Cetoni GmbH, Germany), and controlled by a backpressure regulator – BPR (15-300 psi, VICI AG International, Switzerland). The total outlet flow was measured with a microfluidic Coriolis flow sensor – F (mini CORI-FLOW, Elveflow, France). By adjusting the back-pressure regulator, the system pressure was adjusted to 0, 6, or 11 bar(g), the latter being the upper pressure limit of the chip holder pressure resistance. The flowmeter readings indicated temporary decline of the flow rate, which came back to the original level and stabilized within 20 s, and the reverse happened when decreasing the pressure. All reported pressures refer to the outlet pressure after flow rate stabilisation. The temperature was not controlled, but was constant throughout the experiment (ca. 22 °C).

The interactions between the droplets were observed with a high-speed camera (AX100, Photron, Japan), connected to an inverted microscope (Ti-U Eclipse, Nikon, Japan) with an external LED light source (HDF7010, Hayashi, Japan).

Table 2
Overview of the experimental conditions in different report sections.

Results subsection	Flow rate [μl min^{-1}]			Pressure [bar g]	Dispersed phase	Approx. droplet size [μm]
	Continuous phase	Dispersed phase	Continuous phase – additional inlet			
Heptane vs xylene	160	20	–	0; 6; 11	Heptane	56
					Xylene	56
Dispersed phase volume fraction (SI)	160	20	0	0; 6	Xylene	56
			50			56
Droplet size	120	15	–	0; 6	Xylene	66
	160	20	–	0; 6		56
	200	25	–	1; 6		48
	240	30	–	1; 6		41
Model oil vs crude oil	160	20	–	0; 6	HX	56
					Crude oil in HX	52

3.3. Data acquisition and image analysis

Two sets of images were recorded for each experiment at 8 500 fps. The inlet of the coalescence chamber (A in Fig. 1) was recorded in order to retrieve the initial size and number of the droplets. Afterwards, 10 000 frames were recorded further down the chamber for the analysis of coalescence events. The distance between the first and the second recording point was either 15.6 or 26 mm (B and C in Fig. 1, respectively). The shorter distance was used for the model fluids that coalesced more readily than the crude oil systems.

The images were processed with ImageJ software: first, the frames were converted from greyscale images into binary, after which the areas and centre of mass coordinates (X,Y) of the droplets were obtained using the Analyse Particle feature. The height and width of the detection box was set to 500 μm and 301.2 μm, respectively; the lower size limit for droplets was set at 200 μm^2 to prevent detection of small satellite droplets, sometimes created at the *T*-junction [34]. The circularity parameter was in the range 0.8–1 to disregard polygonal shapes occurring in the voids formed between droplets; and to detect only complete droplets, the exclusion on edges feature was used. As the majority of drops were smaller than the detection box, a single drop was detected in tens of frames (frames 2, 3, 7 and 12 in Fig. S1 in SI). In total, tens of thousands of objects were detected.

The data were copied to Microsoft Excel to calculate the average drop velocity. It is worth pointing out that the velocity of the drops was 20–40% lower than the velocity of the continuous phase, due to drag forces that reduced the droplet velocity, also confirmed by previous findings of Krebs et al. [27]. The drop velocity and the length of the channel were used to obtain the residence time (t_{res}).

The areas of the droplets increased proportionally with the number of coalescence events and, based on this, they were sorted into several size classes. The calculated average velocity, the width of the detection box and the average droplet diameter of each of the size classes were used to convert the dataset of tens of thousands of objects to the estimated number of observed droplets of different sizes (N_f). Fig. 2 displays a typical outcome as the number distribution of droplets of different size classes at the second recording point.

The size distribution was transferred to Matlab, with which the probability density functions were calculated with the distribution-fitting tool. The probability density functions (PDF) generally showed a good fit, as the typical deviations from the average values in the histogram were lower than 5%. Therefore, all subsequent size distributions were presented as PDFs. The number of droplets at the inlet (N_{in}) was estimated by Eq. (1):

$$N_{in} = \sum_{i=1}^{i} n_i * \frac{A_{f_i}}{A_{in}} \quad (1)$$

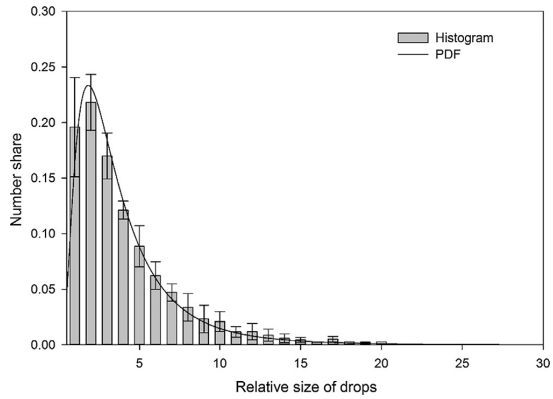

Fig. 2. Droplet size distribution at the second recording point (based on ca. 600 droplets) and a calculated probability density function. Data for heptane droplets in Std-Brine at lowest pressure. Data are for three repeated experiments.

where n_i was number of droplets in class i, A_{fi} the area of class i droplets at the second recording point and A_{in} the area of a drop formed at the *T*-junction. N_{in} was usually above 2000. The percentage of non-coalesced droplets at the end of the channel was given by $\left(\frac{n_1}{N_{in}}\right) * 100\%$, with n_1 the number of the droplets of initial size. The number of droplets retrieved from the inlet image series was used as a control to compare with the estimated N_{in}.

Similarly to the method presented by Krebs et al. [27], the ratio between N_{in} and N_f gave the mean relative size of a droplet and number of coalescence events ($(N_{in}/N_f) - 1$); a droplet of size 3 undergoes 2 coalescence events. The coalescence frequency follows from Equation (2):

$$f = \frac{\frac{N_{in}}{N_f} - 1}{t_{res}} \quad (2)$$

Statistical analysis (*t*-Student, $\alpha = 0.05$) was performed for all results to determine whether the differences between data sets were statistically significant or not.

4. Results & discussion

4.1. Heptane vs xylene

Fig. 3 shows the average coalescence frequency at different system pressures for heptane and xylene drops in standard and degassed brines.

Most coalescence was observed in the standard brine at ambient system pressure, with slightly higher coalescence frequency for heptane than for xylene. The coalescence frequency in standard brine decreased with the increase of system pressure, and the reduction was somewhat larger for xylene than for heptane. In the degassed brine, the coalescence frequency was practically independent of the system pressure. The coalescence frequencies that were found seem similar to those found for standard brine at elevated pressure for xylene, while they are slightly lower for heptane. Notably, we found no effect of the dissolved gas on the droplet size during formation of the droplets.

The probability density functions for the experimental conditions used above (Fig. S2 in the Supporting Information) were wider, and more positively skewed at standard conditions, and ambient pressure, which implies more polydisperse systems, whereas the samples without dissolved gas and at elevated pressure in standard brine had the smallest drop sizes and narrowest size distributions. In order to investigate the effect of dissolved gas further, additional experiments were performed to test the degassing method (Fig. 4).

No statistically significant differences were observed for brines degassed by ultrasonication and the freeze-thaw method. Removing the dissolved gas from xylene further increased the stability of the oil droplets against coalescence, although the reduction of the coalescence frequency was not as marked as found for degassed brine.

When reducing the volume fraction of the dispersed phase (from ca. 0.17 to 0.13) by the additional flow of the continuous phase, the coalescence frequency became lower, which may also be caused by the higher velocity of drops as discussed later. The trends observed for degassing and increasing pressure were similar as mentioned before (see Fig. S3 in the Supporting Information).

For further discussion of our findings, we used various sources available in the literature as the starting point. Experimental observations show that dissolved gas molecules accumulate close to hydrophobic surfaces and thereby affect the orientation of the surrounding water molecules [35]. This imposed ordering of dipole moments can extend into the gap between two surfaces by percolation from gas molecule to gas molecule, resulting in density fluctuations and formation of gaseous bridges that pull the surfaces together and facilitate coalescence. Simultaneously, dissolved gases has been reported to act as nucleation sites for cavitation and thus enhance coalescence [36]. The effect of dissolved gas on surfactant-free emulsions has been investigated by Pashley et al. [12,13,36], who revealed that the removal of dissolved gas

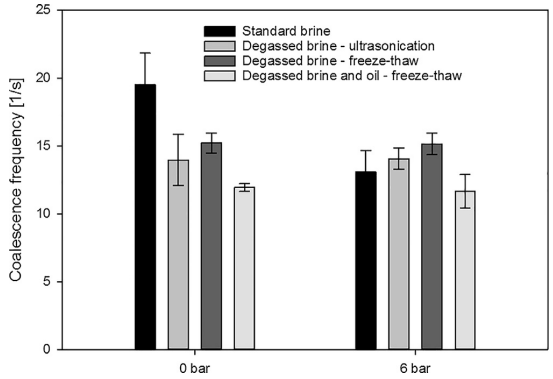

Fig. 4. Coalescence frequencies of xylene in brines degassed by using different methods.

improved dispersion by reduction of the hydrophobic interactions. This was attributed to the formation of smaller droplets in the absence of dissolved gas [12], while re-gassing of already formed emulsions did not influence their stability. Furthermore, it was suggested that freshly created oil-water interfaces quickly acquired a negative charge by adsorption of OH^- ions, which provided some stability towards coalescence through electrical double layer repulsion, which was confirmed by reducing the pH decrease, which led to rapid growth of droplet size [37]. In our experiments, the high salt concentration compressed the double layer thickness considerably and effectively removed electrostatic repulsion. Additionally, the drop sizes in our study were 2–3 orders of magnitude larger than in the investigations referred to. This may have increased the extent of hydrophobic interactions, resulting in less stable droplets in our case (see section below).

The difference in coalescence frequency between heptane and xylene in standard brine can be assigned to the lower interfacial tension between xylene and brine (Table 1). This corresponds to stronger adhesive interactions between the aromatic π-electrons in xylene and the brine, rather than between the saturated hydrocarbons in heptane and the brine, which could affect the drainage time and consequently coalescence frequency. Indeed, the coalescence time [26] of xylene drops was longer, compared to heptane (Fig. S6 in the Supporting Information) when measured in a different microfluidic chip (details in the Supporting Information), which was also in line with the findings of Kourio et al. [38].

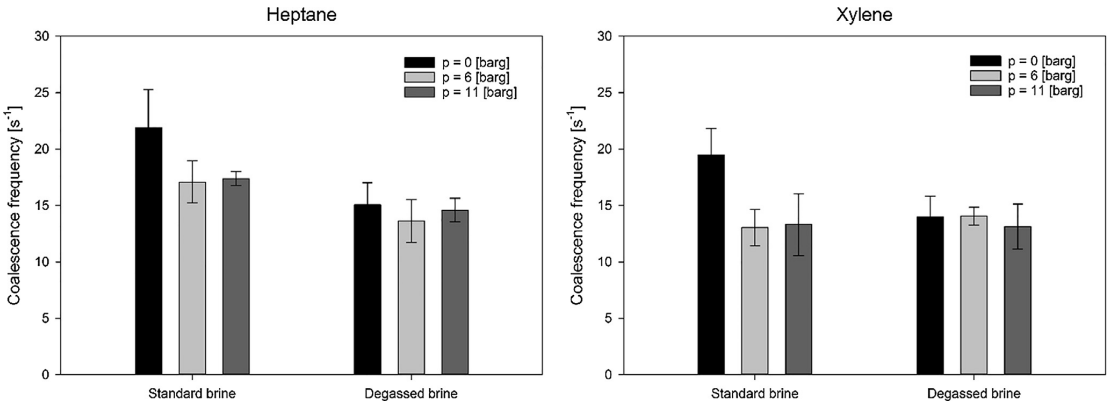

Fig. 3. Coalescence frequencies of heptane and xylene at various pressures in Std-Brine and Deg-Brine.

The variation in interfacial tension shows that heptane is more hydrophobic than xylene. Furthermore, partitioning of compounds between octanol and water, and the logarithm of the resulting value (log K_{OW}) is a common way of assigning hydrophobicity values to organic compounds [39]. Log K_{OW} values of 4.66 and 3.15 for heptane and xylene, respectively, further demonstrate higher degree of hydrophobicity of heptane. This also implies that more dissolved gas molecules are expected to accumulate close to the heptane-water interface and promote coalescence as outlined above. When the system pressure is increased in standard brine, the increased gas solubility results in less nucleation of the dissolved gas, and therefore less cavitation and vapour bridge formation, leading to a reduction in coalescence upon increasing the system pressure. Higher dissolved gas concentration at water-heptane interface could also be the reason for the somewhat higher coalescence frequency in this case. The independence of coalescence frequency on system pressure in the degassed systems confirms the importance of the dissolved gas on additional "hydrophobic" attraction in standard brines, whereas that fact that coalescence frequency is very similar for heptane and xylene in degassed brine, suggests that truly hydrophobic, short-ranged interactions were not observed in our experiments.

When zooming in on the three methods used for degassing: ultrasonication, vacuum and freeze-thaw procedure it should be mentioned that the removal efficiency of the first method was probably not as high as the other two [40]; vacuum degassing should remove up to 95–97%, and freeze-thawing was reported to remove virtually all dissolved gas molecules [12]. Since there was hardly any difference in coalescence frequency in our dynamic interface system, it seems that the level of degassing did not play a major role in the stability of oil droplets. It should also be noted that even with partial deaeration, the effects of the decreased attractive forces should still be observable [7,8,11]. Degassing of the oil phase led to a small decrease in coalescence frequency, but was not as significant as the effect of degassing the water phase.

In summary, when comparing coalescence in standard and degassed brines, it is evident that the removal of dissolved gas results reduced the additional "hydrophobic" attraction that, probably combined with a slight change in density of water, increased the drainage time and reduced coalescence for both heptane and xylene at ambient pressure.

4.2. Droplet size

We next investigated the coalescence frequency of xylene droplet of various sizes (Fig. 5).

The coalescence frequencies decreased as the droplets became smaller, and this trend prevailed independent of the system pressure or the absence of dissolved gases. For all drop sizes, coalescence frequency decreased upon degassing at ambient pressure, whereas the coalescence frequency at higher system pressures resembled that of the degassed brine.

The models for drainage time t_{dr} have the general form of [41]:

$$t_{dr} = k\frac{\mu * R^a}{\gamma^c * B^d}(\Delta\rho g)^b \tag{3}$$

where μ is the viscosity of the continuous phase, R is the radius of the coalescing droplet, γ is the interfacial tension, B is the modified Hamaker constant, $\Delta\rho$ is the density difference, g is the gravitational acceleration and a, b, c, d, k are positive constants. According to Eq. (3), drainage times are expected to increase with droplet size, although literature is not unanimous on that account [42–44]. In our experiments the opposite was found, and an explanation could be that the modified Hamaker constant is an oversimplified approximation of the surface forces, acting on the droplets, as suggested by Grimes with regards to the coalescence in complex crude oil systems [45].

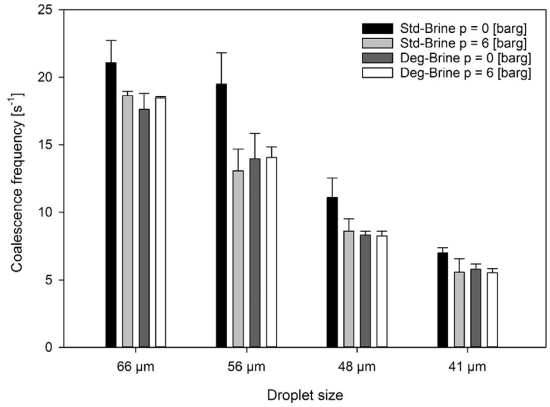

Fig. 5. Coalescence frequencies of drops with different initial sizes in Std- and Deg-Brine at different pressure levels.

In our case, however, it is entirely possible that the hydrophobic interactions could have been incorrectly neglected in Eq. (3) and when taking them into account, the total interaction energy between two drops can be expressed with the following equation [36]:

$$V_S(kT) = \frac{R}{kT}\left[2\pi\epsilon_0\epsilon\psi_0^2\exp(-\kappa H) - \frac{A_{121}}{12H} - A_1\exp\left(-\frac{H}{\lambda_1}\right) - A_2\exp\left(-\frac{H}{\lambda_2}\right)\right] \tag{4}$$

where V_S is the total interaction energy between spheres in kT units, R is the spherical droplet radius, $\epsilon_0\epsilon$ is the permittivity of water, ψ_0 is the particle's electrostatic potential, κ^{-1} is the Debye length, H is the distance between the droplet surfaces and A_{121} is the Hamaker constant. The values of constants A_1, A_2 and λ_1, λ_2 (decay lengths) are experimentally determined. The first term within the parentheses accounts for the repulsive double layer interactions and can be neglected in our case, due to the high salt concentration. The second term represents the attractive van der Waals interactions, included in Eq. (3) as the modified Hamaker constant, while the last two terms account for attractive hydrophobic interactions, which we showed to have an effect on the coalescence times between drops. It can be then concluded from Eq. (4) that the interaction strength increases with droplet size and compensates for the larger volume of drained liquid, which is in agreement with the higher coalescence frequency found for the larger droplets.

In addition, we also have to consider the increased total flow rate, necessary for achieving the smaller sized droplets (see Table 2). This had a marked effect on the drop velocity and the initial amount of droplets, possibly leading to changes in the hydrodynamic forces, although Krebs mentioned that their effect on droplet coalescence was at most in the order of 25% where we find larger effects. Also other have stated that the coalescence frequency could be affected with substantiating to which extent [26,27,46,47].

4.3. Model oil vs diluted crude oil

In crude oil systems, surface-active components will be present, and that is discussed next. The coalescence frequencies of a model oil, consisting of a heptane-xylene mixture, and a crude oil diluted with similar heptane-xylene mixture are compared in Fig. 6.

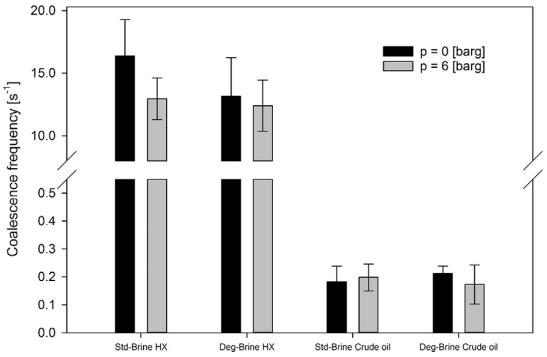

Fig. 6. Comparison of coalescence frequencies between the model oil and diluted crude oil in Std- and Deg-Brine at different pressure levels.

The behaviour of the model oil was similar as observed for other model oils used before: removal of dissolved gas resulted in slightly lower coalescence frequency at ambient pressure, while it had no effect at higher pressure. The diluted crude oil showed a reduction in coalescence frequency by a factor of 100, compared to the model oils. The number of non-coalesced drops was 5–20% for the model oils, while this was more than 90% for the diluted crude oil. If coalescence took place, a droplet coalesced only once or twice for the explored conditions. Furthermore, gas removal had no effect on the coalescence frequency irrespective of the applied pressure.

The different behaviour of the diluted crude oil systems can be attributed to the presence of resins and asphaltenes, which are responsible for the time-dependent alteration of the interfacial properties of crude oils [48]. Although, the crude oil used in this study was light and contained relatively low amounts of resins and asphaltenes (5.1% and 0.3%, respectively), these amounts are more than sufficient to cover the oil water interface. In previous research we have shown that the asphaltenes can build up elastic layers at oil-water interfaces and increase the coalescence time [49], which may lead to a reduced coalescence frequency between crude oil drops. The lack of response to the removal of dissolved gas can also be explained by the presence of the interfacially active components. When these components (which contain heteroatoms such as oxygen, nitrogen and sulphur) adsorb at the oil-water interface, they will reduce the hydrophobicity of the drops. In accordance with the mechanism outlined above, this would result in less accumulation of dissolved gas close to the surface of the drops, which would lower the possibility of cavitation or vapour bridge formation between the droplets.

5. Conclusions

The effect of the dissolved gas on oil droplet coalescence in water (3.5% brine) was studied with microfluidic tools at ambient and elevated pressures. At ambient pressure, our results were in agreement with previous reports [9–11], where removal of dissolved gas resulted in enhanced emulsion stability. We observed no influence of the dissolved gas on emulsion droplet formation [12,36]; however, coalescence between oil drops was affected, most probably through reduced cavitation, or vapour bridge formation. At elevated pressures, the removal of dissolved gas caused minor reduction in the coalescence for heptane, the most hydrophobic oil in our study, and no effects were noted in other emulsions.

Furthermore, the coalescence frequency of smaller droplets was lower than for large droplets, which could be explained by the theory for two interacting spheres. Therefore, it is likely that the increased interaction force for larger particles, together with the lack of electrostatic repulsion, have played a crucial role for the coalescence behaviour in our systems. We have also shown the drastic decrease of coalescence frequency for the diluted crude oil and its insensitivity to the presence of dissolved gases. Both the formation of viscoelastic films by resins and asphaltenes, as well as absence of hydrophobic nucleation sites may have contributed to the overall effect.

By utilizing microfluidic methods, it was possible to evaluate the oil droplet coalescence in standard and degassed conditions, at elevated pressure and by direct measurement. Since in the microfluidic devices process conditions can be varied systematically, we think that this type of study will greatly help in expanding the current knowledge base on droplet behaviour in general and on coalescence more specifically. Further work will include developing new methods for the measurements of coalescence frequency and time at higher system temperature and pressure, as a next step toward industrial applications.

Acknowledgments

This work was carried out as a part of SUBPRO, a Research-based Innovation Centre within Subsea Production and Processing. The authors gratefully acknowledge the financial support from SUBPRO, which is financed by the Research Council of Norway, major industry partners and NTNU. We additionally thank Maurice Strubel from Wageningen University for his technical advice and help during development of the setup.

Appendix A. Supplementary material

Supplementary data associated with this article can be found, in the online version, at https://doi.org/10.1016/j.jcis.2018.05.083.

References

[1] Y. Liao, D. Lucas, A literature review on mechanisms and models for the coalescence process of fluid particles, Chem. Eng. Sci. 65 (10) (2010) 2851–2864.
[2] R. Shinnar, J.M. Church, Statistical theories of turbulence in predicting particle size in agitated dispersions, Ind. Eng. Chem. 52 (3) (1960) 253–256.
[3] A.K. Chesters, The modelling of coalescence processes in fluid-liquid dispersions: a review of current understanding, Chem. Eng. Res. Des. 69 (A4) (1991) 259–270.
[4] C. Tanford, The Hydrophobic Effect: Formation of Micelles and Biological Membranes, 2nd ed., Wiley, New York, 1980.
[5] J. Israelachvili, R. Pashley, The hydrophobic interaction is long range, decaying exponentially with distance, Nature 300 (5890) (1982) 341–342.
[6] H.K. Christenson, P.M. Claesson, Direct measurements of the force between hydrophobic surfaces in water, Adv. Colloid Interface Sci. 91 (3) (2001) 391–436.
[7] E.E. Meyer, Q. Lin, J.N. Israelachvili, Effects of dissolved gas on the hydrophobic attraction between surfactant-coated surfaces, Langmuir 21 (1) (2005) 256–259.
[8] A. Faghihnejad, H. Zeng, Hydrophobic interactions between polymer surfaces: using polystyrene as a model system, Soft Matter 8 (9) (2012) 2746–2759.
[9] M.E. Karaman, B.W. Ninham, R.M. Pashley, Effects of dissolved gas on emulsions, emulsion polymerization, and surfactant aggregation, J. Phys. Chem. 100 (38) (1996) 15503–15507.
[10] N. Ishida, M. Sakamoto, M. Miyahara, K. Higashitani, Attraction between hydrophobic surfaces with and without gas phase, Langmuir 16 (13) (2000) 5681–5687.
[11] M. Alfridsson, B. Ninham, S. Wall, Role of Co-ion specificity and dissolved atmospheric gas in colloid interaction, Langmuir 16 (26) (2000) 10087–10091.
[12] R.M. Pashley, Effect of degassing on the formation and stability of surfactant-free emulsions and fine teflon dispersions, J. Phys. Chem. B 107 (7) (2003) 1714–1720.
[13] M.J. Francis, N. Gulati, R.M. Pashley, The dispersion of natural oils in de-gassed water, J. Colloid Interface Sci. 299 (2) (2006) 673–677.

[14] B. Sowa, X.H. Zhang, K. Kozielski, P.G. Hartley, N. Maeda, Influence of dissolved atmospheric gases on the spontaneous emulsification of alkane–ethanol–water systems, J. Phys. Chem. C 115 (17) (2011) 8768–8774.
[15] M. Karagianni, A. Avranas, The effect of deaeration on the surface tension of water and some other liquids, Colloids Surf. A 335 (1–3) (2009) 168–173.
[16] R.M. Pashley, M. Rzechowicz, L.R. Pashley, M.J. Francis, De-gassed water is a better cleaning agent, J. Phys. Chem. B 109 (3) (2005) 1231–1238.
[17] M. Rzechowicz, R.M. Pashley, The effect of de-gassing on the efficiency of reverse osmosis filtration, J. Membr. Sci. 295 (1–2) (2007) 102–107.
[18] M.J. Francis, R.M. Pashley, The effects of feed water temperature and dissolved gases on permeate flow rate and permeate conductivity in a pilot scale reverse osmosis desalination unit, Desalin. Water Treat. 36 (1–3) (2011) 363–373.
[19] C.-X. Zhao, A.P.J. Middelberg, Two-phase microfluidic flows, Chem. Eng. Sci. 66 (7) (2011) 1394–1411.
[20] H. Gu, M.H.G. Duits, F. Mugele, Droplets formation and merging in two-phase flow microfluidics, Int. J. Mol. Sci. 12 (4) (2011) 2572.
[21] N. Bremond, J. Bibette, Exploring emulsion science with microfluidics, Soft Matter 8 (41) (2012) 10549–10559.
[22] T. Krebs, C.G.P.H. Schroën, R.M. Boom, Coalescence kinetics of oil-in-water emulsions studied with microfluidics, Fuel 106 (2013) 327–334.
[23] L. Mazutis, A.D. Griffiths, Selective droplet coalescence using microfluidic systems, Lab Chip 12 (10) (2012) 1800–1806.
[24] L. Mazutis, J.-C. Baret, A.D. Griffiths, A fast and efficient microfluidic system for highly selective one-to-one droplet fusion, Lab Chip 9 (18) (2009) 2665–2672.
[25] M. Lee, J.W. Collins, D.M. Aubrecht, R.A. Sperling, L. Solomon, J.W. Ha, G.R. Yi, D. A. Weitz, V.N. Manoharan, Synchronized reinjection and coalescence of droplets in microfluidics, Lab Chip 14 (3) (2014) 509–513.
[26] T. Krebs, K. Schroen, R. Boom, A microfluidic method to study demulsification kinetics, Lab Chip 12 (6) (2012) 1060–1070.
[27] T. Krebs, K. Schroën, R. Boom, Coalescence dynamics of surfactant-stabilized emulsions studied with microfluidics, Soft Matter 8 (41) (2012) 10650–10657.
[28] J.M. Köhler, T. Henkel, A. Grodrian, T. Kirner, M. Roth, K. Martin, J. Metze, Digital reaction technology by micro segmented flow—components, concepts and applications, Chem. Eng. J. 101 (1) (2004) 201–216.
[29] T.H. Ting, Y.F. Yap, N.-T. Nguyen, T.N. Wong, J.C.K. Chai, L. Yobas, Thermally mediated breakup of drops in microchannels, Appl. Phys. Lett. 89 (23) (2006) 234101.
[30] H. Feng, D. Ershov, T. Krebs, K. Schroen, M.A. Stuart, J. van der Gucht, J. Sprakel, Manipulating and quantifying temperature-triggered coalescence with microcentrifugation, Lab Chip 15 (1) (2015) 188–194.
[31] T. Krebs, D. Ershov, C.G.P.H. Schroen, R.M. Boom, Coalescence and compression in centrifuged emulsions studied with in situ optical microscopy, Soft Matter 9 (15) (2013) 4026.
[32] M.T. Timko, S. Marre, A.R. Maag, Formation and characterization of emulsions consisting of dense carbon dioxide and water: ultrasound, J. Supercrit. Fluids 109 (2016) 51–60.
[33] M. Dudek, E. Kancir, G. Øye, Influence of the crude oil and water compositions on the quality of synthetic produced water, Energy Fuels 31 (4) (2017) 3708–3716.
[34] O. Carrier, D. Funfschilling, H.Z. Li, Effect of the fluid injection configuration on droplet size in a microfluidic T junction, Phys. Rev. E, Stat., Nonlin., Soft Matter Phys. 89 (1) (2014) 013003.
[35] B.W. Ninham, P. Lo Nostro, Molecular Forces and Self Assembly in Colloid, Nano Sciences and Biology, 1st ed., Cambridge University Press, Cambridge, 2010.
[36] N. Maeda, K.J. Rosenberg, J.N. Israelachvili, R.M. Pashley, Further studies on the effect of degassing on the dispersion and stability of surfactant-free emulsions, Langmuir 20 (8) (2004) 3129–3137.
[37] M.J. Francis, R.M. Pashley, Further studies into oil droplet size manipulation, Colloids Surf. A 334 (1) (2009) 100–106.
[38] M.J. Kourio, C. Gourdon, G. Casamatta, Study of drop-interface coalescence: Drainage time measurement, Chem. Eng. Technol. 17 (4) (1994) 249–254.
[39] K. Holmberg, B. Jönsson, B. Kronberg, B. Lindman, Surfactants and Polymers in Aqueous Solution, Wiley, 2002.
[40] I.B. Butler, M.A.A. Schoonen, D.T. Rickard, Removal of dissolved oxygen from water: a comparison of four common techniques, Talanta 41 (2) (1994) 211–215.
[41] J.C. Slattery, L. Sagis, E.S. Oh, Interfacial Transport Phenomena, Springer, US, 2007.
[42] P. Ghosh, A Comparative study of the film-drainage models for coalescence of drops and bubbles at flat interface, Chem. Eng. Technol. 27 (11) (2004) 1200–1205.
[43] P. Ghosh, V.A. Juvekar, Analysis of the drop rest phenomenon, Chem. Eng. Res. Des. 80 (7) (2002) 715–728.
[44] S.B. Lang, C.R. Wilke, A hydrodynamic mechanism for the coalescence of liquid drops. II. Experimental studies, Ind. Eng. Chem. Fundam. 10 (3) (1971) 341–352.
[45] B.A. Grimes, Population balance model for batch gravity separation of crude oil and water emulsions. Part I: model formulation, J. Dispersion Sci. Technol. 33 (4) (2012) 578–590.
[46] Q. Zhou, Y. Sun, S. Yi, K. Wang, G. Luo, Investigation of droplet coalescence in nanoparticle suspensions by a microfluidic collision experiment, Soft Matter 12 (6) (2016) 1674–1682.
[47] K. Muijlwijk, I. Colijn, H. Harsono, T. Krebs, C. Berton-Carabin, K. Schroën, Coalescence of protein-stabilised emulsions studied with microfluidics, Food Hydrocolloids 70 (2017) 96–104.
[48] J. Sjöblom, N. Aske, I. Harald Auflem, Ø. Brandal, T. Erik Havre, Ø. Sæther, A. Westvik, E. Eng Johnsen, H. Kallevik, Our current understanding of water-in-crude oil emulsions: recent characterization techniques and high pressure performance, Adv. Colloid Interface Sci. 100–102 (2003) 399–473.
[49] B. Gaweł, C. Lesaint, S. Bandyopadhyay, G. Øye, Role of physicochemical and interfacial properties on the binary coalescence of crude oil drops in synthetic produced water, Energy Fuels 29 (2) (2015) 512–519.

Paper 3

Microfluidic Tools for Studying Coalescence of Crude Oil Droplets in Produced Water

Microfluidic tools for studying coalescence of crude oil droplets in produced water

Marcin Dudek[1], Are Bertheussen[1], Thomas Dumaire[2] and Gisle Øye[1,†]

[1] Ugelstad Laboratory, Department of Chemical Engineering, Norwegian University of Science and Technology (NTNU), Trondheim, Norway

[2] Sorbonnes Universités, UPMC University of Paris 6, Paris, France

† Corresponding author: gisle.oye@chemeng.ntnu.no; Sem Sælandsvei 4, 7491 Trondheim, Norway

ABSTRACT

The major contaminant targeted during the treatment of the oilfield produced water is dispersed oil. The efficiency of most separation processes highly relies on the size of the droplets, which can be increased through coalescence. Crude oil has a complex and field-dependent composition, which can affect the interfacial properties of the drops, and consequently the merging process in different ways. This study focused on the development of microfluidic techniques for investigating coalescence between crude oil drops. The experiments were performed with six diluted crude oils and three neat oils, the latter in the presence of an oil-soluble surfactant. The composition of the water phase was systematically varied (pH, ionic composition, presence of dissolved components). In general, crude oil droplets coalesced more readily in lower or neutral pH. The addition of dissolved Fluka acids to the water phase had a unique effect on each crude oil, reflecting their composition. What is more, this effect was similar to the presence of water-soluble crude oil components in the aqueous phase. The pressure did not have a significant effect on the coalescence, which was explained by the lack of the lightest components (C1-C4) in the system. In summary, the results revealed several trends, however it was clear that the coalescence highly depended on the oil composition. This underlined the necessity for experimental methods, such as microfluidics, which allow for quick assessment of the stability of crude oil droplets.

KEYWORDS

Coalescence; Drop; Emulsion; Microfluidics; Produced water.

1. INTRODUCTION

During petroleum production, large volumes of water are co-produced with crude oil and natural gas. This produced water (PW) can be composed of formation water, injected fluids (e.g. seawater or production chemicals), dispersed crude oil, solid particles, and dissolved inorganic and organic components. Globally, it is estimated that the produced water to oil ratio is approximately 3:1[1].

Before the produced water is disposed of (e.g. by re-injection to the reservoir or discharge), it has to undergo quality improving treatment. The main contaminant targeted during the produced water treatment (PWT) processes is the dispersed crude oil. The limit for the discharge of the PW to the sea is between 30 and 40 ppm of oil in water (OiW), depending on the local regulation. However, due to increasing environmental concerns, many countries push for even stricter regulations[2]. The 'Zero Harmful Discharge' policy, initiated at the Norwegian Continental Shelf, not only decreases the limit of the dispersed OiW concentration, but also underlines the necessity for targeting dissolved components during water treatment. Re-injection of the produced water can waive the problem of aquatic pollution, as the oily water is pumped back to an underground formation. Moreover, it can also be used as an increased oil recovery technique that sustains the pressure in the production reservoir. Nevertheless, to avoid formation damage, the requirements for the quality of the produced water must be tailored to the reservoir characteristics and can be similar to those for the discharge[3].

A typical offshore produced water system is composed of a bulk gravity separator, a sand handling system, a hydrocyclone and a gas flotation unit (Figure 1).

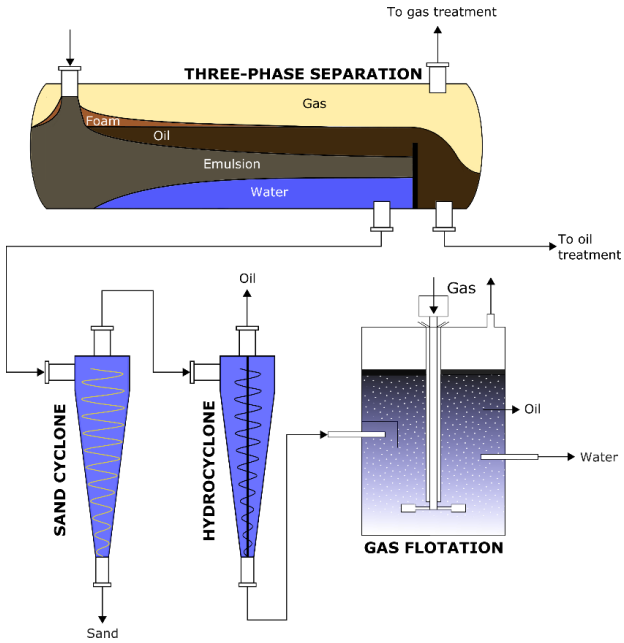

Figure 1 Typical produced water treatment process

The water leaving the gravity separator typically contains 1000 ppm or less of crude oil. The hydrocyclone treatment reduces it further down to 100-300 ppm of OiW, while the gas flotation unit can decrease the oil concentration below the discharge limit. As the oil fields mature, the water cut increases and can reach as high as 95%. Therefore, at some point of the production, the handling of the produced water can bottleneck the entire process. For this reason, subsea treatment of the produced water is considered as a viable alternative to the topside PWT.

Subsea production and processing of crude oil and gas is one of the few options when moving into deeper and more remote waters. In the past two decades, the underwater installations around the world evolved from single satellite wells to complex systems that can perform boosting, compression and separation operations[4]. The subsea treatment of the produced water not only carries the advantage of the reduced volumes of pumped fluids and decreased pressure drop, but can also be beneficial to the separation process. Higher pressure and temperature, maintained in the subsea separation system, can enhance the density difference between the separated phases and reduce the viscosity of the fluids. As a result, the separation efficiency should be higher subsea, compared to the topside conditions[5].

Most of the produced water treatment processes, such as gravity separation, hydrocyclone or gas flotation, highly rely on the droplet size. As described by Stokes law, the creaming velocity in the gravity separators is directly proportional to the square of the drop diameter. In addition, larger drops are easier to encounter by gas bubbles during gas flotation. With the increase of the drop size, the PWT processes are quicker and more effective, resulting in less dispersed OiW in the discharged or reinjected water.

Coalescence is the main process controlling the droplet growth. It can be split into three steps[6]: (1) droplet approach (and collision), (2) thin film drainage and (3) film rupture and fusion of two drops into one. Since the stability of emulsions is an important aspect of many industrial processes, either as a goal to reach or a problem to overcome, it has been extensively studied for many years. Several studies of the coalescence of model oil-in-water drops had been conducted[7-9]. Regarding the crude oil systems, the researchers have paid more attention to the coalescence of water drops in the continuous oil phase[10-13], leaving the crude oil-in-water systems a relatively unexplored topic[14-15]. Crude oil has a very complex composition and can contain a variety of species that influence their interfacial properties, such as resins, asphaltenes[16-17], and acidic species[18]. The dissolved components in the water, partitioned from the oil phase[19], can also adsorb at interfaces[20] and affect the coalescence process. Moreover, crude oil drops may behave differently, when subjected to subsea conditions (i.e. high pressure or temperature). To the best of our knowledge, the effect of pressure on the merging of crude oil drops has not been reported in the literature.

Microfluidics proved to be a very useful tool for studying emulsion stability. Both model oil-in-water[21-23] and water-in-oil systems[24-26] were previously reported in the literature. In the petroleum science, however, the focus of microfluidic applications is rather shifted towards fluid analysis[27-29] and very few papers concerning separation can be found[30].

Previously we have presented a microfluidic approach to study the coalescence of model oil-in-water systems at increased pressure[31]. The objective of the current work was to develop methodology for studying coalescence of crude oil drops under different conditions using microfluidics. The investigated parameters included the composition of the oil phase (different crude oils, diluted and neat), water phase (salinity, pH, dissolved components) and pressure.

2. EXPERIMENTALS

2.1. Chemicals. The physical and chemical properties of six crude oils, produced at the Norwegian Continental Shelf, are summarized in Table 1. Additional characterization (except of crude oil F) and description of methods were reported elsewhere[32].

Table 1 Physicochemical properties of crude oils.

Crude oil	API [°]	Viscosity [mPa s] @20°C	TAN [mg KOH/ g oil]	TBN [mg KOH/ g oil]	SARA [% wt.]			
					Saturates	Aromatics	Resins	Asphaltenes
A	19.2	354.4	2.2	2.8	50.6	31.2	15.7	2.5
B	35.8	14.2	ND	1.0	84.0	13.4	2.3	0.3
C	23.0	74.4	2.7	1.1	64.9	26.3	8.4	0.4
D	36.3	10.2	0.2	1.1	71.5	23.1	5.1	0.3
E	37.9	8.3	0.5	0.4	74.8	23.2	1.9	0.1
F	39.7	7.5	0.1	0.6	78.5	18.9	2.5	0.1

The crude oils were initially diluted to 25% wt. with xylene (Mix of isomers, AnalaR, VWR, USA) to be used as the dispersed phase in the microfluidic investigations. During further tests, three crude oils (B, E, F) were used without dilution and upon addition of 200 ppm of a de-emulsifier. Unless stated otherwise, the measurements were performed with one de-emulsifier (A few experiments in the Section 3.2.1. were also conducted with another de-emulsifier). These additives will later be referred to as oil-soluble surfactants.

Two types of brine were used to simulate produced water salinities at the Norwegian Continental Shelf[33] and to investigate the effect of the divalent ions on the coalescence of the crude oil droplets. Both brines had equal ionic strength (I=0.59M). The first brine, referred to as Na-Brine, contained only sodium chloride (p.a., Merck Millipore, USA). The other, NaCa-Brine, was a mixture of NaCl and $CaCl_2$ (p.a., Sigma-Aldrich, USA) with Ca/Na molar ratio of 1:35. The brines were adjusted to pH 4 and 10 by using solutions of diluted HCl (AnalaR, VWR, USA) and dissolved NaOH (AnalaR, VWR, USA). The natural pH of the brines, later referred to

as pH 6, ranged between 5.8 and 6.6. All aqueous solutions were prepared with deionized water (Millipore Simplicity Systems, Darmstadt, Germany).

2.2. Dissolved components. Three kinds of components were dissolved in water and used as the continuous phase in different microfluidic experiments.

2.2.1. *4-Heptyl benzoic acid (4-HBA).* 100 ppm of the 4-HBA (99+%, Alfa Aesar, USA) was dissolved in Na-Brine at high pH. Subsequently, the solution was adjusted to pH 10.

2.2.2. *Fluka acids.* The water phase with a commercial naphthenic acid mixture (Fluka, Sigma Aldrich, USA; later denoted as Fluka acids) was obtained through partitioning. Heptane (HPLC ≥99%, Sigma-Aldrich, USA) containing Fluka acids was poured into Schott bottles with buffered Na-Brine at pH 6 and 9, respectively. After 12 hours of horizontal shaking, the phases were separated by centrifugation (30 min at 11000 rpm). Part of the water was acidified to pH<2 with hydrochloric acid and shaken with pure heptane to back-extract the organic content for concentration measurement. Samples were silanized with N-tert-Butyldimethylsilyl-N-methyltrifluoroacetamide (MTBSTFA) with 1% tert-Butyldimethylchlorosilane (Sigma-Aldrich, USA) and then analysed with GC/MS for quantification. Finally, the samples were diluted with Na-Brine to contain 100 ppm of acids and adjusted to pH 6 and 10, respectively.

2.2.3. *Dissolved components from crude oils.* Each of the crude oils were mixed with Na-Brine at pH 4, 6 and 10 in order to saturate the water phase with water-soluble oil components. Approximately 100 ml of brine and crude oil were poured into Schott bottles and put on a vertical shaker (200 rpm) for 48 hours. Subsequently, the water phase was extracted and centrifuged to remove any dispersed oil. The pH was measured and afterwards readjusted to the original level. Some water phase was collected, acidified to pH<2 with sulphuric acid, and analysed for the total organic carbon content (TOC-L_{CPH} Analyser, Shimadzu, Japan). The measurements were performed at GIG Research Institute in Katowice, Poland.

2.3. Microfluidic chips and setup. The design of the chips and the microfluidic setup is illustrated in Figure 2.

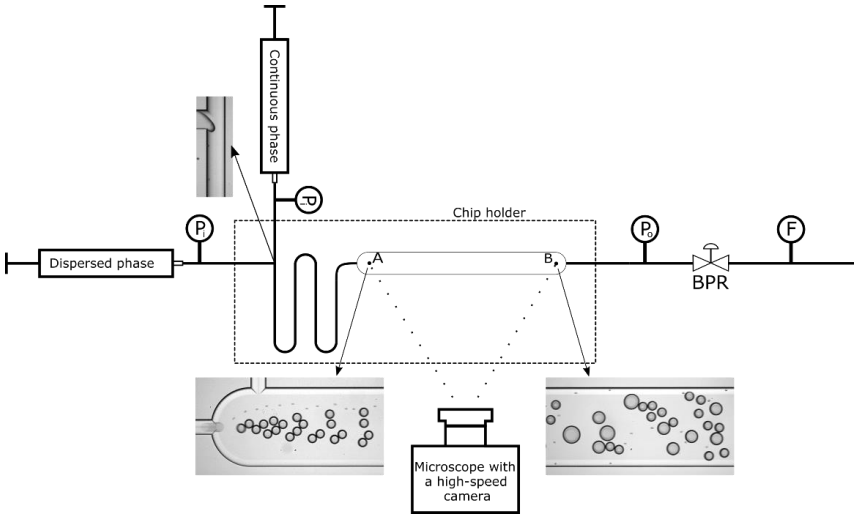

Figure 2 Illustration of the microfluidic setup and chips.

Custom-designed glass microfluidic chips were delivered by Micronit Microtechnologies B.V. (The Netherlands). The inlet channels had a width of 100 µm and led to a T-junction, where the droplets were generated. The drops then passed a meandering channel and entered a coalescence chamber with the width of 500 µm and length of ca. 33 mm, where they could get in contact and possibly undergo coalescence. The wider channel led to the outlet of the chip. All channels had a uniform depth of 45 µm. During the experiments, the chip was placed in a chip holder (Fluidic Connect PRO, Micronit Microtechnologies B.V., The Netherlands) and connected to the rest of the flow setup with FFKM ferrules and PEEK tubing (inner diameter 250 µm, Sigma-Aldrich, USA). The high-pressure measurements were performed with another chip holder (Fluidic Connect 4515, Micronit Microtechnologies B.V., The Netherlands). After the experiment, the chips were cleaned through sonication in three different solvents: toluene/acetone mixture (3:1 v/v), isopropanol and deionized water. Each cleaning step lasted 15 min. Finally, the chips were dried with compressed air and baked in an ashing furnace for six hours at 475°C. Shortly before the experiments, the chips were treated in low-pressure oxygen plasma chamber (Zepto, Diener electronic GmbH, Germany) for 10 minutes.

The liquids were pumped with syringe pumps (neMESYS mid-pressure module V3, Cetoni GmbH, Germany). The pressure level in the system was controlled by a backpressure

regulator (BPR in Figure 2, JR-BPR2, VICI AG International, Switzerland) and monitored with pressure sensor modules (Qmix P, Cetoni GmbH, Germany) at the inlet and outlet of the chip (P_i and P_o in Figure 2, respectively). The flow was measured with a flowmeter (F in Figure 2, mini CORI-FLOW, Elveflow, France). The droplets were observed with a high-speed camera (AX100, Photron, Japan), connected to an inverted microscope (Ti-U Eclipse, Nikon, Japan) with an external LED light source (HDF7010, Hayashi, Japan) at a constant framerate of 8500 frames per second.

2.4. Microfluidic experiment, data acquisition and image analysis.

The experiments were conducted similar to a previous report[31]. In short, the oil and water flow rates were set to 10 and 160 µl/min, respectively. In these conditions the droplets had a diameter of approx. 50 µm. Due to the smaller channels at the inlet of the chip, the readings from the pressure sensor located there indicated approx. 2 bar higher pressure, compared to the outlet of the chip. This pressure drop was present in all tested pressure levels. Two sets of images were taken for each experiment – at the inlet and the outlet of the microfluidic chip (points A and B in Figure 2, respectively). The series from the inlet was used to retrieve the initial size and number of the droplets, and additionally used to verify the accuracy of the recordings from the outlet of the chip. Next, a series of 7000 frames was recorded at the end of the coalescence chamber to assess the extent of coalescence. Both image sequences were processed with the ImageJ software. The frames were first converted into a binary mask and then the areas and the centre of mass coordinates of droplets were retrieved with the Analyse Particle feature. The data was then copied to a Microsoft Excel spreadsheet. It was found that the droplet area increased proportionally with the number of coalescence events. For this reason, the droplets could be sorted into several size classes. It is worth pointing out that the same droplets were detected several times in the consecutive frames. Therefore, the actual number of droplets in each size class (N_f), used for further analysis, was calculated with the average droplet velocity, the width of the detection box and the mean droplet diameter in each size class. The number of initially created droplets (N_{in}) was given by $N_{in} = \sum_{i=1}^{i} n_i * \frac{A_{f_i}}{A_{in}}$, where n_i was the number of class *i* drops, A_{fi} the area of class *i* droplets at the outlet of the channel and A_{in} the area of the initially formed droplets. On average, each dataset consisted of 1500 droplets of the original size. The coalescence frequency was the main parameter for

the comparison between different conditions. It was calculated by $f = \left(\frac{N_{in}}{N_f} - 1\right)/t_{res}$, where t_{res} is the residence time of droplets in the channel (channel length divided by the average drop velocity). All reported values are an average of three parallels with standard deviation.

2.5. Interfacial tension measurements.

The interfacial tension (IFT) measurements were conducted using a pendant drop tensiometer (PAT-1M, Sinterface Technologies, Germany). Images of a crude oil drop, immersed in a brine solution were recorded over time. The measurements lasted 100 seconds. The interfacial tensions were calculated by fitting the drop profiles to the Young-Laplace equation. All measurements were performed at room temperature (22°C).

3. RESULTS AND DISCUSSION

3.1. Diluted crude oils

Initially, we tried to use crude oils as is, however they partially wetted and adsorbed to the glass surface, which prevented droplet generation. Diluting crude oils with an aromatic solvent (xylene) mitigated that issue, allowing us to study the effect of the crude oil chemistry and water composition. The coalescence frequencies of the diluted crude oils are illustrated in Figure 3.

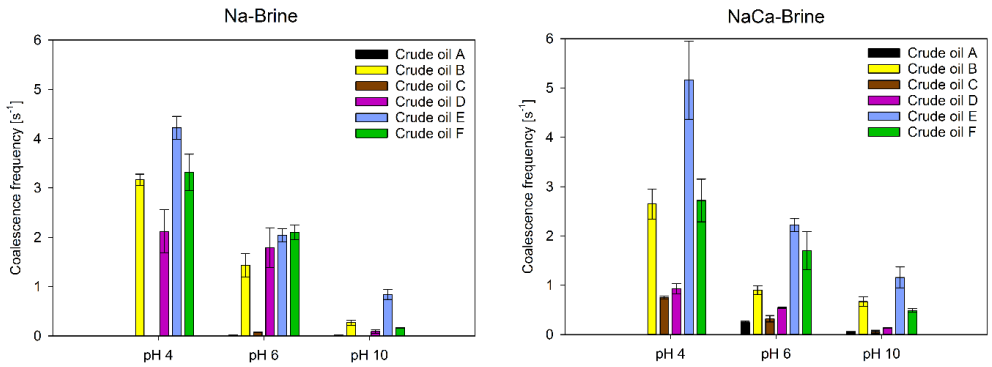

Figure 3 Coalescence frequencies of diluted crude oils in Na- and NaCa-Brine at three pH levels.

In general, the coalescence between the light crude oil drops (B, D, E, F) was more extensive, compared to the heavier ones (A and C). Notably, the viscosity of the oil phases after dilution did not vary much. The final droplet size also depended on the water phase. The highest coalescence frequency was usually observed at the lowest pH and it declined with increasing pH of the water. At low pH, the coalescence between heavier crude oils was difficult to measure, most likely due to the higher TBN values and the fact that in lower pH the glass surfaces often become wetted by crude oils[34] (Figure S1 in SI). In addition, it was impossible to measure the coalescence frequency of crude oil C at pH 10 (Na-Brine) due to the formation very small droplets (Figure S2 in SI), most likely because of high TAN. When calcium was added to the system, the most systematic trend was noticed at pH 10, where its presence boosted the coalescence in almost all cases, compared to the brine without divalent ions. At the other pHs, we did not see any systematic changes in the coalescence frequencies.

Crude oils contain many surface-active components that can be more or less interfacially active in specific conditions. Their interfacial tension (IFT) varies with the pH of the water

phase[35]. This is attributed to the presence of protonated basic species at low pH or dissociated acidic components at higher pH. In general, basic components do not lower the IFT as much as the acids, which has been confirmed both for model[19] and crude oil[36] systems. This effect was reflected in the present coalescence studies, where the droplets coalesced more readily in pH 4 or 6. When the pH was increased to 10, the oil-water interface was controlled by the acids and prevented the droplets from merging with each other through increased interfacial concentration of surface-active components. The acidic species in crude oils are often called naphthenic acids. This group includes a wide range of short- and long-chained carboxylic acids, often with aromatic moieties. They can contribute to a variety of undesirable phenomena during the crude oil production, such as emulsion formation, precipitation or corrosion of the pipelines and process units[18]. Due to their amphiphilic nature, they can adsorb at the oil-water interface[35] or even, in the case of low molecular weight compounds, partition to the water phase[37]. Their interfacial activity in neutral or higher pH is probably the main reason behind the increased stability of droplets. The increase of pH deprotonates more acidic species, which leads to increased interfacial concentration and provides additional stability against coalescence. Moreover, this mechanism is further supported by the results obtained with NaCa-Brine at pH 10. Depending on the molecular structure, naphthenic acids in the presence of an electrolyte in water can form soaps or deposits[38]. These complexes are generally more stable with multivalent ions. High-molecular tetraprotic acids, so called ARN acids, are more likely to form scale[39], whereas low molecular monoacids contribute to forming stable emulsions[40]. In the case of water-in-crude oil emulsions, the latter naphthenates can agglomerate at the interface and lead to problems in flow assurance or separation process[41]. In the case of oil-in-water emulsions, however, it is likely that the addition of calcium removed acids from the interface. These acid-calcium complexes are less interfacially active and more lipophilic in character, which facilitates their diffusion from the interface to the oil phase[42], and most likely resulted in the increased coalescence.

Figure 4 depicts the coalescence frequencies plotted against TAN and TBN values.

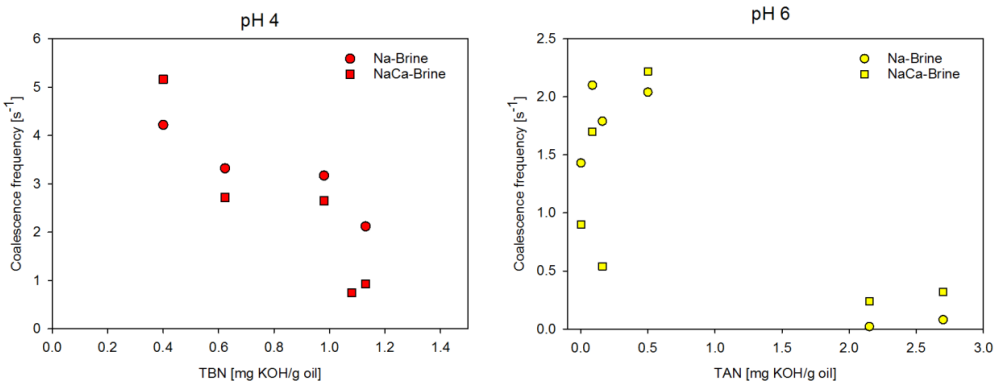

Figure 4 Coalescence frequencies of diluted crude oil plotted against TBN (left) and TAN (right) values of crude oils. The order of crude oils from left to right: E, F, B, C, D (TBN) and B, F, D, E, A, C (TAN).

The crude oils used in this study had the total base numbers ranging from 0.4 to 2.8. At pH 4, the coalescence frequency was found to be inversely proportional to the TBN of the crude oils. This effect was similar for both brines. The total base number is traditionally considered as an indicator for the basic species in crude oils. At lower pH, these components become protonated and affect the interfacial properties of the crude oil drops[36]. This effect can depend both on the type of the basic components and their concentration, as observed in our case. We could not find an explanation for the decrease or increase of coalescence upon addition of calcium.

The coalescence behaviour at higher pH was explained with the total acid number values, as the interfacial properties of crude oil drops are governed by the acidic species. At pH 6 and 10 in Na-Brine, the crude oils could be divided into two groups (plot for pH 10 in Figure S3 in SI). Crude oils with lower TAN value (<0.5) coalesced quite extensively, while hardly any coalescence was observed for the crude oils with high TAN values (>2). This effect can be related to the concentration of the acidic species in the crude oils. At pH 6 only the crude oils with TAN value equal to or higher than 0.5 (A, C, E) experienced an increase of coalescence when calcium was present in the water phase. At pH 10, however, all crude oils experienced an increase of coalescence upon addition of calcium, as discussed before. The results at pH 6 can be interpreted in two ways. First, the interfacial concentration of the naphthenic acids in the less acidic oils might have been too low to observe an effect of calcium. Secondly, the

type of acidic components and the extent of dissociation at the oil-water interface could have played a role[43-44]. We could not find an explanation for why some of the crude oils had consistently lower coalescence frequencies at low or neutral pH upon addition of calcium ions.

A trend was also observed when the coalescence frequencies were plotted against the sum of resin and asphaltene weight fractions of the crude oils (Figure 5).

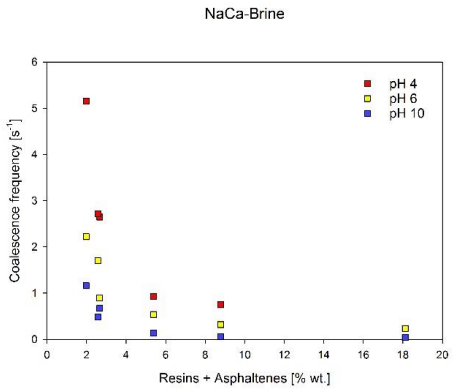

Figure 5 Coalescence frequencies of diluted crude oils plotted against the sum of resins and asphaltenes of respective crude oils.

The coalescence frequencies decayed exponentially with the increasing total resin and asphaltene weight fractions of the crude oils. The coalescence of crude oils with the lowest concentration of these fractions was quite extensive, whereas very little merging occurred at the highest amounts. These trends were similar regardless of the pH or ionic composition (Figure S4 in SI).

The majority of the interfacially active molecules can be found in the resin and asphaltene fractions, which explains their significance for the coalescence frequency. The presence of these species can affect the coalescence between oil drops in several ways. First, the dissociated, charged groups can create electrostatic repulsion, analogous to the effect of ionic surfactants. However, in our system this type of repulsion was significantly decreased due to high electrolyte concentrations. Secondly, the approach and collision between drops may cause gradients in the interfacial concentrations. This will cause a flux of surface-active molecules in the opposite direction of the film drainage process (Marangoni effect), which will impede drainage. Notably, the crude oils were diluted with an aromatic solvent, which

effectively eliminated any asphaltene solubility issues. Nevertheless, asphaltenes in a good solvent could still be present as nanoaggregates[45] and impact the formation of viscoelastic films, and subsequently influence the coalescence between oil drops. In general, the emulsion stability is enhanced with the increase of the elastic properties of the interface[46]. Solutions of asphaltenes in aromatic solvents typically exhibit a maximum of elasticity at a certain concentration[47-48]. In our case, the decreasing coalescence frequency with increasing weight fraction of resins and asphaltenes could also be seen for the increasing percentage of asphaltenes alone (Table 1).

3.2. Crude oils

Method development revealed that the addition of an oil-soluble surfactant facilitated the droplet generation process for some of the crude oils without the need of dilution. Therefore, three light crude oils (B, E, F) were used to investigate the effect of the water composition on the coalescence of *non-diluted* crude oil drops.

3.2.1. Water phase effect.

Figure 6 depicts the coalescence frequencies for the non-diluted crude oils in different brines.

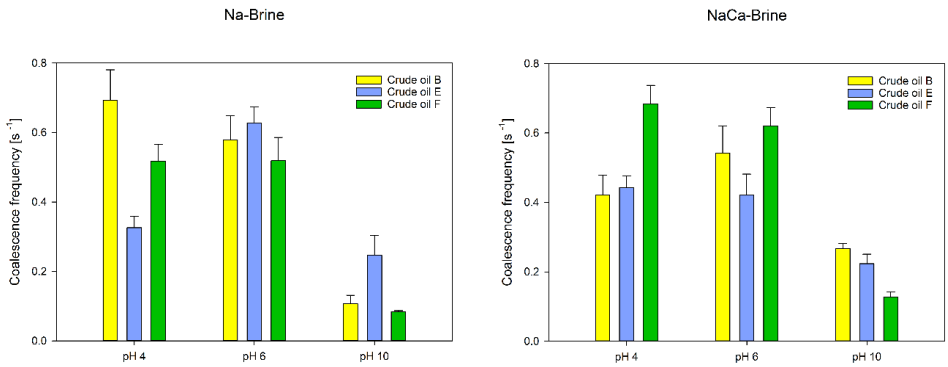

Figure 6 Coalescence frequencies for three crude oils in Na- and NaCa-Brines at different pH levels.

Notably, all coalescence frequencies were significantly lower than for the diluted crude oils. In both brines, the highest coalescence frequencies were observed at pH 4 or 6, and the lower values at pH 10. When considering the effect of divalent ions at pH 10, the coalescence was

either higher (B, F) or did not change (E) upon the addition of calcium. The effect of calcium at other pH varied with the crude oil type.

The complex composition of crude oils will definitely have an impact on the coalescence process during the produced water treatment. Like in the Section 3.1, we attempted to connect the crude oil physical and chemical properties to the observed coalescence behaviour. In this case, however, the addition of the oil-soluble surfactant affected the interfacial behaviour of the crude oil droplets, rendering any analysis based on composition unclear. In general, crude oils react differently to various types and concentrations of oil-soluble surfactants. This was confirmed by the experiments performed with another oil-soluble surfactant (Figure S5 in SI). Nevertheless, the trends observed upon changing the water composition remained quite similar to the results obtained with the diluted crude oils.

3.2.2. Dissolved components – model systems.

Certain components of crude oils are water-soluble. Their partitioning to the water phase can occur in the geological formation, where the two phases spend millions of years in contact, and additionally during the production process, where pressure drops and turbulent flow create further opportunities for mixing and mass transfer. The concentration of the dissolved components is highly field-dependent, but it can reach several hundreds of ppm in the discharged PW[49]. These components can be toxic and pollute the marine environment[50]. Furthermore, they can affect the oil-water separation process. Our group has previously demonstrated the effect of the dissolved components on the air-water interface[20, 51-52] and the flotation performance[53]. In this section we discuss their influence on the coalescence between crude oil droplets.

The results of the coalescence frequency in Na-Brine with and without the partitioned naphthenic acids at pH 6 is shown in Figure 7.

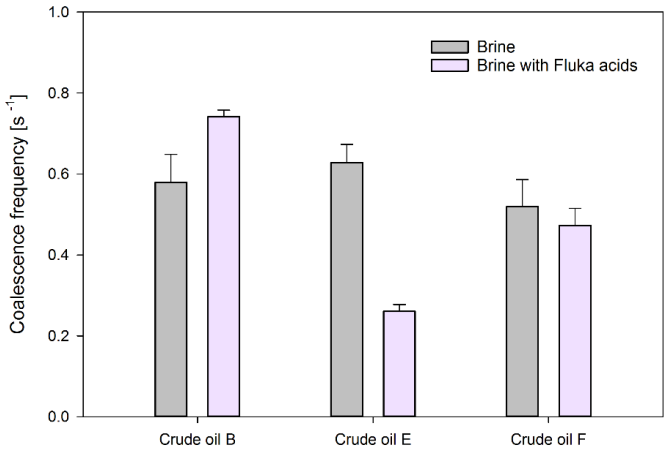

Figure 7 Coalescence frequency of Na-Brine at pH 6 with and without partitioned Fluka naphthenic acids.

Each of the crude oils reacted uniquely to the presence of the dissolved components in the water phase. An increase of coalescence was observed for crude oil B, while the opposite effect was noticed for crude oil E. The dissolved components had little effect on the coalescence with crude oil F. Similar results were obtained for the Fluka acids partitioned at higher pH, presented in Figure 8, together with the results for the 4-heptylbenzoic acid. Also in this case the effect of the dissolved Fluka acids was crude oil-dependent. The acids either promoted coalescence (B, slight increase in F) or reduced it (E).

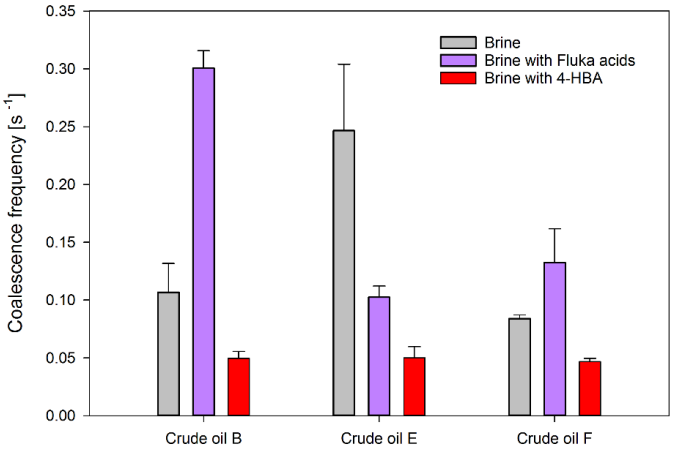

Figure 8 Coalescence frequency of Na-Brine at pH 10 with Fluka partitioned acids, dissolved 4-HBA and without any dissolved components.

Noteworthy, all the oils reacted in a very similar way to the presence of 4-HBA in the continuous phase. The coalescence frequency was reduced to almost identical values of 0.05 s^{-1}, meaning approximately 20 coalescence events for more than 1500 droplets during the recording time.

One possible explanation for the oil-specific response to the presence of the dissolved components is the oil composition, or more precisely the nature of the surface-active components in the crude oils. In the diluted system, crude oil B had lower coalescence frequencies than the other oils. It also had lower resin to asphaltene ratio (R/A) and less aromatic components. Resins are the most polar fraction that is soluble in aliphatic solvents. Although surface-active, they cannot stabilize emulsions by themselves[54]. They are, however, crucial in the emulsion stabilization mechanisms provided by the asphaltenes. Resins were found to increase the stability of asphaltenes in crude oils through solvation[55], and their weight ratio to asphaltene in crude oils correlates inversely with the water-in-oil emulsion stability[54, 56]. Additionally, the R/A ratio has an effect on the film rigidity, which also corresponds to the stability of emulsions[57]. Furthermore, the low fraction of aromatics can contribute to destabilization of asphaltenes. Crude oil B hat the lowest R/A ratio (ca. 8) and lowest aromatic weight fraction. This might have affected the stability of asphaltenes and

increased the film rigidity in the system with standard brine. Upon the addition of dissolved acids, the less stable asphaltenes might have been replaced by the smaller acidic species, diffusing from the water phase, at the interface. Short-chained acids that partitioned at pH 6 might not retard the coalescence between drops to the same extent as the polar, high-molecular weight components from crude oil B. In addition, crude oil B has also slightly higher viscosity, which reduced the diffusion rate from the oil phase to the interface.

In the case of crude oil E and F, the smaller amount of more stable asphaltenes (R/A values of 19 and 25, respectively) should have less effect on the coalescence process. While there was hardly any difference in the coalescence behaviour for crude oil F, the crude oil E experienced a significant decrease of coalescence in the presence of the dissolved acids. Taking the TOC values from Table 2 into consideration, it could be noticed that crude oil F had almost twice as much components that partitioned to the water phase as crude oil E. Moreover, these were predominantly short-chained acids, as the decrease of pH from the initial pH 6 value was much more substantial for that crude oil. Therefore, a competitive mass transfer probably took place between the short-chained acids coming from bulk oil and the acidic species diffusing from the water phase. Even though crude oil E has the highest TAN, it probably contains larger acidic molecules that will diffuse more slowly and will be replaced at the interface by the more mobile short-chained Fluka acids. In addition, it could be possible that some of the acidic species in the water phase partitioned into the oil droplet. Groothuis and Zuiderweg[58] stated that the decreased coalescence rate was expected in systems where mass transfer occured from the continuous to the dispersed phase. These observations were later confirmed by other groups, who reported that the direction of mass transfer affected the film drainage time[59]. This phenomenon is often explained with the Marangoni effect. If the mass transfer occurs from the dispersed to the continuous phase, the concentration of the transferred solute in the thin film region is increased, which will often decrease the local interfacial tension. The interfacial tension gradient will facilitate movement of the fluid outside of the film region, thus promoting film drainage[60]. Conversely, mass transfer from the continuous to the dispersed phase will retard the drainage process by pushing the liquid into the thin film region. In our case, the mass transfer from the water phase to the crude oil E droplet might have inhibited coalescence, compared to the standard brine. Crude oil F

contained more water-soluble acidic components, which possibly limited the mass transfer to the oil phase at pH 6, and did not affect the coalescence in the same way.

Interestingly, the dissolved Fluka acids at pH 6 did not influence the interfacial tension of crude oils (Table 2).

*Table 2 Interfacial tensions of crude oils against different water phases. *value reported after 50s; †value reported after 10s. The shorter measurements were due to instability of the generated drop.*

		Interfacial tension [mN/m]								
Brine type		**Na-Brine**			**NaCa-Brine**			**Dissolved components**		
Oil phase↓	**pH→**	**4**	**6**	**10**	**4**	**6**	**10**	**6 (Fluka)**	**10 (Fluka)**	**10 (4-HBA)**
Crude oil B		14.9	14.1	6.2*	14.6	13.8	8.7	13.5	4.9	3.8†
Crude oil E		14.9	12.9	9.1	12.8	13.1	10.9	13.5	7.9	4.5†
Crude oil F		6.0*	5.6*	5.8†	5.7*	5.8*	5.6*	5.6*	4.7†	-

The oil-soluble surfactant significantly changed the interfacial properties of the oils. The values without the surfactant ranged from 12 to 22 mN/m (for precise values, please refer to our previous report[32]). In some cases, the drop could not be held for longer than 50 or even 10 seconds. Nevertheless, some trends can be observed. At low and neutral pH, the interfacial tension was almost identical, even when using the brine with Fluka acids. Crude oil F had similar values, regardless of the composition of the water phase. For the two other oils, the IFT at pH 10 was lower. However, it increased upon the addition of calcium, which agrees with the previously proposed mechanisms for the calcium – naphthenic acids interactions. The values of the interfacial tension at pH 10 were somewhat lower when Fluka acids were present, whereas the detection limit (ca. 5 mN/m) of the instrument was reached within 10 seconds after generating the droplet for the brine with 4-HBA. The distributions of Fluka acids are depicted in Figures S6 and S7 in SI.

In all cases, Fluka acids at pH 6 had no effect on the interfacial tension and in the same time affected the coalescence frequency in different ways. This might indicate that their limited surface-activity could have played a role in either increasing the coalescence frequency by

replacing some of the high-molecular weight molecules in the case of crude oil B or decreasing it through diffusion from the continuous phase to the oil phase in the case of crude oil E. Finally, all the crude oils experienced a universal drop of coalescence frequency when 4-HBA was in the water phase. At this high pH, 4-heptylbenzoic acid has very high affinity to the oil-water interface[61], significantly reduces the IFT and stabilizes the droplets against coalescence. The 4-HBA completely filled the oil-water interface and 'neutralized' the indigenous surfactants. In contrast to the polydisperse species in the Fluka acids solutions, the 4-heptylbenzoic acid is a single molecule, that packed more efficiently at the interface.

3.2.3. Dissolved components – water-soluble crude oil species.

Table 3 shows the total organic carbon and pH (before readjustment) after 48 hours of contact between the crude oil and water.

Table 3 TOC and pH values of water after contact with crude oils.

Initial pH	Crude oil B		Crude oil E		Crude oil F	
	TOC [ppm]	pH	TOC [ppm]	pH	TOC [ppm]	pH
pH 4	21	4.33	31	4.93	52	4.07
pH 6	17	5.90	30	6.03	49	4.61
pH 10	21	8.91	33	8.67	52	7.21

The amount of the organic content that partitioned from the oil to the water phase depended on the oil, but also differed slightly with the pH. In some cases, the change of pH after mixing was quite significant, which indicated the nature of the partitioned components. In all cases, the lowest amount of TOC was obtained for the neutral pH, while the most marked pH changes were observed at the highest pH. The water phase from crude oil B contained the smallest amount of dissolved organics and experienced relatively small changes of pH, indicating high molecular weights of both acidic and basic species. Similar observations can be made for crude oil E, with a small exception at pH 4, suggesting the presence of smaller basic molecules, which is supported by the significant decrease of coalescence at that pH for that oil. Brines after mixing with crude oil F contained twice the amount of the detected

organic carbon compared to other oils, and experienced significant decreases of pH at pH 6 and 10. This implied significant amount of short-chained acids.

The coalescence frequencies in the water phase containing dissolved crude oil components are illustrated in Figure 9.

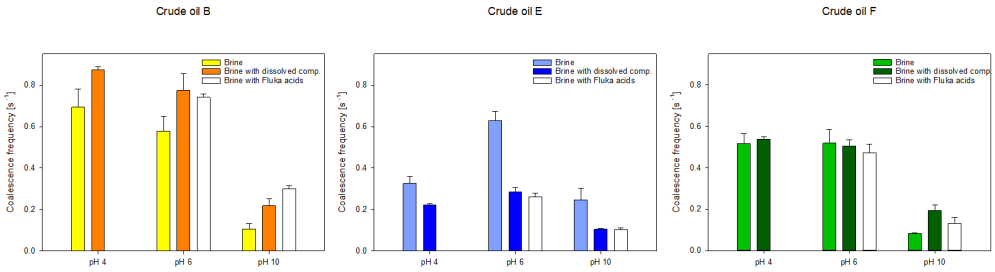

Figure 9 Coalescence frequency of different crude oils in Na-Brines with dissolved crude oil components and Fluka acids.

Also here, the values were oil-specific. The presence of any dissolved components generally resulted in increased coalescence for crude oil B. The opposite effect was observed for crude oil E, while crude oil F experienced only minor changes in coalescence behaviour, limited to the highest pH. Remarkably, the results for the brines with dissolved crude oil components resembled the values acquired with the water phase containing Fluka acids (white bars in Figure 9).

Water-soluble crude oil species are not only of growing environmental concern, but can also affect some aspects of the PW treatment processes. There was no correlation between the crude oil properties and the amount of dissolved organics in the water phase. Moreover, the concentration of the dissolved components did not affect the coalescence frequency in any systematic way. The biggest effects were observed for crude oils B and E, which water phases contained significantly less TOC compared to crude oil F. The results were very similar to the ones presented in the Section 3.2.2., so the previously discussed effect of the dissolved components on the coalescence process also applies here. Since our study was performed with only three crude oils, it is difficult to unambiguously state the impact of the dissolved components on the coalescence process. However, the results demonstrate that their presence in the produced water cannot be neglected. It should also be noted that the striking similarity of coalescence between the water-soluble crude oil components and Fluka acids

suggests that the majority of surface-active components affecting coalescence has acidic nature.

3.2.4. Pressure

Two oils and brines were chosen for experiments at elevated pressure conditions. The results are depicted in Figure 10.

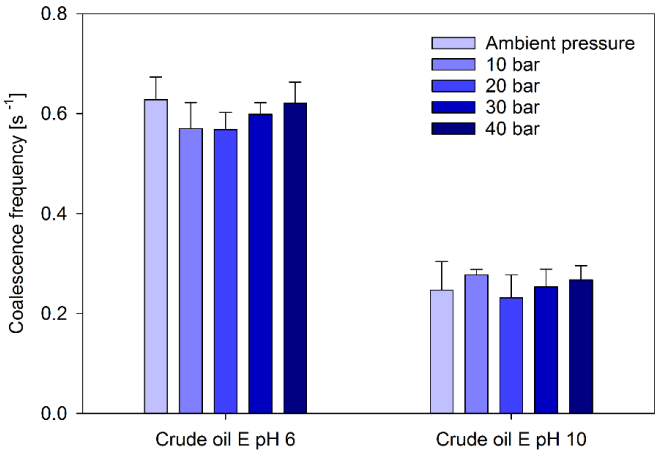

Figure 10 Coalescence frequencies for crude oil E in Na-Brines pH 6 and pH 10 at elevated pressures.

The results show that in the tested pressure range, the extent of coalescence between oil droplets was relatively similar, independent of the pH of the brine and the crude oil (data for crude oil F shown in Figure S8 in SI). The data analysis proved that the differences between the values were statistically insignificant (t-Student, α=0.05).

During the course of experiments, we used 'dead' crude oils, meaning that the samples were depressurized and stored at ambient conditions. As a result, the samples were missing the lightest components (C_1-C_4) that usually flash off during depressurization. This means that, in this range, pressure had minor effect on the physical properties of the crude oils[62-63]. Increased system pressure would lead to increased solubility of the shortest hydrocarbons in the crude oil. This would have several effects on the sample, such as decrease of density or viscosity, and change in the interfacial tension. Higher pressure and change in the crude oil composition can also affect other phenomena associated with crude oil, for instance wax crystallization[64] and asphaltene behaviour[65], which can cause further variations in the oil-

water interface and alter the coalescence between drops. Nevertheless, our results showed that the drop fusion remained unaffected by the increased system pressure, showing that the pressure factor will only contribute to the changes in the chemistry of crude oil drops and not influence the mechanisms of the coalescence process.

4. CONCLUSIONS

We have presented microfluidic methods for investigating coalescence between crude oil drops in water phase. The experiments were first performed with diluted crude oils, followed by a study conducted on crude oil drops with the addition of an oil-soluble surfactant. It was demonstrated that both the composition of the oil and water phases influenced the extent of coalescence in our systems. We have also shown that the dissolved components in the water phase can play a crucial role in the merging process and that this effect is likely to be oil-specific. Furthermore, amongst the various water-soluble components from crude oils, the effect of the acids is dominant in the interfacial behaviour of crude oil drops in water. The pressure did not affect coalescence in any way, which was attributed to the lack of light components (C1-C4) in the crude oils.

We believe that the microfluidic coalescence tool in the present paper will help to understand the role of crude oil chemistry in the produced water treatment, and become a useful method for probing the stability of crude oil drops in water.

ACKNOWLEDGMENTS

This work was carried out as a part of SUBPRO, a Research-based Innovation Centre within Subsea Production and Processing. The authors gratefully acknowledge the financial support from SUBPRO, which is financed by the Research Council of Norway, major industry partners and NTNU. We additionally thank Kelly Muijlwijk, Karin Schroën and Maurice Strubel for their assistance and advice during the method development process.

REFERENCES

1. Fakhru'l-Razi, A.; Pendashteh, A.; Abdullah, L. C.; Biak, D. R.; Madaeni, S. S.; Abidin, Z. Z., Review of technologies for oil and gas produced water treatment. *J Hazard Mater* **2009,** *170* (2-3), 530-51.

2. Igunnu, E. T.; Chen, G. Z., Produced water treatment technologies. *International Journal of Low-Carbon Technologies* **2014,** *9* (3), 157-177.

3. Bader, M. S. H., Seawater versus produced water in oil-fields water injection operations. *Desalination* **2007,** *208* (1), 159-168.

4. Lim, D.; Gruehagen, H., Subsea Separation and Boosting—An Overview of Ongoing Projects. In *Asia Pacific Oil and Gas Conference & Exhibition*, Society of Petroleum Engineers: Jakarta, Indonesia, 2009.

5. Bringedal, B.; Ingebretsen, T.; Haugen, K., Subsea Separation and Reinjection of Produced Water. In *Offshore Technology Conference*, Offshore Technology Conference: Houston, Texas, 1999.

6. Chesters, A. K., The modelling of coalescence processes in fluid-liquid dispersions: a review of current understanding. *Chemical Engineering Research and Design* **1991,** *69* (A4), 259-270.

7. Kourio, M. J.; Gourdon, C.; Casamatta, G., Study of drop-interface coalescence: Drainage time measurement. *Chemical Engineering & Technology* **1994,** *17* (4), 249-254.

8. Podgórska, W., Influence of Dispersed Phase Viscosity on Drop Coalescence in Turbulent Flow. *Chemical Engineering Research and Design* **2007,** *85* (5), 721-729.

9. Kamp, J.; Kraume, M., Influence of drop size and superimposed mass transfer on coalescence in liquid/liquid dispersions – Test cell design for single drop investigations. *Chemical Engineering Research and Design* **2014,** *92* (4), 635-643.

10. Bhardwaj, A.; Hartland, S., Kinetics of coalescence of water droplets in water-in-crude oil emulsions. *Journal of Dispersion Science and Technology* **1994,** *15* (2), 133-146.

11. Frising, T.; Noïk, C.; Dalmazzone, C., The Liquid/Liquid Sedimentation Process: From Droplet Coalescence to Technologically Enhanced Water/Oil Emulsion Gravity Separators: A Review. *Journal of Dispersion Science and Technology* **2006,** *27* (7), 1035-1057.

12. Bresciani, A. E.; Alves, R. M. B.; Nascimento, C. A. O., Coalescence of water droplets in crude oil emulsions: Analytical solution. *Chemical Engineering and Technology* **2010,** *33* (2), 237-243.

13. Opedal, N. v. d. T.; Kralova, I.; Lesaint, C.; Sjöblom, J., Enhanced Sedimentation and Coalescence by Chemicals on Real Crude Oil Systems. *Energy & Fuels* **2011,** *25* (12), 5718-5728.

14. Sterling Jr, M. C.; Ojo, T.; Autenrieth, R. L.; Bonner, J. S.; Page, C. A.; Ernest, A. N. S. In *Coalescence kinetics of dispersed crude oil in a laboratory reactor*, Environment Canada Arctic and Marine Oil Spill Program Technical Seminar (AMOP) Proceedings, 2002; pp 741-753.

15. Gaweł, B.; Lesaint, C.; Bandyopadhyay, S.; Øye, G., Role of Physicochemical and Interfacial Properties on the Binary Coalescence of Crude Oil Drops in Synthetic Produced Water. *Energy & Fuels* **2015,** *29* (2), 512-519.

16. Poteau, S.; Argillier, J.-F.; Langevin, D.; Pincet, F.; Perez, E., Influence of pH on Stability and Dynamic Properties of Asphaltenes and Other Amphiphilic Molecules at the Oil−Water Interface†. *Energy & Fuels* **2005,** *19* (4), 1337-1341.

17. Sjöblom, J.; Marit-Helen, E.; Wanzhen, L.; Xiaoli, Y., Film Properties of Asphaltenes and Resins. In *Encyclopedic Handbook of Emulsion Technology*, CRC Press: 2001; pp 525-540.

18. Havre, T. E.; Sjöblom, J.; Vindstad, J. E., Oil/Water-Partitioning and Interfacial Behavior of Naphthenic Acids. *Journal of Dispersion Science and Technology* **2003,** *24* (6), 789-801.

19. Bertheussen, A.; Simon, S.; Sjöblom, J., Equilibrium partitioning of naphthenic acids and bases and their consequences on interfacial properties. *Colloids and Surfaces A: Physicochemical and Engineering Aspects* **2017,** *529* (Supplement C), 45-56.

20. Eftekhardadkhah, M.; Kløcker, K. N.; Trapnes, H. H.; Gaweł, B.; Øye, G., Composition and Dynamic Adsorption of Crude Oil Components Dissolved in Synthetic Produced Water at Different pH Values. *Industrial & Engineering Chemistry Research* **2016,** *55* (11), 3084-3090.

21. Krebs, T.; Schroën, K.; Boom, R., Coalescence dynamics of surfactant-stabilized emulsions studied with microfluidics. *Soft Matter* **2012,** *8* (41), 10650-10657.

22. Krebs, T.; Schroën, C. G. P. H.; Boom, R. M., Coalescence kinetics of oil-in-water emulsions studied with microfluidics. *Fuel* **2013,** *106*, 327-334.

23. Mazutis, L.; Griffiths, A. D., Selective droplet coalescence using microfluidic systems. *Lab Chip* **2012,** *12* (10), 1800-6.

24. Tan, Y.-C.; Ho, Y. L.; Lee, A. P., Droplet coalescence by geometrically mediated flow in microfluidic channels. *Microfluidics and Nanofluidics* **2007,** *3* (4), 495-499.

25. Baret, J.-C.; Kleinschmidt, F.; El Harrak, A.; Griffiths, A. D., Kinetic Aspects of Emulsion Stabilization by Surfactants: A Microfluidic Analysis. *Langmuir* **2009,** *25* (11), 6088-6093.

26. Zagnoni, M.; Cooper, J. M., On-chip electrocoalescence of microdroplets as a function of voltage, frequency and droplet size. *Lab on a Chip* **2009,** *9* (18), 2652-2658.

27. Fisher, R.; Shah, M. K.; Eskin, D.; Schmidt, K.; Singh, A.; Molla, S.; Mostowfi, F., Equilibrium gas-oil ratio measurements using a microfluidic technique. *Lab Chip* **2013,** *13* (13), 2623-33.

28. Alabi, O. O.; Bowden, S. A.; Parnell, J., Simultaneous and rapid asphaltene and TAN determination for heavy petroleum using an H-cell. *Analytical Methods* **2014,** *6* (11), 3651-3660.

29. Floquet, C. F. A.; Sieben, V. J.; MacKay, B. A.; Mostowfi, F., Determination of boron concentration in oilfield water with a microfluidic ion exchange resin instrument. *Talanta* **2016,** *154*, 304-311.

30. Nowbahar, A.; Whitaker, K. A.; Schmitt, A. K.; Kuo, T.-C., Mechanistic Study of Water Droplet Coalescence and Flocculation in Diluted Bitumen Emulsions with Additives Using Microfluidics. *Energy & Fuels* **2017**.

31. Dudek, M.; Muijlwijk, K.; Schroen, C. G. P. H.; Øye, G., The Effect of Dissolved Gas on Coalescence of Oil Drops Studied with Microfluidics. *Submitted to Journal of Colloid and Interface Science*.

32. Dudek, M.; Kancir, E.; Øye, G., Influence of the Crude Oil and Water Compositions on the Quality of Synthetic Produced Water. *Energy & Fuels* **2017,** *31* (4), 3708-3716.

33. *Produced Water: Technological/Environmental Issues and Solutions*. Springer US: 1992; Vol. 46, p 632.

34. Brown, C. E.; Neustadter, E. L., The Wettability of Oil/Water/Silica Systems With Reference to Oil Recovery. **1980**.

35. Arla, D.; Sinquin, A.; Palermo, T.; Hurtevent, C.; Graciaa, A.; Dicharry, C., Influence of pH and Water Content on the Type and Stability of Acidic Crude Oil Emulsions. *Energy & Fuels* **2007,** *21* (3), 1337-1342.

36. Nenningsland, A. L.; Simon, S.; Sjöblom, J., Surface Properties of Basic Components Extracted from Petroleum Crude Oil. *Energy & Fuels* **2010,** *24* (12), 6501-6505.

37. Hutin, A.; Argillier, J.-F.; Langevin, D., Mass Transfer between Crude Oil and Water. Part 1: Effect of Oil Components. *Energy & Fuels* **2014,** *28* (12), 7331-7336.

38. Hurtevent, C.; Rousseau, G.; Bourrel, M.; Brocart, B., Production Issues of Acidic Petroleum Crude Oils. In *Emulsions and Emulsion Stability*, Sjöblom, J., Ed. Taylor & Francis Group LLC: Boca Raton, FL, 2006; pp 477-516.

39. Sjöblom, J.; Simon, S.; Xu, Z., The chemistry of tetrameric acids in petroleum. *Advances in Colloid and Interface Science* **2014,** *205*, 319-338.

40. Mapolelo, M. M.; Rodgers, R. P.; Blakney, G. T.; Yen, A. T.; Asomaning, S.; Marshall, A. G., Characterization of naphthenic acids in crude oils and naphthenates by electrospray ionization FT-ICR mass spectrometry. *International Journal of Mass Spectrometry* **2011,** *300* (2), 149-157.

41. Havre, T. E., Near-IR spectroscopy as a method for studying the formation of calcium naphthenate. *Colloid and Polymer Science* **2004,** *282* (3), 270-279.

42. Tichelkamp, T.; Teigen, E.; Nourani, M.; Øye, G., Systematic study of the effect of electrolyte composition on interfacial tensions between surfactant solutions and crude oils. *Chemical Engineering Science* **2015,** *132*, 244-249.

43. Dyer, S. J.; Graham, G. M.; Arnott, C., Naphthenate Scale Formation - Examination of Molecular Controls in Idealised Systems. In *International Symposium on Oilfield Scale*, Society of Petroleum Engineers: Aberdeen, United Kingdom, 2003.

44. Brandal, Ø.; Sjöblom, J., Interfacial Behavior of Naphthenic Acids and Multivalent Cations in Systems with Oil and Water. II: Formation and Stability of Metal Naphthenate Films at Oil-Water Interfaces. *Journal of Dispersion Science and Technology* **2005,** *26* (1), 53-58.

45. Mullins, O. C., The Modified Yen Model. *Energy & Fuels* **2010,** *24* (4), 2179-2207.

46. Georgieva, D.; Schmitt, V.; Leal-Calderon, F.; Langevin, D., On the Possible Role of Surface Elasticity in Emulsion Stability. *Langmuir* **2009,** *25* (10), 5565-5573.

47. Angle, C. W.; Hua, Y., Dilational Interfacial Rheology for Increasingly Deasphalted Bitumens and n-C5 Asphaltenes in Toluene/NaHCO3 Solution. *Energy & Fuels* **2012,** *26* (10), 6228-6239.

48. Nenningsland, A. L.; Simon, S.; Sjöblom, J., Influence of Interfacial Rheological Properties on Stability of Asphaltene-Stabilized Emulsions. *Journal of Dispersion Science and Technology* **2014,** *35* (2), 231-243.

49. Hansen, B. R.; Davies, S. H., Review of potential technologies for the removal of dissolved components from produced water. *Chemical Engineering Research and Design* **1994,** *72* (A2), 176-188.

50. Rogers, V. V.; Wickstrom, M.; Liber, K.; MacKinnon, M. D., Acute and Subchronic Mammalian Toxicity of Naphthenic Acids from Oil Sands Tailings. *Toxicological Sciences* **2002,** *66* (2), 347-355.

51. Eftekhardadkhah, M.; Reynders, P.; Øye, G., Dynamic adsorption of water soluble crude oil components at air bubbles. *Chemical Engineering Science* **2013,** *101* (Supplement C), 359-365.

52. Eftekhardadkhah, M.; Øye, G., Dynamic Adsorption of Organic Compounds Dissolved in Synthetic Produced Water at Air Bubbles: The Influence of the Ionic Composition of Aqueous Solutions. *Energy & Fuels* **2013,** *27* (9), 5128-5134.

53. Eftekhardadkhah, M.; Aanesen, S. V.; Rabe, K.; Øye, G., Oil Removal from Produced Water during Laboratory- and Pilot-Scale Gas Flotation: The Influence of Interfacial Adsorption and Induction Times. *Energy & Fuels* **2015,** *29* (11), 7734-7740.

54. Spiecker, P. M.; Gawrys, K. L.; Trail, C. B.; Kilpatrick, P. K., Effects of petroleum resins on asphaltene aggregation and water-in-oil emulsion formation. *Colloids and Surfaces A: Physicochemical and Engineering Aspects* **2003,** *220* (1), 9-27.

55. Murgich, J.; Strausz, O. P., Molecular Mechanics of Aggregates of Asphaltenes and Resins of the Athabasca Oil. *Petroleum Science and Technology* **2001,** *19* (1-2), 231-243.

56. Schorling, P. C.; Kessel, D. G.; Rahimian, I., Influence of the crude oil resin/asphaltene ratio on the stability of oil/water emulsions. *Colloids and Surfaces A: Physicochemical and Engineering Aspects* **1999,** *152* (1), 95-102.

57. Strassner, J. E., Effect of pH on Interfacial Films and Stability of Crude Oil-Water Emulsions. **1968**.

58. Groothuis, H.; Zuiderweg, F. J., Influence of mass transfer on coalescence of drops. *Chemical Engineering Science* **1960,** *12* (4), 288-289.

59. Chevaillier, J. P.; Klaseboer, E.; Masbernat, O.; Gourdon, C., Effect of mass transfer on the film drainage between colliding drops. *Journal of Colloid and Interface Science* **2006,** *299* (1), 472-485.

60. Kopriwa, N.; Buchbender, F.; Ayesterán, J.; Kalem, M.; Pfennig, A., A Critical Review of the Application of Drop-Population Balances for the Design of Solvent Extraction Columns: I. Concept of Solving Drop-Population Balances and Modelling Breakage and Coalescence. *Solvent Extraction and Ion Exchange* **2012,** *30* (7), 683-723.

61. Spildo, K.; Høiland, H., Interfacial Properties and Partitioning of 4-Heptylbenzoic Acid between Decane and Water. *Journal of Colloid and Interface Science* **1999,** *209* (1), 99-108.

62. Al-Besharah, J. M.; Akashah, S. A.; Mumford, C. J., The effect of temperature and pressure on the viscosities of crude oils and their mixtures. *Industrial & Engineering Chemistry Research* **1989,** *28* (2), 213-221.

63. Karnanda, W.; Benzagouta, M. S.; AlQuraishi, A.; Amro, M. M., Effect of temperature, pressure, salinity, and surfactant concentration on IFT for surfactant flooding optimization. *Arab J Geosci* **2013,** *6* (9), 3535-3544.

64. Vieira, L. C.; Buchuid, M. B.; Lucas, E. F., Effect of Pressure on the Crystallization of Crude Oil Waxes. I. Selection of Test Conditions by Microcalorimetry. *Energy & Fuels* **2010,** *24* (4), 2208-2212.

65. Golkari, A.; Riazi, M., *Experimental Investigation of Miscibility Conditions of Dead and Live Asphaltenic Crude Oil-CO۲ Systems*. 2016; Vol. 7.

Paper 4

Removal of Crude Oil Droplets through Spreading on Gas Bubbles Studied with Microfluidics

Removal of Crude Oil Droplets through Spreading on Gas Bubbles Studied with Microfluidics

Marcin Dudek[1] and Gisle Øye[1,†]

[1] Ugelstad Laboratory, Department of Chemical Engineering, Norwegian University of Science and Technology (NTNU), Trondheim, Norway

† Corresponding author: gisle.oye@chemeng.ntnu.no; Sem Sælandsvei 4, 7491 Trondheim, Norway

ABSTRACT

Gas flotation process is often used during treatment of the oilfield produced water. It relies on the generation of gas bubbles and their attachment to oil drops, for example by forming an oil film on the surface of a gas bubble. In this paper we present a microfluidic technique for investigating the removal efficiency of crude oil drops by gas bubbles through spreading mechanism. The developed method allowed us to systematically study the effect of the oil, water and gas phases. The highest removal efficiencies were observed at low or neutral pH. By reducing the salinity, the electrostatic repulsion increased, which had a negative effect on the removal efficiency. The addition of the dissolved components stabilized the oil drops and gas bubbles, which decreased their removal through spreading. Using methane instead of nitrogen improved the interactions between bubbles and oil droplets, leading to more oil being removed.

INTRODUCTION

Produced water (PW) is a major by-product during crude oil and natural gas production. It is composed of both dissolved and dispersed components[1], of which some need to be removed for the water to be discharged to the sea or re-injected to an underground formation[2]. The commonly targeted pollutant during PW treatment is the dispersed crude oil. After initial treatment processes, the water typically contains up to 250-300 ppm of crude oil droplets that are smaller than 25 µm. These oil droplets are meta-stable in water due to their size and the presence of indigenous surfactants in the petroleum. The target is to reduce the concentration down to 30-40 ppm, which is the universally accepted limit for discharge to the sea[1].

Gas flotation is one of the common produced water treatment processes, and uses the dispersed or nucleated gas bubbles to enhance the density difference between oil and water. The generated bubbles can attach to oil drops and form aggregates that are both bigger and less dense, and thereby easier to remove. This attachment can occur through different mechanisms[3], such as formation of an oil film or lens, point attachment, entrapment in a turbulent wake or physical lifting of oil droplets by flocculated gas bubbles. The oil film on the gas bubble provides the most stable bubble-drop aggregate. Generally, it can be divided into three stages[4]: (1) approach and thin film formation, (2) film drainage and (3) film rupture and spreading of oil over the surface of a gas bubble. These processes are depicted in Figure 1.

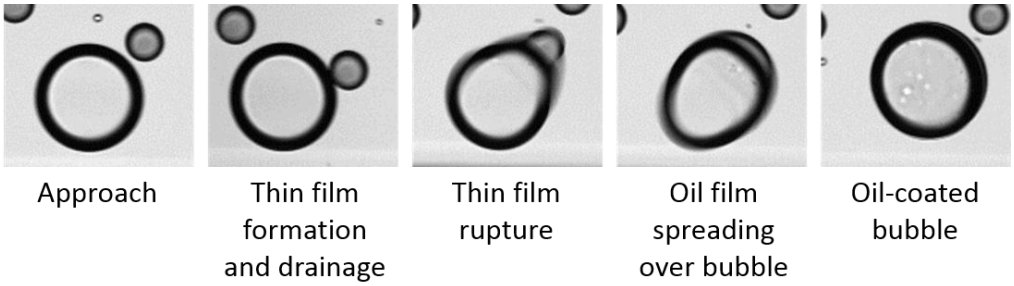

Figure 1 The stages of bubble-drop interactions, leading to formation of an oil film on a gas bubble.

The collisions between bubbles and drops, together with the characteristic drainage time, govern the total removal efficiency through this mechanism[5]. Thin film drainage is a

complicated process, depending both on the interfacial properties of all three phases (gas, oil and water), and on the hydrodynamic forces inside the process unit.

Crude oil is a complex mixture of hydrocarbons and other organic species. Certain fractions of crude oil, like resins, asphaltenes or naphthenic acids, are surface-active and can influence the interfacial behaviour of crude oil drops in water[6-7]. Furthermore, water-soluble components can partition to the water phase and affect the gas-water interfaces[8]. For the water produced at the Norwegian Continental Shelf, these dissolved species are predominantly of acidic nature[9]. The crude oil-indigenous amphiphilic molecules can affect the stability of the thin film and the drainage process during bubble-droplet interactions. They give raise to additional repulsive forces (electrostatic or steric), and can also retard the film drainage time through the Marangoni effect[10].

The role of interactions between gas bubbles and crude oil droplets during gas flotation has scarcely been reported in the literature. Nikolov et al. studied the thin film stability between crude oil droplets and air bubbles[11]. Another study, conducted by Oliveira et al., tried to relate the fundamental interactions between gas bubbles and oil droplets to the flotation efficiency with the use of well-defined systems[12]. The effect of solvent on the induction time in bitumen-air systems was studied by He et al.[13]. Recently, Chakibi et al. reported the role of salinity on induction time and laboratory flotation performance of crude oil emulsions[14]. Our group has also contributed to the field by studying the film drainage times between bubbles and crude oil drops[15], which was later related to the performance of a pilot-scale flotation[16]. Interestingly, none of the groups used similar experimental setup for studying the interactions between bubbles and drops, which indicates that the existing methodology may not be sufficient.

Microfluidics has recently emerged as a new tool for studying the fundamental aspects of dispersions and their stability[17]. It has been extensively used to investigate coalescence in emulsions[18-20], recently also in the petroleum field[21-22]. While three-phase systems were studied with microfluidic tools[23-25], the application of these systems was limited to foam flooding in petroleum research[26-28]. No reports on the microfluidic studies of crude oil droplet spreading on gas bubbles were found.

In this work we present a new, microfluidic method to probe the interactions between bubbles and crude oil droplets that normally occur during a gas flotation process, by investigating the spreading of oil drops over the gas bubble surface inside a microchannel, and reporting the oil removal efficiency. We systematically varied the water and oil composition, as well as the droplet number and size. The effect of the gas phase on the spreading efficiency by using both nitrogen and methane bubbles was also reported.

EXPERIMENTALS

Chemicals.

Brines. Two types of brine were used as the continuous phase during most experiments. The first brine (later referred to as Na-Brine) was composed of 3.5% wt. sodium chloride (p.a., Merck Millipore, USA). The second brine was a mixture of sodium chloride and calcium chloride (p.a., Sigma-Aldrich, USA), with a Ca/Na molar ratio of 1:35. Both solutions had the same ionic strength and were prepared with deionized water (Millipore Simplicity Systems, Darmstadt, Germany). They were adjusted to pH 4 and 10 by using solutions of diluted HCl (AnalaR, VWR, USA) and dissolved NaOH (AnalaR, VWR, USA). The natural pH of the brines, later referred to as pH 6, ranged from 5.8 to 6.6. The low salinity brine, used in the Brine Effect section, consisted of 20 mM of sodium chloride.

Dissolved components. The water phase with dissolved naphthenic acids (Fluka, Sigma Aldrich, USA; later denoted as Fluka acids) was prepared through partitioning from heptane (HPLC ≥99%, Sigma-Aldrich, USA). Buffered Na-Brines at pH 6 and 9, and solutions of Fluka acids in heptane were poured into Schott bottles and mixed on a horizontal shaker for 12 hours. After shaking, the water phase was extracted and centrifuged (30 min, 11 000 rpm). Some of the water was acidified to pH <2 with hydrochloric acid and mixed with heptane to back-extract the acids for concentration measurement. The samples were silanized with N-tert-Butyldimethylsilyl-N-methyltrifluoroacetamide (MTBSTFA) with 1% tert-Butyldimethylchlorosilane (Sigma-Aldrich, USA) and then analysed with GC/MS. With the known concentration, the samples were diluted with Na-Brine to contain 100 ppm of acids and re-adjusted to pH 6 and 10. The solution of 4-heptylbenzoic acid (4-HBA, 99+%, Alfa Aesar, USA) was prepared by dissolving 100 ppm of the acid in Na-Brine at high pH. After dissolution, the solution was readjusted to pH 10.

The surface tension measurements of brines, with and without the dissolved components, were conducted with a Du Noüy ring tensiometer (Sigma 70, KSV, Finland). The reported values were noted after 24 hours of measurement.

Crude oils. Three crude oils, produced at the Norwegian Continental Shelf and with the addition of 200 ppm of a de-emulsifier, were used as the dispersed phase. The summary of the physical and chemical properties is presented in Table 1. The full characteristics of the crude oils and description of experimental methods were reported elsewhere[29] (crude oil F was not included in that study).

Table 1 Physicochemical properties of the crude oils.

Crude oil		Density [g/cm^3] @20°C	Viscosity [mPa s] @20°C	TAN [mg KOH/ g oil]	TBN [mg KOH/ g oil]	SARA [% wt.]			
						Saturates	Aromatics	Resins	Asphaltenes
	B	0.841	14.2	ND	1.0	84.0	13.4	2.3	0.3
	E	0.831	8.3	0.5	0.4	74.8	23.2	1.9	0.1
	F	0.822	7.5	0.1	0.6	78.5	18.9	2.5	0.1

Gas phase. Most experiments were performed with nitrogen (grade 5.0). The measurements in the Gas Phase Effect section were also conducted with methane (grade 3.5).

Microfluidic chips and setup.

The design of the chips and the microfluidic setup used during the microfluidic gas flotation experiments is illustrated in Figure 2.

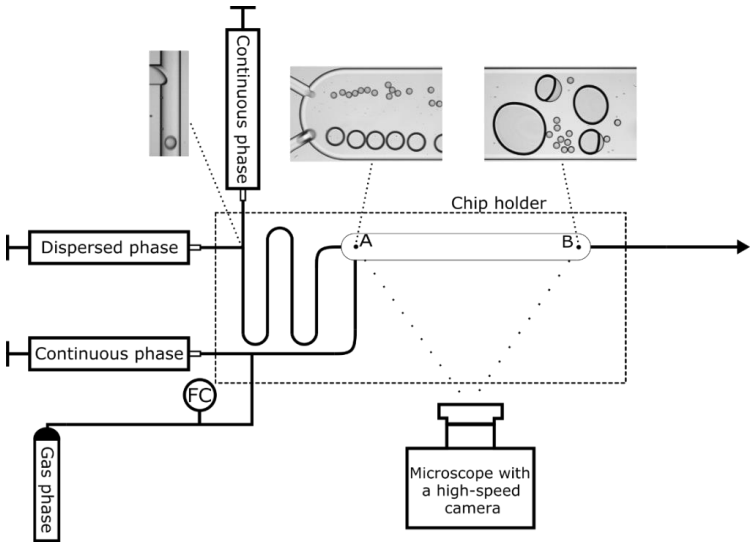

Figure 2 Microfluidic setup and chips.

Custom-designed glass microfluidic chips were purchased from Micronit Microtechnologies B.V. (The Netherlands). They had two T-junctions, where the simultaneous generation of gas bubbles and oil droplet took place. The inlet channels, leading to and from the T-junctions, had a width of 100 µm. The wider channel, where the bubbles and droplet met, was 750 µm wide and 33 mm long.
All channels had a uniform depth of 45 µm. After entering the wider channel, the fluid particles started to intermingle, which resulted in some of the oil droplets spreading on the gas bubble surface. During the measurements, the chip was placed in a chip holder (Fluidic Connect PRO, Micronit Microtechnologies B.V., The Netherlands) and connected to the flow setup with FFKM ferrules and PEEK tubing (inner diameter 250 µm, Sigma-Aldrich, USA). After the experiment, the chips were cleaned through sonication in three different solvents: toluene/acetone mixture (3:1 v/v), isopropanol and deionized water. Each cleaning step lasted 15 min. Finally, the chips were baked in an ashing furnace for six hours at 425°C. Shortly before the experiments, the chips were treated in low-pressure oxygen plasma chamber (Zepto, Diener electronic GmbH, Germany) for 10 minutes.

The liquids were pumped with syringe pumps (neMESYS mid-pressure module V3, Cetoni GmbH, Germany). The flow of gas was controlled with a gas flow controller (EL-Flow Prestige, Bronkhorst High-Tech B.V., The Netherlands). The flow conditions in the respective experiments are presented in Table 2.

Table 2 Experimental conditions of the respective sections.

Section	Droplet generation			Bubble generation		
	Continuous phase flow [µl/min]	Dispersed phase flow [µl/min]	Droplet diameter [µm]	Continuous phase flow [µl/min]	Dispersed phase flow [µl/min]	Bubble diameter [µm]
Brine Effect	160	6	55	120	43	150
Concentration Effect	160	4 6 8	55			150
Drop Size Effect	120 160 200	8 6 4	70 55 40			150
Dissolved Comp. Effect	160	6	55			100-110
Gas Phase Effect	160	6	55			150

The provided value of the bubble diameter in all sections except the Dissolved Components Effect was a result of quick coalescence between the generated 110 µm bubbles in the beginning of the channel. During the experiments with dissolved components, the bubbles were stabilized against coalescence by the acidic species, present in the water phase. The number of droplets generated in unit time was proportional to the dispersed flow rate. In the Concentration Effect section, the lowest flow rate allowed production of ca. 1000 drops/s, 6 µl/min produced around 1400 drops/s, whereas the highest flow rate resulted in approx. 1800 droplets/s. In all other sections, the flow rates were set so the number of droplets entering the wider channel in unit time was similar (approx. 1400 drops/s).

The droplets were observed with a high-speed camera (AX100, Photron, Japan), connected to an inverted microscope (Ti-U Eclipse, Nikon, Japan) with an external LED light source (HDF7010, Hayashi, Japan) at a constant framerate speed of 8500 frames per second.

Data acquisition and image analysis.

The image analysis method was based on the one reported before[30-31], with a few modifications. Two sets of ca. 16000 frames at the inlet and outlet of the chip (points A and B in Figure 2, respectively) were taken for each of the experiment. The images from the inlet were used to retrieve the number and size of the generated droplets. The number of the remaining drops, not removed by gas bubbles, was determined from the outlet images. Both image sequences were processed with ImageJ software. The frames were first converted into a binary mask and then the areas and the centre of masses coordinates of droplets were retrieved with the Analyse Particle feature, available in the ImageJ software. Due to the limited coalescence between oil drops, the remaining drops were always significantly smaller than the gas bubbles. This made it possible to differentiate them from the bubbles with the use of a size limitation feature, as shown in Figure 3.

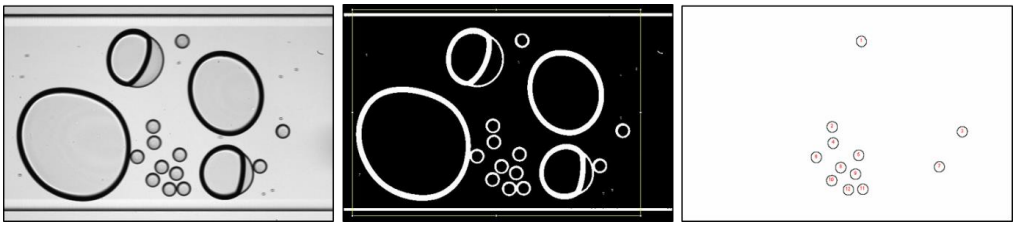

Figure 3 The stages of image analysis. From left: original image, frame converted to a binary mask and detected objects.

Subsequently, the data was copied to a Microsoft Excel spreadsheet. Even though the coalescence between drops was practically negligible, the detected droplets at the end of the channel were sorted into several size classes. The droplet area increased proportionally with the number of coalescence events, which allowed recalculating the drops of different sizes to the number of drops of the initial size that formed them. Since the same droplets were detected several times within the detection frame, the actual number of droplets in each size class was calculated with the use of the average droplet velocity, the width of the detection box and the mean droplet diameter in each size class. The removal efficiency (RE) was the main parameter used to compare different experimental conditions. It was calculated with Equation 1:

$$Removal\ efficiency\ [\%] = \frac{drops_{in} - drops_{out}}{drops_{in}} \quad (1)$$

where $drops_{in}$ and $drops_{out}$ are the number of drops detected in the inlet and outlet of the chips in unit time. In the Drop Size Effect section, the removal efficiency was normalized with respect to the residence times, in order to eliminate its effect on the final result. The normalization was done by multiplying the number of droplets removed during the experiment by the ratio between the average residence time for the middle-sized drops and the calculated residence time for the specific experiment. All values are reported as the average of three measurements and the standard deviation.

RESULTS AND DISCUSSION

Brine Effect.

The oil removal efficiencies resulting from oil spreading on gas bubbles for three crude oils in two different brines are presented in Figure 4.

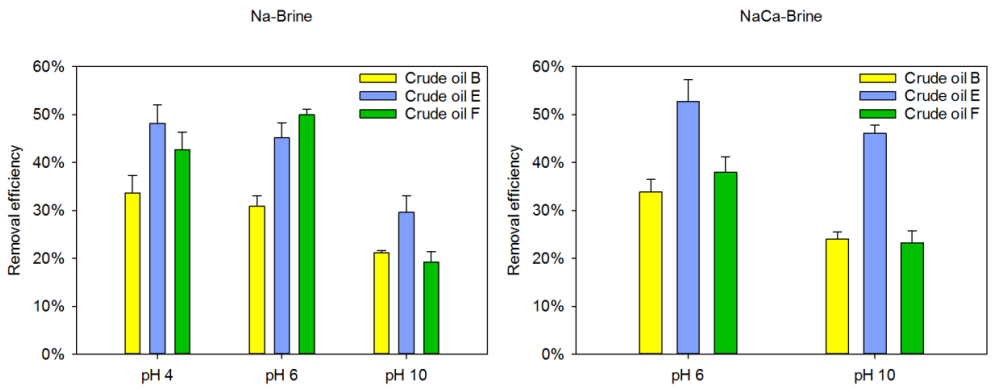

Figure 4 Removal efficiencies of three crude oils in Na- and NaCa-Brine at three pH levels.

The highest removal efficiencies (RE) were found in the lower pH levels. All the oils gave a significant decrease of RE when the pH was raised to 10. When comparing both brines at pH 6, more droplets were removed for two of the oils (B, E), whereas less droplets spread on the gas bubbles in the case of crude oil F. At pH 10 in NaCa-Brine, the removal efficiency improved compared to the systems without calcium ions. In many cases crude oil B had the lowest RE.

The pH level of the aqueous phase will determine the type of surface-active components present at the crude oil-water[32] and the gas-water[33] interface. Crude oil is a complex mixture of hydrocarbons and various organic species. Some of them, typically found in the resin and asphaltene fractions, are polar due to high aromaticity and the presence of heteroatoms, such as nitrogen, oxygen and sulphur[34]. These components can accumulate at interfaces, reduce the interfacial tension and also lead to the formation of viscoelastic interfacial layers that retard the drainage process. At low pH, the basic components diffuse to the interface and become protonated, whereas at neutral and higher pH the acids control the crude oil interfacial activity. In general, the acidic species in crude oil are considered to be more surface-active because of less complex structure and higher affinity to the water phase in

wider range of pH. This would explain the significantly lower removal efficiencies, achieved at higher pH levels. Furthermore, at high pH some water-soluble crude oil components may partition from the oil to the water phase[35]. These dissolved components can then accumulate at the surfaces of bubbles and will be an additional factor in the reduction of removal efficiency at high pH. The detailed mechanisms involving dissolved components are explained later. When calcium was present at high pH, the removal efficiency increased in all cases. This effect can be attributed to the complexing ability of divalent ions with the dissociated naphthenic acids[36]. The formed complexes are less hydrophilic than the charged species, and may partition back to the oil phase. This phenomenon may effectively reduce the interfacial concentration of surfactants at both oil-water and gas-water interfaces and lead to an increase of the interfacial tension[37], which explains the improved removal efficiency in the NaCa-Brine at pH 10. He et al., who studied the induction time of bitumen on gas bubbles, had similar observations[13].

The slightly higher viscosity of crude oil B might explain the overall lower removal efficiency of this oil. The drainage and rupture process of the thin film between oil droplet and gas bubble is sometimes divided into induction (drainage) time and coverage (spreading) time. Some authors reported a dependence of the oil viscosity on the latter[14-15].

The effect of salinity level on the removal efficiency of two crude oils is presented in Figure 5.

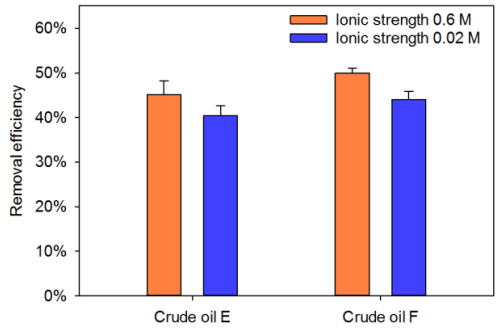

Figure 5 Comparison of removal efficiencies of two oils in high and low salinity brines.

Both oils experienced a decrease in the removal efficiency upon reduction of the salinity. The level of salinity plays an important role for the interfacial properties of both air-water and oil-water interfaces during gas flotation. In the case of oil droplets, high salinity (HS) can screen

negative charges acquired by crude oil drops in the water phase[38], thus decreasing the repulsion between them. At the same time, the abundant presence of an electrolyte will also promote packing of surface-active species at the interface, which will have a negative effect on the bubble-drop interactions. Similar to the oil droplets, gas bubbles in water are also negatively charged due to the preferential adsorption of hydroxyl ions and adsorbed components at the vicinity of gas/water interfaces[39]. In HS brine, the electrical double layer is significantly compressed by the electrolyte, however in low salinity (LS) the overlapping electrical double layers will provide negative interactions between droplets and bubbles. In addition, it has been reported that the coalescence of gas bubbles greatly depends on the concentration of salt in the solution[40-41]. A recent microfluidic study confirmed that the amount and type of the electrolyte influences the coalescence between bubbles[42]. The salinity level in our system could also have an effect on the bubble size distribution in the microfluidic channel which, as discussed later, can affect the spreading of oil droplets on gas bubbles. Nevertheless, the trends agree with other reports demonstrating the decreased induction time and improved flotation performance with increased salinity[12, 14-15].

Concentration Effect.

The effect of the droplet generation rate (i.e. oil concentration) on the removal efficiency of two crude oils is depicted in Figure 6.

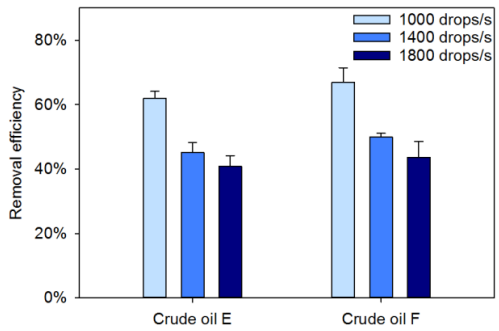

Figure 6 Effect of droplet production rate (i.e. oil concentration) on the removal efficiencies of two crude oils.

Both oils showed similar, declining trend of the removal efficiency when increasing the number of produced drops. In general, flotation units underperform when the influent has

more than 500-1000 mg/L of dispersed oil and the droplets are larger than 200 µm in diameter[43], and they are typically preceded by hydrocyclones. Therefore, the tendencies observed here are reasonable. Interestingly, if the absolute number of removed drops is considered, the trend is reversed. The microfluidic gas flotation at the highest concentration (ca. 1800 drops/s) removed between 700 and 750 drops per second, whereas at the lowest concentration (1000 drops/s), the amount of removed drops was close to 600 droplets per second. This was most likely due to the mechanism, speculated by Strickland[5], in which the oil coated bubbles are more probable to merge with free oil droplets than the non-coated bubbles. Indeed, upon visual inspection of the recorded images, we observed bigger bubbles for the lower concentration (Figure 7A), whereas smaller bubbles with thicker oil films were seen when the concentration was higher (Figure 7B).

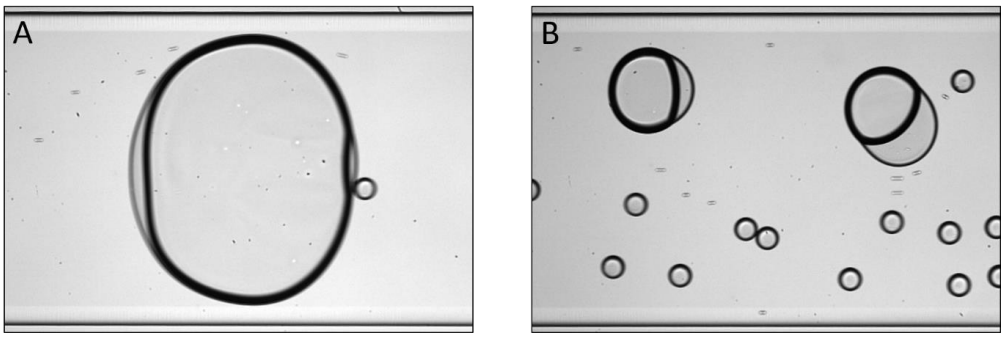

Figure 7 Snapshots from low (A) and high (B) oil concentration experiments.

Bubbles with more oil on their surface were more prone to detachments events, which led to the formation of relatively big oil droplets. While they could have been excluded with the size limitation of the detection tool, this would only decrease the removal efficiency, therefore the observed trends would be unaffected. Less collisions with smaller amount of oil drops could also lead to more extensive coalescence between gas bubbles, as oil film inhibits bubble-bubble coalescence. The change in the bubble size distribution can affect the spreading of oil droplets over the gas bubbles[3]. The droplet sizes can affect the removal efficiency in a similar way, and this is discussed next.

Oil Droplet Size Effect.

The removal efficiency of the droplets of different sizes for two crude oils is shown in Figure 8.

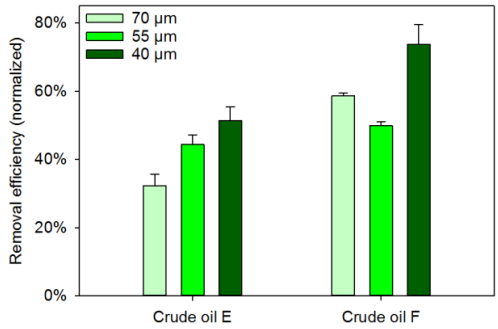

Figure 8 The influence of drop size on the removal efficiencies of two crude oils.

The smallest droplets (approx. 40 µm) had the highest RE in both cases. The trend was not consistent in the remaining two sizes (ca. 55 and 70 µm). Noteworthy, the number of drops produced in unit time was kept constant. The results were normalized to include the effect of the differences in the residence times caused by the changes in the total flow rates.

Typically, gas flotation treatment follows a gravity-based separator (e.g. hydrocyclone), which removes the largest drops from the water phase. For this reason, the PW entering a flotation unit usually contains drops below 25 µm in diameter[2]. However, in some cases the flotation system may consist of several cells, which makes it capable of being a single-step water treatment process[44]. Nevertheless, the effect of the droplet size on the performance of gas flotation can be quite convoluted. On the one hand, bigger droplets should be easier to encounter and consequently be removed by the gas bubbles during the flotation process, which was confirmed by several experimental studies[5, 45]. In addition, larger drops experience higher buoyancy forces that increase their rising velocity, consequently adding the gravity separation effect to the overall efficiency. On the other hand, the bubble-droplet size ratio is also important for determining the mechanisms, with which the dispersed particles are removed[3]. In our system, the removal efficiency depended solely on the spreading of oil over gas bubbles, so the comparison with the total flotation performance might not be very accurate. The fact that the smallest drops were removed more efficiently in our system could

be explained by the differences in drainage time. During a collision between a bubble and a droplet, a thin water film is formed. Its thickness is proportional to the droplet radius[46-47] and is an important parameter determining the film drainage rate[48]. If all other parameters, such as physicochemical properties, bubble numbers and sizes, and hydrodynamic forces (the total flow rate in the channel was only slightly different for each drop size), are kept constant, then the decrease in the film thickness should also reduce the drainage time. Consequently, smaller droplets needed less time to spread over the surfaces of gas bubbles, which increased the RE, as observed in our case.

Dissolved Components Effect.

The effect of the dissolved components was studied in Na-Brine at pH 6 and 10, and compared to the results obtained with Na-Brine only. The results are presented in Figure 9.

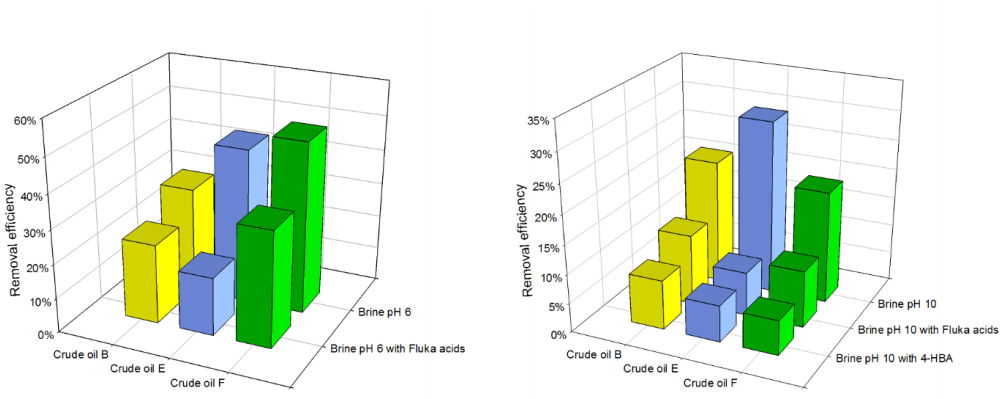

Figure 9 Comparison the removal efficiencies in Na-Brines with and without dissolved components at pH 6 (left) and pH 10 (right).

The presence of dissolved components caused a reduction of the removal efficiency in all cases, and the decrease of spreading of oil on bubbles was found to be both oil- and water-dependent. The dissolved Fluka acids at pH 6 reduced the RE 1.5-2.5 times, whereas the same concentration of acids at pH 10 decreased the removal efficiency by a factor of 2-4. The results obtained with the 4-HBA were similar for all of the oils (RE of 6-8%). The removal efficiency of crude oil B was least affected by the presence of the dissolved components, while crude oil E had the highest decrease of RE. The dissolved components also had a visible effect on the bubble stability. Compared to the standard brines, where the coalescence between bubbles

was extensive, the dissolved acidic species reduced the bubble growth. The stability of bubbles depended on the type of the dissolved matter (Figure 10).

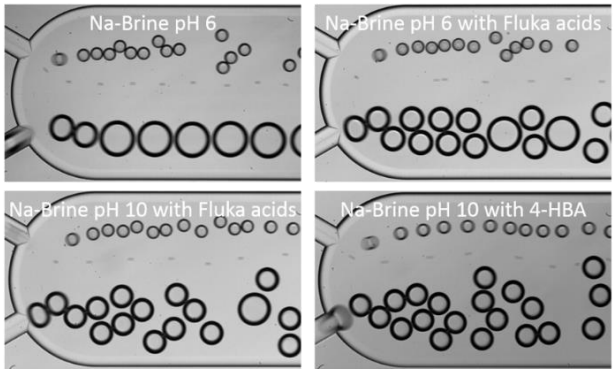

Figure 10 Snapshots of the channel inlet in different brine compositions.

In standard brine at pH 6, the generated 110 µm bubbles coalesced quickly in the beginning of the channel to form bubbles of 150 µm in diameter. Upon addition of Fluka acids, the bubbles were more stable, but coalescence still occurred. The Fluka acids at pH 10 provided more extensive stabilization against merging of bubbles and slightly reduced the size of generated bubbles (ca. 100 µm). While the size of bubbles at the end of the channels was only somewhat different from the standard brine for the brine with Fluka acids at pH, the effect of the Fluka acids at pH 10 was more substantial. Many bubbles were still of initial size and only some of them coalesced to form bigger bubbles. Even more stable bubbles were obtained with the 4-HBA. In this case the generated bubbles had similar size to the bubbles formed in Fluka pH 10 and virtually all of them retained their original size at the end of the channel. The enhanced stability of bubbles is supported by the surface tension values for different brines (Table 3).

Table 3 Surface tension measurements of the brines with and without dissolved components.

Brine	Na-Brine at pH 6	Na-Brine with Fluka acids at pH 6	Na-Brine with Fluka acids at pH 10	Na-Brine with 4-HBA at pH 10
Surface Tension [mN/m]	72.5 ±0.7	69.1 ±1.5	62.3 ±0.5	37.4 ±0.5

The Fluka acids at pH 6 were not very surface-active and reduce the surface tension only slightly, compared to the brine without any dissolved components. Naphthenic acids extracted at higher pH have a higher affinity to the air-water surface, providing a larger reduction of surface tension. Largest surface pressure was obtained for the 4-HBA, which confirmed its high surface activity, reported by others[49]. The difference between the two Fluka acid solutions can be explained by their composition. The acidic species extracted at pH 6 have generally shorter carbon chains and less aromatic structure, compared to the acids from the other solution (Figures S1 and S2 in SI). The presence of the dissolved organic components in produced water is a result of partitioning of water-soluble crude oil components and the addition of production chemicals to the petroleum fluids[9]. The effect of these components on the air-water interface was studied in our group by Eftekhardadkhah et al.[8, 33, 50]. Additionally, drop-bubble micromanipulator studies showed that the presence of dissolved components increases the drainage time between a crude oil droplet and a gas bubble[15]. The results from that report agree with our findings. The dissolved components, adsorbing at interfaces, can increase the potential energy barrier, stabilizing the thin film against rupture. In addition, the presence of the surface-active molecules in the thin film may give rise to the Marangoni effect. When a bubble and a droplet approach each other, an interfacial tension gradient is formed in the thin film region as a result of the surface concentration changes. The molecules will diffuse from the low interfacial tension region towards the high, creating a flux acting in the opposite direction of the film drainage process. Then, the drainage time can become longer than the contact time, which will decrease the removal efficiency as observed in our case. Furthermore, the 4-HBA reduced the RE for all oil to more or less the same value. Previously, we have reported the effect of this component on the coalescence of crude oil drops[31], where it completely stabilized the droplets against merging. The 4-HBA had a similar effect on the oil drops, and in addition stabilized the gas

bubbles. This single component can greatly increase the efficiency of packing at both oil-water and gas-water interfaces. As a result, it stabilized the system to a greater extent than both Fluka acids solutions.

Gas Phase Effect.

During offshore separation processes using gas flotation, natural gas is predominantly used as the gas phase due to its availability and compatibility with the dispersed oil phase. However, in some cases nitrogen or carbon dioxide are also utilized[44]. To bring our studies closer to real systems, we also investigated the effect of the gas phase. Figure 11 compares the removal efficiencies of crude oil E when using nitrogen and methane, with and without Fluka acids in the water phase.

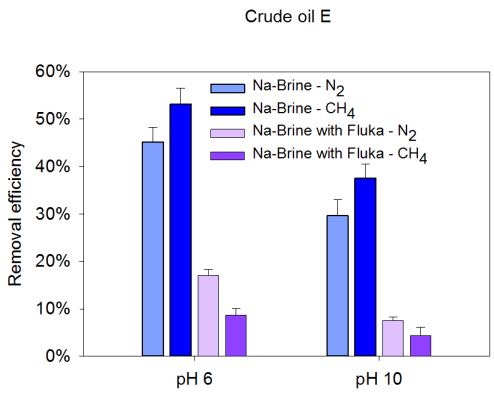

Figure 11 Comparison of removal efficiencies for crude oil E when using nitrogen and methane, with and without the dissolved components.

Methane led to higher removal efficiency in almost all cases (the results for the remaining oils are presented in Figures S3 and S4 in SI). No significant changes in the initial bubble size nor coalescence between them were observed, when methane was used as the gas phase. For two of the oils (E, F), we performed tests with methane and dissolved Fluka acids at pH 6 and 10. When the dissolved components were added to the system containing methane bubbles, the RE decreased dramatically and were lower than in the analogous system with nitrogen.

The surface tensions of nitrogen and methane against seawater are comparable, both being around 72-73 mN/m [51]. Nevertheless, methane, being the simplest hydrocarbon, will probably have higher affinity to the hydrocarbon structure of crude oil. The interaction

between the two might be more favourable due to the increased mutual solubility, which could have been promoted by the slightly higher pressure in the microchannel. The hydrocarbon gas is also less dense than nitrogen (0.7 kg/m^3 and 1.2 kg/m^3, respectively). All these factors might have contributed to the enhanced spreading of oil droplets over gas bubbles. However, upon addition of the dissolved Fluka acids, the removal efficiency dropped significantly. The naphthenic acids, present in the water phase, typically consisted of a long hydrocarbon chain (>C10), sometimes with an aromatic moiety in their structure. It could be argued that these molecules, originally coming from the crude oil, will adsorb more readily to the methane-water surface than to nitrogen-water surface. Still, we have not observed increased stability of methane bubbles at the inlet nor significant changes in the bubble size distribution at the end of the channel.

CONCLUSIONS

We have presented a new, microfluidic method for studying the removal of oil droplets through spreading of oil the surfaces of gas bubbles. Crude oil was used as one of the dispersed phases, as similar bubble-drop interactions would be expected to occur in a gas flotation treatment of the petroleum produced water. We have systematically investigated the effect of various parameters on the oil removal efficiency by spreading. It was shown that the removal efficiency was highest at low or neutral pH, and lowest at highest pH, which was explained by the increased interfacial activity of acidic species in crude oils. The reduction of salinity increased the electrostatic repulsion between bubbles and drops, and resulted in decreased spreading. The smallest drops and the lowest concentration of oil drops were found to improve the removal efficiency. The dissolved components in the water phase had a dramatic effect on the stability of oil drops and gas bubbles, which probably increased the drainage time and greatly reduced the spreading of oil over the gas surfaces. In addition, the effect of the gas phase was studied, where it was found that methane bubbles increased removal of oil drops.

We believe that this microfluidic method can be very useful in studying fundamental aspects of gas flotation in the petroleum industry. Oil films on gas bubbles is the most stable aggregate out of all flotation mechanisms. The knowledge about the parameters promoting the spreading or the effect of various additives on this process may be valuable, and this will be the scope of our further work.

ACKNOWLEDGMENTS

This work was carried out as a part of SUBPRO, a Research-based Innovation Centre within Subsea Production and Processing. The authors gratefully acknowledge the financial support from SUBPRO, which is financed by the Research Council of Norway, major industry partners and NTNU.

REFERENCES

1. Fakhru'l-Razi, A.; Pendashteh, A.; Abdullah, L. C.; Biak, D. R.; Madaeni, S. S.; Abidin, Z. Z., Review of technologies for oil and gas produced water treatment. *J Hazard Mater* **2009,** *170* (2-3), 530-51.

2. Judd, S.; Qiblawey, H.; Al-Marri, M.; Clarkin, C.; Watson, S.; Ahmed, A.; Bach, S., The size and performance of offshore produced water oil-removal technologies for reinjection. *Separation and Purification Technology* **2014,** *134*, 241-246.

3. Rawlins, C. H., Flotation of Fine Oil Droplets in Petroleum Production Circuits. *Recent Advances in Mineral Processing Plant Design* **2009**, 232.

4. Niewiadomski, M.; Nguyen, A. V.; Hupka, J.; Nalaskowski, J.; Miller, J. D., Air bubble and oil droplet interactions in centrifugal fields during air-sparged hydrocyclone flotation. *International Journal of Environment and Pollution* **2007,** *30* (2), 313-331.

5. Strickland, W. T., Jr., Laboratory Results of Cleaning Produced Water by Gas Flotation. *Society of Petroleum Engineers Journal* **1980**, 175-181.

6. Poteau, S.; Argillier, J.-F.; Langevin, D.; Pincet, F.; Perez, E., Influence of pH on Stability and Dynamic Properties of Asphaltenes and Other Amphiphilic Molecules at the Oil−Water Interface†. *Energy & Fuels* **2005,** *19* (4), 1337-1341.

7. Spiecker, P. M.; Gawrys, K. L.; Trail, C. B.; Kilpatrick, P. K., Effects of petroleum resins on asphaltene aggregation and water-in-oil emulsion formation. *Colloids and Surfaces A: Physicochemical and Engineering Aspects* **2003,** *220* (1), 9-27.

8. Eftekhardadkhah, M.; Reynders, P.; Øye, G., Dynamic adsorption of water soluble crude oil components at air bubbles. *Chemical Engineering Science* **2013,** *101* (Supplement C), 359-365.

9. Røe Utvik, T. I., Chemical characterisation of produced water from four offshore oil production platforms in the North Sea. *Chemosphere* **1999,** *39* (15), 2593-2606.

10. Chevaillier, J. P.; Klaseboer, E.; Masbernat, O.; Gourdon, C., Effect of mass transfer on the film drainage between colliding drops. *Journal of Colloid and Interface Science* **2006,** *299* (1), 472-485.

11. Nikolov, A. D.; Randie, M.; Shetty, C. S.; Wasan, D. T., Chemical Demulsification of Oil-in-Water Emulsion using Air-Flotation: The Importance of Film Thickness Stability. *Chemical Engineering Communications* **1996,** *152-153* (1), 337-350.

12. Oliveira, R. C. G.; Gonzalez, G.; Oliveira, J. F., Interfacial studies on dissolved gas flotation of oil droplets for water purification. *Colloids and Surfaces A: Physicochemical and Engineering Aspects* **1999,** *154* (1), 127-135.

13. He, L.; Lin, F.; Li, X.; Xu, Z.; Sui, H., Effect of solvent addition on bitumen–air bubble attachment in process water. *Chemical Engineering Science* **2015,** *137*, 31-39.

14. Chakibi, H.; Hénaut, I.; Salonen, A.; Langevin, D.; Argillier, J. F., Role of Bubble–Drop Interactions and Salt Addition in Flotation Performance. *Energy & Fuels* **2018,** *32* (3), 4049-4056.

15. Eftekhardadkhah, M.; Øye, G., Induction and Coverage Times for Crude Oil Droplets Spreading on Air Bubbles. *Environmental Science & Technology* **2013,** *47* (24), 14154-14160.

16. Eftekhardadkhah, M.; Aanesen, S. V.; Rabe, K.; Øye, G., Oil Removal from Produced Water during Laboratory- and Pilot-Scale Gas Flotation: The Influence of Interfacial Adsorption and Induction Times. *Energy & Fuels* **2015,** *29* (11), 7734-7740.

17. Bremond, N.; Bibette, J., Exploring emulsion science with microfluidics. *Soft Matter* **2012,** *8* (41), 10549-10559.

18. Baret, J.-C.; Kleinschmidt, F.; El Harrak, A.; Griffiths, A. D., Kinetic Aspects of Emulsion Stabilization by Surfactants: A Microfluidic Analysis. *Langmuir* **2009,** *25* (11), 6088-6093.

19. Krebs, T.; Schroen, K.; Boom, R., A microfluidic method to study demulsification kinetics. *Lab on a Chip* **2012,** *12* (6), 1060-1070.

20. Krebs, T.; Schroën, K.; Boom, R., Coalescence dynamics of surfactant-stabilized emulsions studied with microfluidics. *Soft Matter* **2012,** *8* (41), 10650-10657.

21. Nowbahar, A.; Whitaker, K. A.; Schmitt, A. K.; Kuo, T.-C., Mechanistic Study of Water Droplet Coalescence and Flocculation in Diluted Bitumen Emulsions with Additives Using Microfluidics. *Energy & Fuels* **2017**.

22. Lin, Y.-J.; Perrard, A.; Biswal, S. L.; Hill, R. M.; Trabelsi, S., Microfluidic Investigation of Asphaltenes-Stabilized Water-in-Oil Emulsions. *Energy & Fuels* **2018**.

23. Xu, J.-H.; Chen, R.; Wang, Y.-D.; Luo, G.-S., Controllable gas/liquid/liquid double emulsions in a dual-coaxial microfluidic device. *Lab on a Chip* **2012,** *12* (11), 2029-2036.

24. Yang, L.; Wang, K.; Mak, S.; Li, Y.; Luo, G., A novel microfluidic technology for the preparation of gas-in-oil-in-water emulsions. *Lab on a Chip* **2013,** *13* (17), 3355-3359.

25. Yue, J.; Rebrov, E. V.; Schouten, J. C., Gas-liquid-liquid three-phase flow pattern and pressure drop in a microfluidic chip: similarities with gas-liquid/liquid-liquid flows. *Lab on a Chip* **2014,** *14* (9), 1632-1649.

26. Conn, C. A.; Ma, K.; Hirasaki, G. J.; Biswal, S. L., Visualizing oil displacement with foam in a microfluidic device with permeability contrast. *Lab on a Chip* **2014,** *14* (20), 3968-3977.

27. Almajid, M. M.; Kovscek, A. R., Pore-level mechanics of foam generation and coalescence in the presence of oil. *Advances in Colloid and Interface Science* **2016,** *233*, 65-82.

28. Xiao, S.; Zeng, Y.; Vavra, E. D.; He, P.; Puerto, M.; Hirasaki, G. J.; Biswal, S. L., Destabilization, Propagation, and Generation of Surfactant-Stabilized Foam during Crude Oil Displacement in Heterogeneous Model Porous Media. *Langmuir* **2018,** *34* (3), 739-749.

29. Dudek, M.; Kancir, E.; Øye, G., Influence of the Crude Oil and Water Compositions on the Quality of Synthetic Produced Water. *Energy & Fuels* **2017,** *31* (4), 3708-3716.

30. Dudek, M.; Muijlwijk, K.; Schroen, C. G. P. H.; Øye, G., The Effect of Dissolved Gas on Coalescence of Oil Drops Studied with Microfluidics. *Submitted to Journal of Colloid and Interface Science*.

31. Dudek, M.; Dumaire, T.; Bertheussen, A.; Øye, G., Microfluidic Tools for Studying Coalescence of Crude Oil Droplets in Produced Water. *Submitted to Fuel*.

32. Farooq, U.; Simon, S.; Tweheyo, M. T.; Øye, G.; Sjöblom, J., Interfacial Tension Measurements Between Oil Fractions of a Crude Oil and Aqueous Solutions with Different Ionic Composition and pH. *Journal of Dispersion Science and Technology* **2013,** *34* (5), 701-708.

33. Eftekhardadkhah, M.; Kløcker, K. N.; Trapnes, H. H.; Gaweł, B.; Øye, G., Composition and Dynamic Adsorption of Crude Oil Components Dissolved in Synthetic Produced Water at Different pH Values. *Industrial & Engineering Chemistry Research* **2016,** *55* (11), 3084-3090.

34. Gaweł, B.; Eftekhardadkhah, M.; Øye, G., Elemental Composition and Fourier Transform Infrared Spectroscopy Analysis of Crude Oils and Their Fractions. *Energy & Fuels* **2014,** *28* (2), 997-1003.

35. Bertheussen, A.; Simon, S.; Sjöblom, J., Equilibrium partitioning of naphthenic acids and bases and their consequences on interfacial properties. *Colloids and Surfaces A: Physicochemical and Engineering Aspects* **2017,** *529* (Supplement C), 45-56.

36. Brandal, Ø.; Sjöblom, J.; Øye, G., Interfacial Behavior of Naphthenic Acids and Multivalent Cations in Systems with Oil and Water. I. A Pendant Drop Study of Interactions Between n-Dodecyl Benzoic Acid and Divalent Cations. *Journal of Dispersion Science and Technology* **2004,** *25* (3), 367-374.

37. Tichelkamp, T.; Teigen, E.; Nourani, M.; Øye, G., Systematic study of the effect of electrolyte composition on interfacial tensions between surfactant solutions and crude oils. *Chemical Engineering Science* **2015,** *132*, 244-249.

38. Farooq, U.; Simon, S.; Tweheyo, M. T.; Sjöblom, J.; Øye, G., Electrophoretic Measurements of Crude Oil Fractions Dispersed in Aqueous Solutions of Different Ionic Compositions—Evaluation of the Interfacial Charging Mechanisms. *Journal of Dispersion Science and Technology* **2013,** *34* (10), 1376-1381.

39. Yoon, R.-H.; Yordan, J. L., Zeta-potential measurements on microbubbles generated using various surfactants. *Journal of Colloid and Interface Science* **1986,** *113* (2), 430-438.

40. Marrucci, G.; Nicodemo, L., Coalescence of gas bubbles in aqueous solutions of inorganic electrolytes. *Chemical Engineering Science* **1967,** *22* (9), 1257-1265.

41. Firouzi, M.; Howes, T.; Nguyen, A. V., A quantitative review of the transition salt concentration for inhibiting bubble coalescence. *Advances in Colloid and Interface Science* **2015,** *222*, 305-318.

42. Wang, J.; Tan, S. H.; Nguyen, A. V.; Evans, G. M.; Nguyen, N.-T., A Microfluidic Method for Investigating Ion-Specific Bubble Coalescence in Salt Solutions. *Langmuir* **2016,** *32* (44), 11520-11524.

43. Moosai, R.; Dawe, R. A., Oily Wastewater Cleanup by Gas Flotation. *West Indian Journal of Engineering* **2002,** *25* (1), 17.

44. Saththasivam, J.; Loganathan, K.; Sarp, S., An overview of oil–water separation using gas flotation systems. *Chemosphere* **2016,** *144*, 671-680.

45. Sylvester, N. D.; Byeseda, J. J., Oil/Water Separation by Induced-Air Flotation. *Society of Petroleum Engineers Journal* **1980**.

46. Ivanov, I. B.; Danov, K. D.; Kralchevsky, P. A., Flocculation and coalescence of micron-size emulsion droplets. *Colloids and Surfaces A: Physicochemical and Engineering Aspects* **1999,** *152* (1–2), 161-182.

47. Boyson, T. K.; Pashley, R. M., A study of oil droplet coalescence. *Journal of Colloid and Interface Science* **2007,** *316* (1), 59-65.

48. Chesters, A. K., The modelling of coalescence processes in fluid-liquid dispersions: a review of current understanding. *Chemical Engineering Research and Design* **1991,** *69* (A4), 259-270.

49. Spildo, K.; Høiland, H., Interfacial Properties and Partitioning of 4-Heptylbenzoic Acid between Decane and Water. *Journal of Colloid and Interface Science* **1999,** *209* (1), 99-108.

50. Eftekhardadkhah, M.; Øye, G., Dynamic Adsorption of Organic Compounds Dissolved in Synthetic Produced Water at Air Bubbles: The Influence of the Ionic Composition of Aqueous Solutions. *Energy & Fuels* **2013,** *27* (9), 5128-5134.

51. Sachs, W.; Meyn, V., Pressure and temperature dependence of the surface tension in the system natural gas/water principles of investigation and the first precise experimental data for pure methane/water at 25°C up to 46.8 MPa. *Colloids and Surfaces A: Physicochemical and Engineering Aspects* **1995,** *94* (2), 291-301.